Sustained Delivery of CZ48,

A Lactone-Stabilized Camptothecin, by Nanosuspensions

A Dissertation Presented to the

Faculty of the Department of Pharmacological and Pharmaceutical Sciences

College of Pharmacy, University of Houston

In Partial Fulfillment of

the Requirements for the Degree of

Doctor of Philosophy

By

Dong Dong

November, 2012

Acknowledgements

I would like to take this opportunity to acknowledge many people who have made my stay at the College of Pharmacy memorable.

Special thanks are reserved for my advisor Dr. Diana S-L Chow for her unwaving guidance and support. You helped and encouraged me all through my graduate years and continuesly to support, inspire and guide me. I know I will continue to lean on you for supports wherever my career takes me to.

I would also like to sincerely thank my dissertation committee members, Dr. Giovanella who provides the proprietary compound, CZ48 and facilities for our efficacy study; Drs. Hu, Liang and Tam who never ceased in helping and sharing their precious time and expertise in the experiment design and data analysis.

I have to also thank Dr. Lucy Liu from CHRISTUS Stehlin Foundation for Cancer Research. She tought me animal skills and gave me a significant help.

I also want to thank Dr. Elimika Pfuma and fellow graduate students, especially Stanley Hsiao, Yang Teng, Tanay Samant, Jie He in the Department of Pharmacological and Pharmaceutical Sciences for all the supports you gave me.

Lastly, thank you my husband Baojian Wu for being there and absorbing all my pains and worries when things did not seem to be moving, for that I will always love you.

Abstract

CZ48, a novel C20-propionate ester of camptothecin (CPT), shows promising antitumor activity as a topoisomerase I (Topo-I) inhibitor. Compeling evidence indicates that CZ48 is more effective and less toxic than other anticancer agents, many of which are in clinical use such as Adriamycin, Alkeran, and 5-FU. However, poor solubility and the effective delivery challenges have been the obstacles for application of the drug to patients.

Interestingly, many studies have shown that a prolonged exposure of Topo-I inhibitors with low concentrations is more efficacious in cancer treatment compared with a short term exposure with high concentrations, though the exact mechanism remains unknown. In an attempt to accelerate the development process and promote the clinical trials of CZ48, we hypothesized that CZ48 can be formulated into nanosuspensions which deliver CZ48 in a sustained fashion. Sustained delivery of CZ48 could provide a prolonged exposure of CPT, the actual active compound, thus leading to an enhanced antitumor activity. The success in formulating the CZ48 nanosuspension will overcome the limitaions of the drug (e.g., the poor solubility and short half-life) and push it into the first line option in cancer chemotherapy based on the achieved outstanding efficacy and low toxicity. Further, the passive targeting property of nanosuspension may provide additional merits for CZ48 chemotherapy.

Toward the goal, our specific aims are: (1) to prepare by wet media milling method and characterize CZ48 nanosuspensions. We aim to obtain two types of nanosuspensions

that differ considerably in the particle size. In vitro release study will be carried out by dialysis bag diffusion technique; (2) to determine the pharmacokinetics and organ distribution of CZ48 (and CPT) from CZ48 nanosuspensions in Sprague-Dawley (SD) rat and Swiss nude mouse models. The pharmacokinetic profiles and biodistribution patterns of CZ48 (and CPT) will be established by administering CZ48 as a nanosuspension following intravenous (i.v.) administration; (3) to determine the efficacy of CZ48 nanosuspension in tumor-bearing athymic mouse model. The lead formulation with the most favorable pharmacokinetic properties will be selected to validate the antitumor activity in a well-established tumor-bearing mouse model. The efficacy will be mainly measured by the suppression of tumor growth and the survival rate.

Two types of CZ48 nanosuspensions with particle sizes of 200 nm (NS-S) and 600 nm (NS-L), respectively, were successfully formulated and extensively characterized. The *in vitro* release study showed a sustained release of CZ48 from nanosuspensions compared with the release from cosolvent (reference). Pharmacokinetic studies in SD rats and Swiss nude mice demonstrated that compared to CZ48 cosolvent, CZ48 nanosuspensions increased the systemic exposure of CZ48 and prolonged the blood circulation of CPT. Moreover, the half-life was much longer and AUC was much larger of CPT from NS-S than those of NS-L. In tested organs, CZ48 nanosuspensions showed the largest value of CZ48 AUC in liver, spleen and lung after the i.v. administration. For both nanosuspensions, a prolonged half-life of CPT was observed in all the test organs compared to those from cosolvent. CZ48-loaded nanosuspension (NS-S) exhibited

significant tumor inhibitory effect with a higher tolerable dose, and an improved survival rate compared to CZ48 cosolvent.

In conclusion, this study for the first time demonstrated that nanosuspension was a viable pharmaceutical carrier that delivered CZ48 in a sustained manner and achieved significant tumor growth suppression at a higher tolerable dose. The study provides a formulation strategy that has a great potential to overcome the delivery barriers for many other anticancer drugs. We anticipate that CZ48 nanosuspention will be a lead candidate for the clinical trials on CZ48 in the near future.

List of Tables

List of Figures

List of Abbreviations

CZ48	Camptothecin-20(S)-O-propionate hydrate
CPT	Camptothecin
Topo-I	Topoisomerase I
NCI	National Cancer Institute
HSA	Human Serum Albumin
PBS	Phosphate Buffered Saline
CEs	Carboxylesterases
DMSO	Dimethyl Sulfoxide
PEG 400	Polyethylene Glycol 400
RES	Reticuloendothelial system
i.v.	Intravenous
T-80	Polysorbate 80 (Tween 80)
MPS	Mononuclear Phagocyte System
CCD	Cental Composite Design

SCLC	Small Cell Lung Cancer
NSCLC	Non Small Cell Lung Cancer
TPT	Topotecan
CPT-11	Irinotecan
EGFR	Epidermal Growth Factor Receptor
EPR	Enhanced Permeability and Retention
PI	Polydispersity Index
F-108	Pluronic® F108
ANOVA	Analysis of Variance
NS-S	Nanosuspension with particle size of 200 nm
NS-L	Nanosuspension with particle size of 600 nm
IACUC	Institutional Animal Care and Use Committee
IS	Internal Standard
ACN	Acetonitrile
NIH	National Institutes of Health

L,W,H	Low. Medium. High
NT	No Treatment
CP	Cosolvent Placebo
NP	Nanosuspension Placebo
Co	Cosolvent
V	Volume
Kp	Tissue/Plasma Partition Coefficient
LLOQ	Low Limit of Quantification

Contents

Chapter 1 Review of the Literature

CZ48 (Figure 1a), a novel C20-propionate ester of camptothecin (CPT) (Figure 1b), was synthesized by the scientists at the CHRISTUS Stehlin Foundation for Cancer Research (Houston, TX). The drug shows promising antitumor activity as a DNA topoisomerase-I (Topo-I) inhibitor. CZ48 is converted to CPT (the actual active moiety) *in vivo* via the esterases (Figure 2). In this regard, CZ48 is considered as a prodrug of CPT.

CZ48 is a novel and potent anticancer agent, currently in Phase-I clinical trials. In addition, CZ48 has the merit of being a CPT ester with a minimal toxicity to animals. Body weight losses, an indicator of toxicity, in nude mice were not observed with oral doses as high as 200 mg/kg (Cao Z et al, 2000). For this reason, CZ48 can be viewed as a low toxicity prodrug reservoir of CPT.

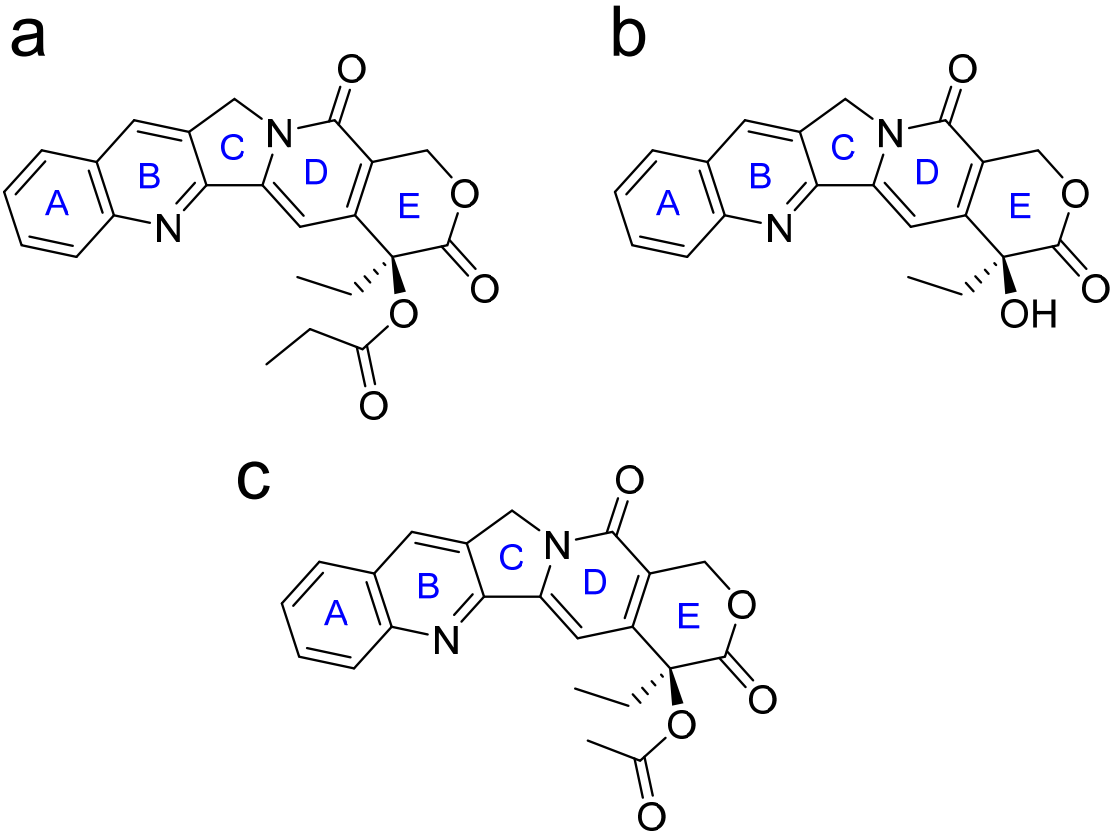

Figure 1 Chemical Structures of CZ48 and Analogs: a. CZ48; b. CPT; c. CZ44

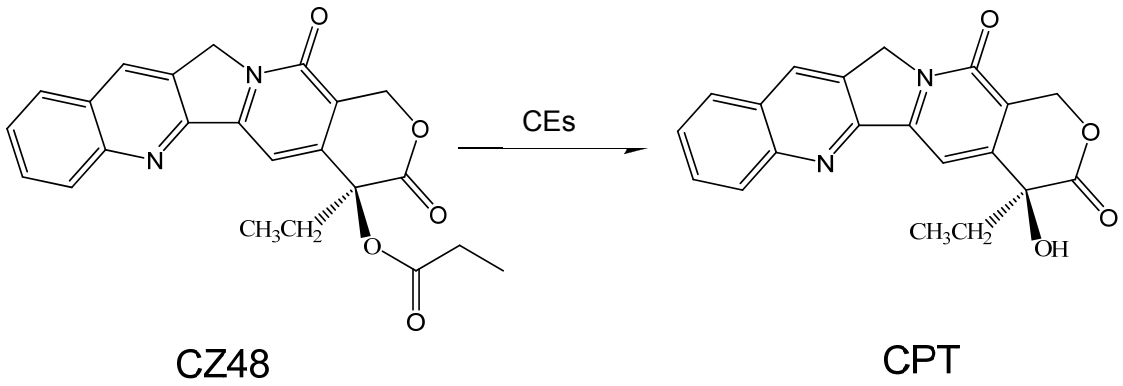

Figure 2 Bio-transformation of CZ48 to CPT

1.1. CPT

1.1.1. Discovery of CPT

In the 1950s, CPT extracts from the wood, leaves, bark and fruit of *Camptotheca acuminata* were found to have anti-tumor effects. In the early 1960s, the National Cancer Institute (NCI) Chemotherapy Program showed that CPT had promising anti-neoplastic activity against murine leukemia tumor L1210 and rat walker carcinoma cell lines (Wall ME et al., 1966). Strong antitumor properties were also observed in other different experimental systems (Gottlieb JA et al., 1970; Muggia FM et al., 1972).

In the 1960s, Due to the limited water solubility of CPT itself, CPT was entered into clinical trial as a water soluble sodium salt. However, it exhibited unpredictable and severe toxicity such as hemorrhagic cystitis, severe diarrhea, thrombocytopenia, and neutropenia which have inhibited the clinical application of CPT (Gottlieb JA and Luce JK, 1972; Moertel CG et al., 1972; Muggia FM et al., 1972). As a result, the clinical development of CPT sodium was halted in the 1970s.

1.1.2. New Interests of CPT

Despite clinical withdrawal of CPT, researchers continued conducting laboratory studies on the drug for the following 20 years. In early 1980s, two major findings renewed the clinical interest in this agent.

The first was that the intact lactone ring is an essential structure for cytotoxicity of CPT and its analogues (Wall ME and Wani MC, 1977). The intact lactone ring was also critical for their in vivo antitumor activity (Schultz AG, 1973; Wani MC, et al., 1980; Hertzberg RP, et al., 1989). The structure of CPT with a closed E-ring is shown in Figure 1b. Unfortunately this lactone ring is susceptible to spontaneous reversible hydrolysis in vivo at the physiological pH of 7.4 and readily opens to yield the opened-ring carboxylate form (Figure 3) (Fassberg J and Stella VJ, 1992). This reaction is reversible, pH-dependent and influenced by the presence of specific binding proteins such as human serum albumin (HSA) in the biological matrix. In human patients, the ratio of CPT-lactone form and CPT-carboxylate form is 1:9, because 1). At physiological pH, the equilibrium favors the CPT-carboxylate form over the lactone form of CPT (Fassberg J and Stella VJ, 1992); 2). The carboxylate form preferentially binds to serum albumin, which results in a more rapid ring opening in CPT circulation. However, the activity of CPT-carboxylate form is about 10-times less potent than CPT lactone form (Hertzberg, 1989). Therefore, the development of CPT analogues aimed at increasing the aqueous solubility of this lipophilic agent as well as improving the lactone stability in vivo for optimum therapeutic efficacy.

The second major finding was the elucidation of the mechanism of the action of CPT as an inhibitor of the mammalian nuclear enzyme, DNA topoisomerase-I (Topo-I) (Hsiang YH and Liu LF, 1988). Interestingly, Topo-I is overexpressed in certain tumor types including cervix (McLeod HL et al., 1994) and colon (Giovanella BC et al., 1989) tumors as significantly increased concentrations of this enzyme, compared to that in normal

colonic mucosa, were found in advanced stages of human colon adenocarcinoma and in xenografts of colon cancer carried by immunodeficient mice. CPT inhibits Topo-I by blocking the rejoining step of the cleavage/religation reaction of Topo-I, resulting in accumulation of a covalent reaction intermediate, cleavable complex (Figure 4). It results in interferences with the relegation step, leading to double stranded DNA breaks and, ultimately, to cell death in the S-phase of cell cycle (Hsiang YH et al., 1985, 1989). In this way, CPTs are S-phase cell cycle specific agents, in which optimal therapeutic efficacy generally requires prolonged exposure of the tumor to drug concentrations exceeding a minimum threshold.

These two findings have revived the interest in CPT and led to the development of more active CPT analogues. Development efforts aimed at increasing the aqueous solubility of this lipophilic agent as well as improving the lactone stability in vivo for optimum therapeutic efficacy.

1.1.3. CPT Analogues

With the clinical interest in CPT revived after the discoveries of its mechanism of action and the importance of the lactone ring, new analogues were being developed. There are several CPT analogues in different stages of development. Two water-soluble CPT analogues Topotecan (Hycamtin®) and Irinotecan (Camptosar®) have been approved by FDA for clinical use. Topotecan is indicated as a second-line therapy for advanced ovarian cancer, small cell lung cancer, and cervical cancer. Irinotecan is indicated as first line therapy in combination with fluorouracil for the treatment of colorectal cancer.

However, the response rates of clinical anticancer activity of these two agents are modest, 12-50% depending on the type of cancer being treated (Takimoto CH et al., 1998).

Previous studies have suggested that prolonged exposure to low concentrations of CPT lactone is more relevant than short-term exposure to high concentrations (Gerrits CJ et al., 1997). For Topotecan, as early as 45 minutes after the start of a 30 minute infusion, the carboxylate form has already exceeded the lactone form level in plasma (Grochow LB et al., 1992). Studies have suggested that the open-ring carboxylate may contribute to myelosuppression. At pH 6, more than 80% of the total Topotecan is in the lactone form, but at physiologic pH, Topotecan is rapidly hydrolyzed to the carboxylate form (Dennis MJ et al., 1997). Irinotecan is a prodrug of the active SN-38, but only 2 ~ 4% of irinotecan is converted to the active drug (Rothenberg ML et al., 1993). All these make a new anticancer drug more urgent.

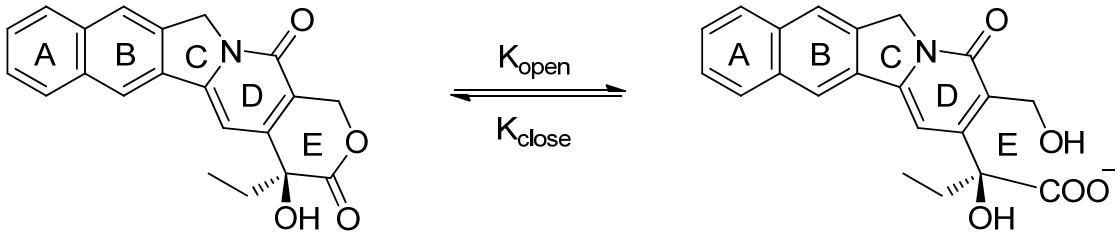

Figure 3 Equilibrium between Lactone and Carboxylate Forms of CPT

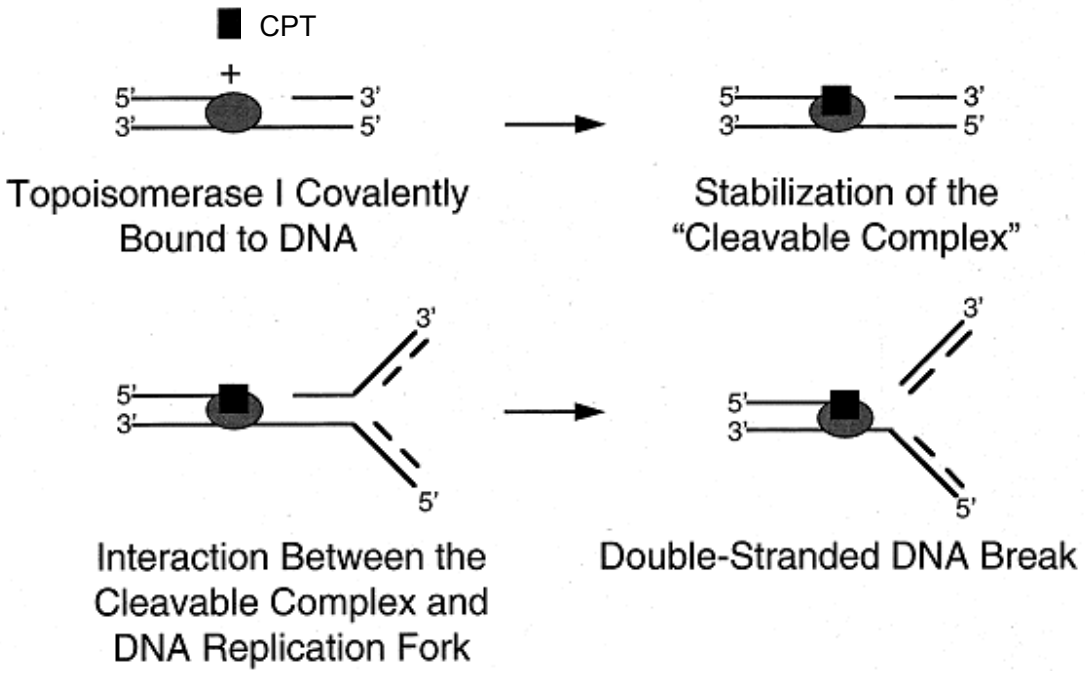

Figure 4 **Mechanism of CPT (Topo-I inhibitor) Action-Stabilization of the DNA-Topo-I Cleavable Complex in the Presence of Ongoing DNA Replication Generates Cytotoxic DNA Damage**

1.2. CZ48

1.2.1. Discovery of CZ48

Recognizing the potential promise and apparent limitations of the available CPT analogues, various alkyl esters of CPT were synthesized by scientists at Christian Stehlin Foundation for Cancer Research (Houston, TX) to circumvent problems of rapid lactone hydrolysis (Cao Z et al., 1998). Among these CPT esters, CZ48, camptothecin-20(S)-O-propionate hydrate, is the most effective candidate in inhibiting growth and inducing apoptosis in HL-60 and U-937 cells (Cao Z et al., 2000). Therefore, CZ48 was considered for further study.

1.2.2. Merits of CZ48

The lactone stability of CZ48 is significantly improved after the substitution of a bulky acyl group on the E-ring to interfere with albumin binding. Incubated in phosphate buffered saline solution (PBS) with the presence of HSA at 37 °C for 4 h, CZ48 is stable and there is no detectable hydrolysis to its carboxylate form (Liehr JG et al., 2000). The bulky ester chain in the vicinity of the lactone moiety interferes with albumin binding and thus inhibits the conversion of the active lactone form of CZ48 to inactive carboxylate form. Moreover, the 20-OH group in conventional CPTs interacts with the carboxylate oxygen by H-bonding and facilitates ring opening. Acylation of this hydroxyl group in CZ48 diminishes H-bonding interactions and results in a slower rate of lactone hydrolysis.

Besides the improved lactone stability, CZ48 has shown anticancer activity against tumor cells in culture. It also has anticancer activity against human tumor xenografts in nude mice with an exceptional lack of toxicity. CZ48 acts as a prodrug and exerts the antitumor activity by carboxylesterases (CEs) mediated hydrolysis to the active metabolite CPT in vivo (Liehr JG et al., 2000). *In vitro* study of CZ48 metabolism has showed that among blood and CE-containing tissues such as liver, spleen, lung and kidney, the liver has the highest metabolic capacity to convert CZ48 to CPT (Satoh T and Hosokawa M, 1998) instead of in blood, consistent with the fact that the highest CEs activity is in the liver.

CZ48 acts as a prodrug reservoir with a low toxicity (Cao Z et al., 2000). CPT converted from CZ48 dosing persists longer in blood circulation than that from CPT dosing. The prolonged persistence may offer an advantage of continuous exposure of CPT at a desired concentration for an extended period of time. As a result, CPT is continuously generated and entering the susceptible S-phase of the cell cycle, which leads to an enhanced therapeutic efficacy of CZ48.

In a word, CZ48 is a promising novel Topo-I inhibitor in the class of CPT anologes, combining the properties of improved lactone stability, reserved antitumor activity and low toxicity. Further studies including administration route and formulation of CZ48 are needed in order to provide guidelines for effective dosing of this agent.

1.2.3. Limitations of CZ48

The poor solubility of CZ48 is a big challenge to administer the drug. A cosolvent formulation, containing Dimethyl sulfoxide (DMSO), polyethylene glycol 400 (PEG400), Ethonal, was developed by Xiaohui Li in 2004 to study the pharmacokinetics of CZ48. It also can be given by i.v. injection. Due to the high content of organic solvent, the injection volume was limited. In addition, multiple doses can not be given because of the severe tissue damage. In addition, Topo-I inhibitors are S-phase cell-cycle specific and *in vitro* and *in vivo* studies have suggested that prolonged exposure to low concentrations might indeed be more relevant for efficacy than short-term exposure to high concentrations (Gerrits CJ et al, 1997). Therefore, developing a sustained release nanoformulation for CZ48 could overcome the administration challenge, provide a prolonged exposure of CPT at the site and the passive targeting of nanoformulation to reticuloendothelial system (RES) rich organs might have additional merits for the CZ48 chemotherapy.

1.3. Nanoformulations

Nanocarriers loaded with chemotherapy drugs have become increasingly attractive to researchers because of the stabilization of nanoparticles and of their capability in uptake by and release from monocytes/macrophages.

Nanoformulations refer to various drug delivery systems wherein the particle size of drug is in a nano range and can be given by various routes of administration, such as oral,

parenteral, and pulmonary pathways. These formulations have been widely used to deliver drugs in a sustained manner and to modulate the drug distribution pattern among tissues. The commonly used nanoformulations include lipospme, microsphere, microemulsion, nanosuspension and so on.

1.3.1. Liposome

Liposomes are spherical vesicles consisting of one or more phospholipid bilayer surrounding an aqueous core. The diameter of the liposomes varies from 0.02 ~ 10 μm (Drulis-Kawa Z and Dorotkiewicz-Jach A, 2010). The vesicles are built by the amphiphilic phospholipids. The polar head groups of the phospholipids form the interface to the aqueous media. The lipophilic agents are incorporated into the bilayer of the membrane while the hydrophilic agents are located within the water phase inside the vesicles (Korting HC and Schäfer-Korting M, 2010). The use of liposomes as a drug delivery system can improve the pharmacological properties of the traditional chemotherapeutics by altering drug pharmacokinetics and biodistribution (Allen TM and Cullis PR, 2004; Cukierman E and Khan DR, 2010).

1.3.2. Microsphere

Polymeric microspheres delivery system is one of the sustained-release systems that can accommodate a variety of drugs including small molecules proteins and nucleic acids. It can be easily injected in the site of action, for example brain tissue, if they have a proper size. Biocompatibility can be achieved by the use of natural polymers such as

cellulose, chitin, and chitosan or by the employment of polymers made from naturally occurring monomers such as lactic and glycolic acids.

1.3.3. Microemulsion

Microemulsions are drug delivery systems that have a considerable potential to act as drug delivery vehicles by incorporating a wide range of drug molecules. They are defined as clear, thermodynamically stable, isotropic mixtures of oil, water and surfactant and frequently in combination with a co-surfactant (Lawrence MJ and Rees GD., 2000). The droplet diameter is usually within the range of 10 ~ 100 nm and they form spontaneously by simple mixing of the various components (auto emulsification) (Vandamme TF, 2002). Microemulsions offer an interesting and potentially quite powerful alternative carrier system for drug delivery because of their high solubilization capacity, transparency, thermodynamic stability, ease of preparation, and high diffusion and absorption rates when compared to solvent without the surfactant system.

1.3.4. Nanosuspension

Nanosuspension formulations are carrier-free colloidal drug delivery systems for water-insoluble drugs. It contains a pure drug nanoparticles and a minimum amount of surface active agents required for stabilization of the suspended drug particles in the aqueous medium (Gao L et al., 2007). Nanosuspensions have revealed their success to solve the problems associated with the delivery of the drugs with poor solubility in water or/and in organic solvent. As nanosuspension is stabilized by the minimum amount of surfactants

and the drugs remain in a solid state, the formulation has low toxicity, higher mass per volume loading, and higher physiochemical stability compared to the drug solution (Keck CM and Müller RH, 2006). The intravenous (i.v.) administration of nanosuspensions results in various pharmacokinetic profiles depending on its physical characteristics. For example, the pharmacokinetic profile and tissue distribution of a fast dissolving nanosuspension will be similar to that of the solution upon injection (Xiong R, et al., 2008). On the other hand, if the nanosuspension particles had a slow dissolution profile, there will be a high possibility to be captured by the macrophages of the mononuclear phagocytic system (MPS), primarily by Kupffer cells in the liver, spleen and lungs in a process known as phagocytosis (Xiong R et al., 2008; Gao L et al., 2007) . Phagocytosis is triggered by the adsorption of certain plasma proteins (opsonins) on the surface of the foreign particles. Some studies showed that nanoparticles coated with polysorbate 80 (T-80) on the surface could anchor apolipoprotein E, which plays an important role in prolonging the drug circulation time in vivo (Sun W et al., 2004).

Compare to other nanoformulations, the advantages of nanosuspensions include (1) Higher drug loading (because drug is suspended in solid state) leads to lower volume of administration. (2) Nanosuspensions present reduced toxicity by using relatively low quantity of stabilizing surfactants (Keck CM and Müller RH, 2006). (3) They can be given by various routes of administration, such as oral, parenteral, pulmonary and ocular pathways, due to their particle size within a nano range (Kesisoglou F et al., 2007; Müller RH and Jacobs C, 2002; Pignatello R et al., 2006). (4) Nano-particles have a high possibility to be taken up by the macrophages in the liver, spleen and lung.

Subsequently, the particles may dissolve in the macrophages slowly and diffuse out of the cells to provide a depot effect (Xiong R et al., 2008; Andes D, 2003; Ganta S et al., 2009).

Recently, there are two basic technologies to prepare nanosuspension: media milling and high-pressure homogenization. Four commercial nanosuspension products have been obtained by media milling. Nanosuspensions can be formed by breaking larger micron-sized particles down by milling. A new surface area is formed which leads to an increase in free-energy in the system. The system becomes unstable due to the increased energy resulting from the creation of new surface area of the milled particles. To correct this energy imbalance, the small particles tend to agglomerate to decrease the surface area and re-stabilize the system. To overcome the self-correction step, a surface active agent is added during the milling step.

1.4. Central Composite Design (CCD)

During the formulation preparation process, many variables show a marked influence on the physicochemical properties of nanosuspensions. Such as milling time, surfactant, surfactant concentration, drug concentration, and so on. Therefore, it is essential to have a clear understanding about how preparation parameters determine particle characteristics and how these variables interact with each other.

Generally, the impact of each variable can be assessed by varying one variable while keeping other factors constant. Such an empirical method is acceptable only when the factors are independent of one another. However, it fails to take into account the interactions between these factors. Factorial designs enable all factors to be varied simultaneously, thus allowing quantization of the effects caused by independent variables and interactions between them; thus, it is an ideal technique for formulation studies (McLeod AD et al., 1988; Molpeceres J et al., 1996). However, in such studies, an increase in the number of factors markedly increases the number of experiments to be carried out. An alternative approach under these circumstances is to include extra center and star points in a two-level factorial design, which is known as central composite design (CCD). CCD is composed by the factorial experiment, axial points and center point. This structure makes it have a better prediction capability than factorial design (Bolton S, 1983; de Boer T et al., 1999).

1.5. Lung Cancer

Lung cancer is the leading cause of death due to cancer, approximately 1/3 of cancer deaths. According to the NCI, there are 226,160 new lung cancer cases yearly and 160,340 deaths in the United States in 2012. Lung cancer patients experience 40% relapse rates and 15% overall survival rates over five years. Considering these numbers, much needs to be done in the treatment of lung cancer.

Based on morphology, there are two types of lung cancer namely small cell lung cancer (SCLC) and non-small cell lung cancer (NSCLC). NSCLC accounts for 70% of all lung cancer cases. The current treatment options in lung cancer are surgery, radiation, chemotherapy, and targeted therapy. SCLC responds to chemotherapy better than NSCLC and chemotherapy is the major treatment option for SCLC. The major areas of focus for SCLC need to be prevention (smoking) and early detection; whereas in NSCLC the latter two are important but treatment options need to be improved.

NSCLC is divided by stages based on the localization of the tumor, lymph node involvement, and metastases to other places. Stage I has no nodular involvement or metastases. Stage II has nodular involvement in nearby lymph nodes but no metastases or has no nodular involvement or metastases but has a tumor size so large that it invades the chest wall but does not cause obstruction of organs. Stage III has nodular involvement in distant lymph nodes but has no metastases or a tumor size so large that it invades the chest wall and causes some obstruction. Stage IV has distant metastases and metastases to a different lobe of the lung.

Stage I, II, and III are considered early stages and treatment focuses on radiation and surgery. Chemotherapy is used in combination with radiation and surgery in earlier stages, and is only used as palliative treatment in stage IV. Palliative treatment includes reduction of tumor size which when too large may cause problems such as intense pain or effect on vital organs. Chemotherapy regimens are platinum based with the agents cisplatin and carboplatin being used in combination with agents such as paclitaxel, docetaxel, topotecan (TPT), irinotecan (CPT-11), vinorelbine, and gemcitabine. In recurrent NSCLC in which platinum agents had previously been used docetaxel may be used and in case of failure the epidermal growth factor receptor (EGFR) inhibitor erlotinib can be used. Based on the NCI record, vinorelbine, paclitaxel, docetaxel, gemcitabine have shown increased survival outcomes, although minimal. The camptothecin derivatives are considered second line, in this way; CZ48 may offer a good alternative.

We then chose to use the tumor bearing Athymic Swiss nude mouse model for efficacy studies because it is a well-established cancer model. The cell line we chose to use was the more aggressive H460 cell line (Mattern J et al., 1985). We deside to characterize the pharmacokinetics of nanosuspension formulations in the Athymic Swiss nude mice before starting the efficacy studies.

1.6. Concepts of Passive Targeting

Tumor blood vessels are generally characterized by abnormalities such as high proportion of proliferating endothelial cells, pericyte deficiency and aberrant basement

membrane formation leading to an enhanced vascular permeability. Particles, such as nanocarriers (in the size range of 20–200 nm), can extravasate and accumulate inside the interstitial space (Danhier F et al., 2010). Endothelial pores have sizes varying from 10 to 1000 nm (Torchilin VP, 2000). Moreover, lymphatic vessels are absent or non-functional in tumor which contributes to inefficient drainage from the tumor tissue. Nanocarriers entered into the tumor are not removed efficiently and are thus retained in the tumor. This passive phenomenon has been called the “Enhanced Permeability and Retention (EPR) effect,” discovered by Matsumura and Maeda (Matsumura Y and Maeda H, 1986). The abnormal vascular architecture plays a major role for the EPR effect in tumor for selective macromolecular drug targeting at tissue level that can be summarized as follows and illustrated in Figure 5:

a. Normal Tissue b. Tumor Tissue

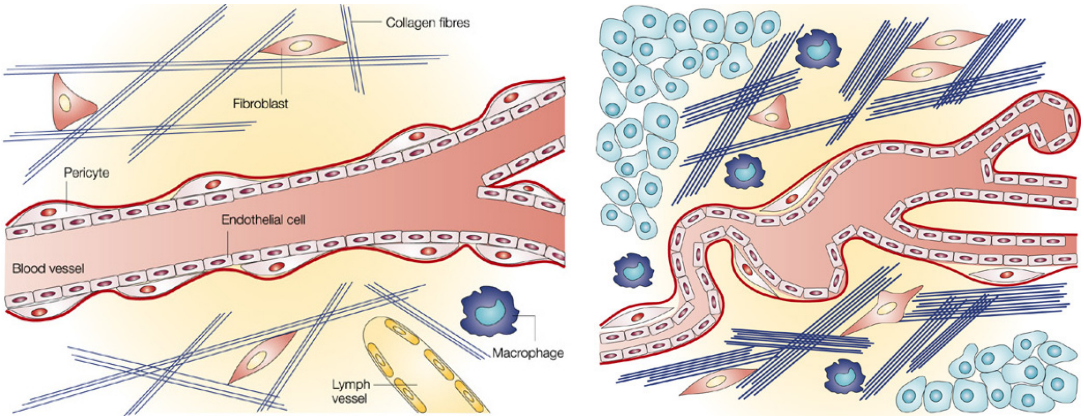

Figure 5 Differences between Normal and Tumor Tissues that Explain the Passive Targeting of Nanocarriers by the Enhanced Permeability and Retention Effect.

a. Normal tissues contain linear blood vessels maintained by pericytes. Collagen fibers, fibroblasts and macrophages are in the extracellular matrix. Lymph vessels are present. B. Tumor tissues contain defective blood vessels with many sac-like formations and fenestrations. The extracellular matrix contains more collagen fibers, fibroblasts and macrophages than in normal tissue. Lymph vessels are lacking. (Heldin CH et al., 2004)

Summary

This suvey of the literature reveals that CZ48, a propionate ester of CPT, was synthesized with superior lactone stability over CPT both *in vitro* and in vivo. However, the poor solubility of CZ48 is a big challenge to administer the drug. In addition, Topo-I inhibitors are S-phase cell-cycle specific and *in vitro* and *in vivo* studies have suggested that, for efficacy, prolonged exposure to low concentrations might indeed be more relevant than short-term exposure to high concentrations. Therefore, developing a sustained release nanoformulation for CZ48 could overcome the administration challenge, provide a prolonged exposure of CPT at the site and the passive targeting of nanoformulation to RES rich organs might have additional merits for the CZ48 chemotherapy.

Chapter 2 Hypotheses and Specific Aims

2.1 Central Hypothesis

In this study, nanosuspensions are selected to formulate and to modify the pharmacokinetics of CZ48. We propose that nanosuspensions can be prepared with the optimal characteristics to deliver CZ48 at a sustained rate. By the continuous delivery of CZ48, a low but effective level of active form of CPT will be constantly converted from the prodrug, CZ48, to achieve a significant anticancer activity and toxicity alleviation. We hypothesize that optimized nanosuspension of CZ48 can provide sustained plasma levels of active CPT.

2.1. Specific Aims

2.1.1. Aim I

To prepare and characterize CZ48 nanosuspensions with different particle sizes

We hypothesize that CZ48 nanosuspensions with a distinct particle size can be developed and the formulations offer a sustained release of CZ48. We will also use the CCD method to optimize the nanosuspensions' properties.

2.1.2. Aim II

To determine the pharmacokinetics and organ distribution of CZ48 and CPT from the NS formulations of CZ48 in rodents

We hypothesize that a prolonged drug exposure *in vivo* will be achieved upon the administration of CZ48 nanosuspensions.

2.1.3. Aim III

To determine the efficacy of CZ48 nanosuspension in tumor-bearing athymic mouse model

We hypothesize that the lead formulation will overcome the limitations of CZ48 and be proven a significant efficacy with a higher tolerable dose in H460 tumor mouse model.

Chapter 3 Materials and Methods

3.1. Materials

3.1.1. Chemicals and Materials

- Acepromazine Maleate Injection (Phoenix, St .Joseph, MO, USA) with Ketamine and xylazine were mixed and injected intramuscularly to provide anesthesia during cannulation surgery and for euthanasia at the end of studies conducted in rats.
- Acetonitrile (ACN) HPLC-grade (EM Science, Gibbstown, NJ, USA) was used in mobile phase for HPLC assay, as well as the extraction of drug from *in vivo* samples for HPLC analysis.
- CPT was purchased from Sigma-Aldrich (St. Louis, MO, USA). CPT was used as standard for HPLC assays.
- CZ48 and CZ44 were kindly given by CHRISTUS Stehlin Foundation for Cancer Research (Houston, TX, USA) as gift. CZ44 was used as internal standard for HPLC assay.
- Dimethylsulfoxide (DMSO) analytical grade (J.T. Baker Chemical Co., Phillipsburg, NJ, USA) was used as solvent for stock solutions of CZ48, CPT and CZ44, as well as a constituent of the cosolvent formulation used for CZ48 studies.
- Double distilled water was produced by a MiliporeMilli-Q system (Billerica, MA, USA).

- Ethanol (EMD, Gibbstown, NJ, USA) was used in the preparation of CZ48 cosolvent formulation,
- F-60 and F-108 were kindly provided by BASF (USA). Tween-80 (T-80) was purchased from Sigma-Aldrich (St. Louis, MO, USA). They are used for formulation preparation.
- Glacial acetic acid (J.T. Baker Chemical Co., Phillipsburg, NJ, USA) was used to keep the pH of the mobile phase at 3.0 in the CZ48 HPLC assay.
- Heparin sodium salt (Sigma Chemical Co., St. Louis, MO, USA) was used to heparinize micro-centrifuge tubes for blood collection in the PK studies.
- Phosphate-buffered saline (PBS) that was made from 0.4 mM KH2PO4 (Sigma Chemicals Co., St. Louis, MO, USA), 2 mM K2HPO4 (Fisher Scientific Co., Fair Lawn, NJ, USA), and 140 mM NaCl (Eastman Kodak Co., St. Louis, MO. USA) was prepared as a receptor medium for *in vitro* release studies.
- Polyethylene glycol 400 (PEG 400) (Merck, Darmstadt, Germany) was used as a component of cosolvent formulations of CZ48.
- Sodium choride (Sigma Chemical Co., St. Louis, MO, USA) was dissolved in double distilled water to prepare normal saline solution.

3.1.2. Surgical Instruments and Supplies

- Alcohol wipes (Webcol® Alcohol Preps, Kendall Healthcare Products Co., Mansfield, MA, USA) were used to disinfect the animal skin surface prior to injection or surgery.

- Cotton swabs (Q-tips, 6 inch) (Tyco healthcare group LP, Mansfield, MA, USA) were used in animal surgery procedures in PK studies.
- Inserts (small volume) for samples in vials for HPLC analysis: Conical, clear glass, 150 µl (Waters Corp., Milford, MA, USA) were used for PK studies with low sample volumes (25-150µl) for HPLC assay. Flat bottom, clear glass, 250 µl (J G Finneran, Vineland, NJ) were used for larger plasma or tumor sample volumes (50-250µl) in microdialysis or efficacy studies for HPLC assay.
- Insulin syringes (1/2 cc, sterile) (Becton Dickinson & Co., Rutherford, NJ, USA) were used to administer the anesthesia intramasularly.
- Membrane filters (47mm, 0.45 µm, hydrophilic polypropylene; Pall Corp., Ann Arbor, MI, USA) were used to filter the mobile phase for the HPLC assays.
- Needles (23G1, sterile single use, Precision Glide Needle, Becton/Dickinson and Company. Sparks, MD, USA) were used with syringe (1 CC, sterile single use, Becton/Dickinson and Company. Sparks, MD, USA) for i.v. drug administration and blood sampling from canular.
- Pipette tips (disposable, 1-10 µl, 10-100 µl and 100-1000 µl, VWR, West Chester,PA, USA) were used with appropriate pipettes (VWR, West Chester,PA, USA) to measure solutions for all experiments.
- Polyethylene tubing (I.D. 0.023", O.D. 0.038", Becton/Dickinson and Company. Sparks, MD, USA) was used to extend the cannula for convenient drug administration and blood sampling.
- Standard silicone tubing (I.D. 0.025", O.D. 0.047", Helix Medical, Carpinteria, CA, USA) were used as cannula.

- Surgical absorbent pads (Medline, Mundelein, IL, USA) were used during animal studies.
- Surgical suture (size 4-0, Deknatel)
- Syringe filters (0.45 μm, HPLC certified) were used to filter CZ48 cosolvent during preparations.

3.1.3. Equipment and Apparatus

- Beckman Coulter Microfuge 22R Refrigerated Microcentrifuge was used to separate plasma from blood, and sample preparation.
- Column (XTerra ® RP18, 5 μm particle, 46 × 150 mm, Waters) was used for all HPLC analysis.
- Dissection equipment set (Miltex ®, Thomas Scientific, Swedesboro, NJ, USA) was used for surgery and cannulation of rats, as well as organ dissection from rats and mice.
- Electronic balance, 0.0001 g sensitivity (Mettler AE100, Mettler Instrument Corporation, Hightstown, NJ, USA) was used to weigh all solid chemicals and animal organs.
- HPLC system (515 HPLC pumps, 717 plus autosampler, and 2475 multi λ fluorescence detector, Waters).
- pH meter (IQ 240, Scientific Instrument, Carlsbad, CZ, USA) was used to measure the pH of the mobile phase.

- Shaking water bath (Model YB-521, American Scientific Products) was used in the preparation of cosolvent formulation and the *in vitro* release study.
- Vortex mixer (Vortex-Genie 2, Scientific Industries, Inc., Bohemia, NY, USA) was used for mixing liquid samples and solutions.
- WinNonlin professional version 3.3 (Pharsight Corporation, Mountainveiw, CA, USA) computer program was used for pharmacokinetic analyses and parameter calculation.

3.1.4. Animals

- Male Sprague Dawley rats (250 ~ 300 g), purchased from Harlan Laboratories (Houston, TX), were used for pharmacokinetic and organ distribution studies.
- Athymic Swiss nude mice (25 ~ 30 g) (CHRISTUS Stehlin Foundation for Cancer Research in Houston, TX, USA) were used for all PK, organ distribution and efficacy studies.

3.2. Methods

3.2.1. CZ48 Nanosuspension Preparation

CZ48 nanosuspensions were prepared by media milling method (shown as Figure 6), as described earlier (Kocbek P et al., 2006). In brief, the mixture of CZ48, stabilizers and water were placed in a 7 ml scintillation vial. Certain amount of glass beads (0.5 ~ 0.75: 0.75 ~ 1: 1 ~ 1.3 μm at 1:1:1) were then added as milling agents. The mixture was milled at the rate of 1,600 rpm for several hours. Each formulation was prepared in duplicate.

3.2.2. CZ48 Nanosuspension Characterization

The particle size, polydispersity index (PI), and zeta potential of each formulation were measured by ZetaPals (Brookhaven Instruments, Holtsville, NY). Samples were diluted to an appropriate concentration by filtered, double-distilled water. Each sample was measured three times, and the average values were employed.

Figure 6 Wet Media Milling Technique for Nanosuspensions Preparation

3.2.3. CZ48 Nanosuspension Optimization-Experimental Design

A Central composite design (CCD) was implemented for the optimization of various response properties. Based on the results of initial studies, the combination of Pluronic® F-108 (F-108) and T-80 as stabilizers yields nanosuspensions with preferred properties and the concentration of CZ48, F-108/CZ48 ratio and T-80/CZ48 ratio were found to influence the properties (particle size and zeta potential) of CZ48 nanosuspensions significantly. In this study, a three-factor five-level CCD was undertaken to investigate the main effects and the interactions of these three critical influencing factors on the two responses (particle size, zeta potential). During the optimization trails, the investigate range of each variable and the experimental codes were shown in Table 1. In the present design, 20 experiments were carried out to determine the model coefficients.

Two optimal experimental responses were studied: Y1, particle size, Y2, zeta potential, and those responses were modeled by the following model quadratic equation:

$$Y = b_0 + b_1X_1 + b_2X_2 + b_3X_3 + b_4X_1^2 + b_5X_2^2 + b_6X_3^2 + b_7X_1X_2 + b_8X_2X_3 + b_9X_1X_3$$

------- (1)

Where X_1, X_2 and X_3 correspond to the studied factors, Y is the measured response, b_0 is an intercept, b_1 ~ b_9 are the regression coefficient.

Data were analyzed by nonlinear estimation using STATISTICA® software. The results of these experiments were compared by Analysis of Variation (ANOVA) to determine if the factors and the interactions between the factors were significant. T-tests were used to

obtain parameters statistically significant in the regression model at α = 0.05 level. An F-test was performed to determine whether there was an overall regression relationship between the response Y and the entire set of variables X at a 95% level of significance.

Response surface delineation was performed according to the fitting model. The surface response plots for particle size and zeta potential as functions of influencing factors were conducted by fixing the least significant factor at the optimized value. The minimum response values and its corresponding experimental settings were solved from the regression equation (2) and (3) by performing a Visual-Basic-language based computer script calculation with step width of 0.1.

A verification test was conducted to prove the accuracy and usefulness of this statistic model under the optimized experimental conditions. The particle sizes of nanosuspension formulations prepared under these conditions were analyzed (n=6).

3.2.4. CZ48 Nanosuspension Stability

The physical stability of the CZ48 nanosuspensions was evaluated at 4 ± 2 °C and 25 ± 2 °C. Prepared nanosuspensions were divided into two parts and kept at 4 °C and 25 °C, and the changes in particle size, PI and zeta potential were recorded over the period of 3 months.

3.2.5. *In-vitro* Drug Release Study

In-vitro release study of CZ48 from cosolvent and nanosuspensions of two particle sizes in both PBS and human plasma were conducted to compare the *in-vitro* rates and extents of CZ48 from different formulations by Dialysis Bag Diffusion Technique (Figure 7) (Kostanski JW and DeLuca PP, 2000).

3.2.5.1 Conditions for HPLC Assay of CZ48 and CPT in Aqueous Solution

The HPLC assay was based on a previously developed isocratic HPLC method (Li XH, 2004) for the simultaneous quantifications of CZ48 and CPT concentrations in aqueous solution. The concentration ranges for CZ48 and CPT were both 12.5 ~ 200 ng/ml. We used a reverse phase C8 column (4.6 mm x 250 mm, particle size of 5 μm) and a fluorescence detector with excitation and emission λ of 360 & 455 nm, respectively. The mobile phase consisted of methanol: acetonitrile: 2% triethylamine (30:28:42, by volumes) with the pH adjusted to 5.0 with acetic acid and a flow rate of 1 ml/min was used to elute the column. The internal standard used was CZ44. The peak area ratios of CZ48/CZ44 or CPT/CZ44 were plotted against the corresponding CZ48 or CPT concentrations. Linear regression was used to determine the slopes of the curves and the y-intercepts. The HPLC assay was repeated to establish within-day (n = 3) and between-day (n = 6) variability.

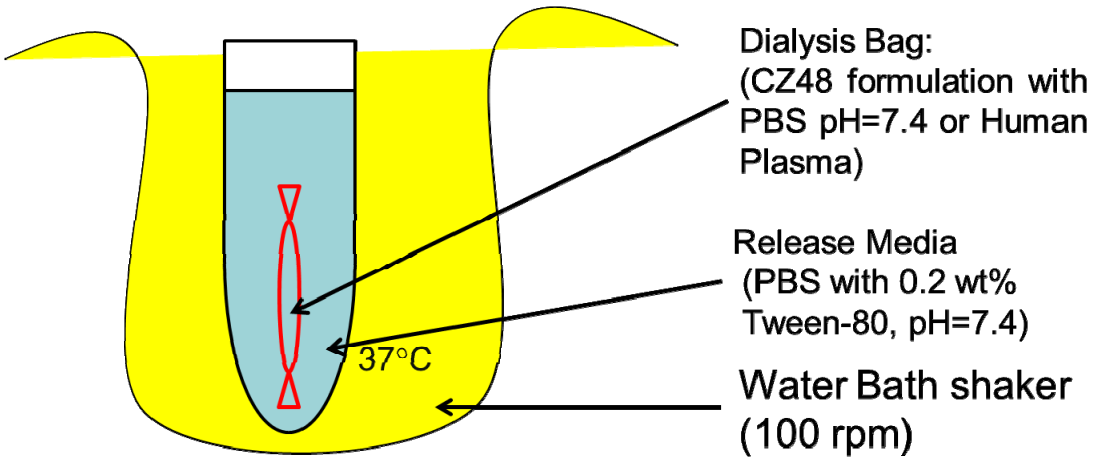

Figure 7 Dialysis Bag Diffusion Technique for *In vitro* Release Study

3.2.5.2 *In-vitro* CZ48 Release from Cosolvent, NS-S, and NS-L in PBS and Human Plasma

The *in-vitro* release studies were performed in human plasma and phosphate buffered saline (PBS) solution (pH 7.4) with 0.2 wt% T-80 (to maintain sink condition), respectively, using dialysis bag diffusion technique reported by Kostanski and DeLuca (Kostanski JW and DeLuca PP, 2000). Approximately 1 mg of the formulation was transferred to the dialysis bag (M.W. cut off 6000 - 8000 Da) in a shaker with the speed of 100 rpm at 37 ± 0.5 °C. Samples (200 µl) were withdrawn at the predetermined time points of 0.25, 0.5, 0.75, 1, 2, 3, 4, and 6 h in PBS or 0.25, 0.5, 0.75, 1, 2, 3, 4, 6, 8, 10, 24, 32 and 48 h in plasma. Samples were assayed for CZ48 by a validated HPLC method.

The profiles of cumulative amount of CZ48 released versus time were constructed. The extent of CZ48 release was calculated as the total release at 6 h (PBS) or 48 h (plasma). To characterize the release profiles, 1st-order, Higuchi, Peppas, Hixson-Crowell and Weibull equations were fitted to the release profiles. 1st-order (Equation 2) as log percent drug remaining vs. time, Higuchi"s model (Equation 3) as cumulative percentage of drug released vs. square root of time and Hixson-Crowell model (Equation 5) as the cube root of the percentage of drug remaining in the matrix vs. time.

$$F = 100 \times (1 - e^{-k_1 t}) \quad \text{..... (2)}$$

$$F = k_H \times t^{0.5} \quad \text{..... (3)}$$

$$F = k_{KP} \times t^{n} \quad \text{..... (4)}$$

$$F = 100 \times [1 - (1 - k_{HC} \times t)^{3}] \quad \text{..... (5)}$$

$$F = 100 \times [1 - e^{-\frac{(t - T_i)^{\beta}}{\alpha}}] \quad \text{..... (6)}$$

3.2.5.3 Statistical Data Analysis

Statistical criteria including the adjusted coefficient of determination (R^2 adjusted), the standard deviation of the residual (MSE_root) and Akaike information criterion (AIC) were used to evaluating the goodness of fit of a model. Release kinetic parameters were obtained by nonlinear regression based on the best fit model using MATLAB software. Data was presented as mean ± standard deviation (n = 3). The significant difference in the parameters among the groups will be statistically evaluated by one-way ANOVA followed by post hoc Tukey's test at $p<0.05$ using MINITAB student 12 software.

3.2.6. Pharmacokinetic and Biodistribution Studies of CZ48 and CPT from CZ48 nanosuspensions in Sprague-Dawley (SD) rats

The aim of this study was to establish the PK of CZ48 and its metabolite, CPT, from the cosolvent, NS-S and NS-L upon intravenous (i.v.) administration to SD rats.

3.2.6.1 Preparation of Dosing Formulations

CZ48 cosolvent (0.8 mg/ml) was prepared as DMSO: PEG400: Ethanol (2:2:1 by volume). CZ48 nanosuspensions were diluted using the double distilled water to the proper concentration at 10 mg/ml.

3.2.6.2 Rats Study Protocol

All experiments were conducted in accordance with National Institutes of Health (NIH) Guideline for the Care and Use of Animals and with approved animal protocol from the University of Houston Institutional Animal Care and Use Committee (IACUC). Male SD rats (250 ~ 300 g) were housed under standardized condition (12 hours light / dark schedule). All animals were kept 1 week prior to experiments for acclimation. Then, the rats were randomly divided into experimental groups (6 rats per group) for treatment with CZ48 formulations. Before CZ48 administration, a cannula was introduced into the jugular vein for injection of formulations and blood collection. The rats were anesthetized by anesthesia cocktail (Ketamine 50 mg/ml, Xylazine 3.3 mg/ml and Acetopromazine 3.3 mg/ml) prior to the jugular vein surgery and administrated carprofen subcutaneously after the surgery.

3.2.6.3 Pharmacokinetic Study

Rats were dosed with CZ48 cosolvent at 5 mg/kg (control group), CZ48 NS-S at 25 mg/kg, or CZ48 NS-L at 25 mg/kg through jugular vein cannula. Blood sample (200 µl) were withdrawn at 5, 15, 30, 45 min, and 1, 2, 3, 4, 6, 8, 10 and 24hr post dose from

jugular vein cannula. The volume of blood removed at each sampling time was replaced with an equal volume of saline. And the blood samples were immediately centrifuged at 10, 000 rpm for 20 min to separate the plasma fraction from the blood cells, and the plasma samples were stored at -80 °C until HPLC analysis.

3.2.6.4 Organ Distribution Study

At 15 min, 30 min, 2 h, 4 h, 8 h, and 24 h after the dose injection, rats (n=4 per time point) were anaesthetized with anesthesia cocktail (Ketamine 50 mg/ml, Xylazine 3.3 mg/ml and Acetopromazine 3.3 mg/ml), and subsequently euthanized by drawing all the blood from the abdominal aorta. Next to blood, heart, liver, spleen, lung, kidney and brain were collected. Organs were weighted and homogenized. All samples were stored at -80 °C until HPLC analysis.

The organ/plasma partition coefficient (Kp) of CZ48 and CPT for the heart, liver, spleen, lung, kidney and brain were obtained experimentally from the organ/plasma ratios toward the end of the study by the following equation (Chow EC et al., 2011):

$$K_p = \frac{AUC(t)_{organ}}{AUC(t)_{plasma}} = \frac{\int_0^t C_{organ}(t)dt}{\int_0^t C_{plasma}(t)dt}$$

3.2.6.5 HPLC Assay of CZ48 and CPT in Rat Plasma and Tissue Samples

The HPLC assay was based on a well-established gradient HPLC method (Liu X et al., 2010) for the simultaneous quantifications of CZ48 and CPT concentrations in plasma samples. The concentration ranges for CZ48 and CPT were both 0.78 ~ 800 ng/ml. We used a reverse phase C8 column (4.6 mm x 250 mm, particle size of 5 μm) and a fluorescence detector with excitation and emission λ of 360 & 455 nm, respectively. The optimized method used a binary gradient mobile phase with 0.1% acetic acid water as mobile phase A (pH 3.0) and acetonitrile (ACN) as mobile phase B. A flow rate of 1.2 ml/min was used with a 10 μl injection volume. The time program of the gradient was listed in Table 1. Each injection was followed by a 3 ~ 5 min equilibrium time before the next injection. The eluted peaks were monitored at excitation and emission wavelengths of 360 and 455 nm, respectively. CZ44 was used as internal standard. The peak area ratios of CZ48/CZ44 or CPT/CZ44 were plotted against the corresponding CZ48 or CPT concentrations. Linear regression was used to determine the slopes of the curves and the y-intercepts.

Table 1 HPLC Mobile Phase Gradient Conditions for Analysis of CZ48, CPT

Time (min)	Flow rate (ml/min)	A%	B%
0.00	1.2	80.0	20.0
15.00	1.2	78.0	22.0
25.00	1.2	55.0	45.0
30.00	1.2	20.0	80.0
31.00	1.2	0.0	100.0
32.00	1.2	80.0	20.0
34.00	1.2	80.0	20.0

3.2.6.5.1 Standard Stock and Working Solutions

Standard stock solutions of CZ48, CPT and internal standard (IS) were all prepared in DMSO at concentrations of 1.0 mg/ml. Stock solutions were stored at -20 °C until they were used for working solutions by adding appropriate volume of ACN.

3.2.6.5.2 Preparation of CZ48 and CPT Rat Plasma Samples

A portion of 100 μl blank mouse plasma, spiked plasma or pharmacokinetics study plasma was transferred to a 1 ml test tube. And then 500 μl of IS working solution (40 ng/ml) was added to the mixture and vortex for 10 s. The mixture was centrifuged at 10,000×g for 15min, and the upper layer was transferred to a clean tube and evaporated to dryness using an evaporator under a stream of nitrogen. Then, the dried extract was reconstituted in 200 μl of water/ACN (50/50, v/v diluent) and a 10 μl aliquot was injected into the chromatographic system. Within-day (n = 3) and between-day (n = 6) variability were also established for both CZ48 and CPT.

3.2.6.5.3 Preparation of CZ48 and CPT Rat Organ Samples

Rat organ samples (0.5 g each, heart, liver, spleen, lung, kidney, or brain) were minced and placed into 7 ml vials and 1 ml of normal saline was added to each sample, The organ samples were then homogenized by a tissue homogenizer. The internal standard working solution in ACN (40 ng/ml, 500 μl) was added to 100 μl of blank organ homogenate, spiked organ homogenate or biodistribution study organ homogenate. The

mixture was vortex for 10 s, and centrifuged at 10,000×g for 15min, and the upper layer was transferred to a clean tube. The extract was evaporated to dryness using an evaporator under a stream of nitrogen and reconstituted in 200 μl of water/ACN (50/50, v/v diluent) and a 10 μl aliquot was injected into the chromatographic system. Within-day (n = 3) and between-day (n = 6) variability were also established for both CZ48 and CPT.

3.2.6.5.4 Determination of Extraction Recovery

The percent drug recovery was calculated as the ratio of the slope of the plasma standard curve to that of the aqueous assay, and accounting for the dilution factor involved. This value can provide the information on the extent of drug loss during the extraction procedures.

3.2.6.6 Pharmacokinetic Analysis

Pharmacokinetic and statistical data analyses were performed using WinNonlin (Professional 3.0 Version). WinNonlin was used to model CZ48 and CPT profiles using a compartmental model for rat samples to estimate the area under the curve (AUC), clearance (CL), elimination rate constant (k_e), volume of distribution (V_d) and elimination half-life ($t_{1/2}$) for the three formulations.

3.2.6.7 Statistical Analysis

Statistical significance was evaluated by ANOVA followed by Tukey's post-hoc for more than two groups with a $P<0.05$ for significance. MINITAB student 15 was used for the

statistical analysis. In case of rat biodistribution study, sparse sampling was used in the collection of in-vivo data; that is, each animal contributed with a single observation and the area under the concentration-time curve was constructed from the mean plasma concentration from multiple rats at each time point.

3.2.7. Pharmacokinetic and Biodistribution Studies of CZ48 and CPT from CZ48 nanosuspensions in Swiss Nude Mice

The aim of this study was to establish the PK of CZ48 and its metabolite, CPT, from the cosolvent, NS-S and NS-L upon intravenous (i.v.) administration to Swiss Nude Mice.

3.2.7.1 Preparation of Dosing Formulations

CZ48 cosolvent (0.8 mg/ml) was prepared as DMSO: PEG400: Ethanol (2:2:1 by volume). CZ48 nanosuspensions were diluted using the double distilled water to the proper concentration at 10 mg/ml.

3.2.7.2 Mice Study Protocol - Pharmacokinetic and Organ Distribution Study

All experiments were conducted in accordance with NIH Guidelines for the Care and Use of Animals and with approved animal protocol from the University of Houston IACUC. Male Swiss athymic nude mice (20 ~ 25 g) were a gift from Stehlin Foundation for Cancer Research (Houston, TX, USA). Mice were maintained in individual ventilated cages under standard laboratory conditions (12-hour light/dark cycle) with free access to

food and water. Then, the mice were randomly divided into experimental groups (6 rats per group) for treatment with CZ48 formulations.

Mice were dosed with CZ48 cosolvent at 5 mg/kg (control group), CZ48 NS-S at 25 mg/kg, or CZ48 NS-L at 25 mg/kg through tail vein. There will be six groups of mice for each formulation which will be named as 15 min, 30 min, 2 h, 4 h, 8 h, and 12 h. The animals of 15 min and 30 min groups were sacrificed after 15 min and 30 min post dose under anesthesia using Avertin (tribromoethanol and amyl alcohol) based on the Christus Stehlin Foundation Standard Operating Procedure (SOP) for mouse anesthesia. A terminal blood collection will be withdrawn from the heart, and the whole body will be flushed by normal saline. Then heart, liver, spleen, lung, kidney, gall bladder, and brain will be harvested.

The animals of 2 h group, before sacrifice, only one additional blood sample was taken at 1 h time point from facial vein, then follow the same procedure as the 15 min and 30 min groups. The animals of 4 h, 8 h, and 12 h groups were treated the same as them in 2 h group. One additional blood sample for each mouse was collected from facial vein before sacrifice, which was at 3 h for 4 h group, 6 h for 8 h group, and 10 h for 12 h group. In this way, the animals in 15 min and 30 min groups were only taken one blood sample for each mouse. The others were taken two blood samples for each mouse.

The blood samples were immediately centrifuged at 10, 000 rpm for 20 min to separate the plasma fraction from the blood cells, and the samples were stored at -80 °C until HPLC analysis.

3.2.7.3 HPLC Assay of CZ48 and CPT in Mouse Plasma and Tissue Samples

The HPLC assay was based on a well-established gradient HPLC method (Liu X et al., 2010) for the simultaneous quantifications of CZ48 and CPT concentrations in plasma samples. This HPLC method also has been validated in section 3.2.6.3 in animal organs.

The pharmacokinetic paramters and Kp were also calculated following the same procedures as we did for the study in the rats.

3.2.7.4 Statistical Analysis

In case of mice study, sparse sampling was used in the collection of in-vivo data; that is, each animal contributed with a single observation and the area under the concentration-time curve was constructed from the mean plasma concentration from multiple rats at each time point.

3.2.8. CZ48 Nanosuspension Efficacy Studies

Before testing the efficacy of CZ48 nanosuspension *in vivo*, we first evaluated the CPT circulation by different formulation dosage. NS-S was selected as lead formulation to perform the efficacy study. NSCLC H460 cell lines were purchased from American Type Culture Collection (ATCC, mansaas, VA) and were widely used in the NSCLC efficacy test in subcutaneous tumor model because of its fast growth rate and high implant successful rate.

3.2.8.1 Passage of Tumor into Mice

The cell lines had been subcultured and frozen (- 40 °C) after the cell culture work to maintain supply. The subculturing was done to divide the cells from one flask to four flasks. The subcultured cell lines were counted using a Z_2 coulter counter and were recorded as cells per ml. After counting, the cells were placed in the freezer (- 40°C) and these were the cells used in the efficacy studies for this project.

For the efficacy studies, the cells were thawed, detached using trypsin, and centrifuged. The pellet was suspended in RPMI 1640 medium at a concentration of 10^7 cells/ml. One-quarter ml of the suspension was injected subcutaneously in the mid dorsal portion of four to six mice with a 25 gauge needle for tumor growth. After two weeks, the tumors were taken out for passage into all the study mice. The mice were sacrificed and the tumors were removed, pooled, minced up, and centrifuged. The supernatant was removed and 1 part of RPMI 1640 media was added to two parts of the tumor pellet and cells were aspirated with 16 gauge needle. About 100 µl of the suspension was injected in the mid-back of the study mice in order to induce the tumor for growth. 10 mice were used in each group for the dose response study based on the power analysis using MINITAB 14.

3.2.8.2 Randomization of Mice into Dosing Groups

When the estimated tumor volumes were about 100 mm^3, the mice were weighed and tumor volumes measured. Calipers were used to measure tumor volume which is

defined as the product of the tumor length (L), width (W), and height (H). The mouse weight and tumor volume were added to Microsoft FoxPro 7.0 with the mouse ID number that was earlier generated using FoxPro 7.0 and the program was used to randomize the mice into groups.

3.2.8.3 Study Design

The mice were dosed and assessed twice weekly. The assessment included body weight for toxicity, as well as tumor size and survival for efficacy. If the body weight loss was >15% or the tumors were >7000 mm^3, the mice were sacrificed. The endpoints of the study were tumor growth rate (defined as V/V_0, V is the tumor volume on the day of sacrifice and V_0 is the tumor volume on the first day of dosing), toxicity (body weight loss >15 %), and survival.

3.2.8.4 Statistical Data Analysis

MINITAB student 14 was used for most of the statistical analysis. ANOVA with Tukey's post-hoc was used for comparisons of tumor growth rate among groups. SASS was used for Kaplan-Meier survival analysis among groups in the efficacy studies.

Chapter 4 Results

The results of this investigation are summarized in the following subtopics: (1) Preparation, optimization and characterization of CZ48 nanosuspensions; (2) Plasma PK and organ distribution of CZ48 and CPT after CZ48 nanosuspensions i.v. administration to rats; (3) Plasma PK and organ distribution of CZ48 and CPT after CZ48 nanosuspensions i.v. administration to mice; (4) Comparison of formulation effects between species; (5) Proof of concept efficacy of NS-S in lung cancer tumor bearing mouse model

4.1. Preparation, Optimization and Characterization of CZ48 Nanosuspensions

4.1.1. CZ48 Nanosuspensions Preparation

Before the statistic experimental design was conducted, three qualitative factors (the type of stabilizers, concentration of stabilizers, and milling time) were prescreened by varying only one factor at a time. Since the influence of each factor on the physicochemical properties unknown when the prescreening study was conducted, the experimental condition was set arbitrarily as follows: drug concentration at 1%, stirring speed at 1,600 rpm.

4.1.1.1 Influence of Stabilizers

In order to identify stabilizer candidates for the nanosuspensions of CZ48, five different stabilizers, polyvinylpyrrolidone (PVP) K40, polyvinyl alcohol (PVA), Pluronic® F68 (F-68), Pluronic® F108 (F-108), and polysorbate 80 (T-80) in three concentrations as stabilizer/CZ48 ratio at 1:1 (H), 1:4 (M), and 1:10 (L) were screened as well as their combination with T-80 (L:L). The results were shown in (Table 2). The particle size in nanosuspensions stabilized with PVA, F-108 and T-80 is significantly smaller than those stabilized with PVP 40 and F-68. However, only F-108 and F-68 could further decrease the particle size significantly when higher concentrations were used ($p<0.05$). Moreover, nanosuspensions with a combination of with T-80 at a very low concentration resulted in a comparable or significantly smaller particle size than those with the single stabilizer alone at a much higher concentration. As stabilizers in combination were reported to achieve a better long-term stabilization, and T-80 uniquely facilitates a longer drug circulation in blood (Lück M et al., 1998), we preferably used stabilizers combing T-80 with another other type of stabilizer for our CZ48 nanosuspensions. According to the screening data in (Table 2), a smaller size (366 ± 13.2 nm) was obtained by using combined F-108 and T-80 as the stabilizer without any formulation optimization. This is consistent with an earlier report that F-108 is excellent in stabilizing nanoparticles, due to its strong affinity to the surface of nanoparticles (Höfig I et al., 2012). In addition, the combination of F-108 and T-80 was the only one pair that can further reduce the particle size by increasing the milling time. The stabilizers of combined F-108 and T-80 were selected for further CCD optimization.

In addition, the polydispersity for all the nanosuspension formulations with different stabilizers were within the acceptable range (0 ~ 0.3), indicating a narrow particle size distribution. The zeta potential of the nanosuspensions was all negative within the range of -19 ~ -32 mV (Table 2).

Table 2 Effect of Different Stabilizers and Combinations with T-80 on Particle Size, PI and Zeta Potential of Nanosuspension by Media Milling Method Preparation

Stabilizer		Particle size (nm)	PI	Zeta Potential (mV)
PVP K40	H	666.0 ± 28.4	0.118 ± 0.022	-19.29 ± 0.85
	M	707.6 ± 13.3	0.132 ± 0.027	-23.35 ± 0.67
	L	679.6 ± 23.5	0.103 ± 0.032	-23.60 ± 1.05
PVA	H	417.5 ± 27.7	0.176 ± 0.050	-25.20 ± 1.06
	M	412.0 ± 32.1	0.154 ± 0.011	-23.52 ± 0.25
	L	-	-	-
F-68	H	793.1 ± 62.8	0.178 ± 0.034	-26.57 ± 0.45
	M	915.7 ± 37.3	0.154 ± 0.011	-27.16 ± 1.25
	L	1034.9 ± 110.9	0.176 ± 0.050	-27.06 ± 0.70
F-108	H	301.3 ± 9.5	0.162 ± 0.026	-31.77 ± 1.23
	M	417.9 ± 12.9	0.150 ± 0.014	-25.82 ± 1.29
	L	578.7 ± 10.1	0.198 ± 0.006	-25.45 ± 0.72
T-80	H	475.4 ± 12.9	0.112 ± 0.028	-32.64 ± 0.64
	M	481.6 ± 22.2	0.123 ± 0.051	-32.73 ± 0.92
	L	455.4 ± 12.7	0.143 ± 0.034	-28.36 ± 1.56
PVP K40 / T-80	(L / L)	581.9 ± 31.2	0.128 ± 0.049	-25.31 ± 0.88
PVA / T-80		414.6 ± 10.7	0.164 ± 0.042	-28.81 ± 1.11
F-68 / T-80		413.5 ± 22.4	0.175 ± 0.053	-32.55 ± 1.78
F-108 / T-80		366.2 ± 13.2	0.140 ± 0.016	-31.80 ± 0.96

- : The drug can not be wetted by the stabilizer.

4.1.1.2 Influence of Milling Time

Milling time (1h ~ 48 h) was also screened by fix all other factors. The results were shown as Figure 8. The particle size decreased with time by wet milling. After 24 h, the mean particle size reached a plateau. Therefore, 24 h was selected as the fixed milling time for further studies.

However, it is premature to draw any conclusion from this preliminary screening data. Nevertheless, this step is necessary to focus on relevant variables as quantitative factors for further optimization using systematic CCD approach.

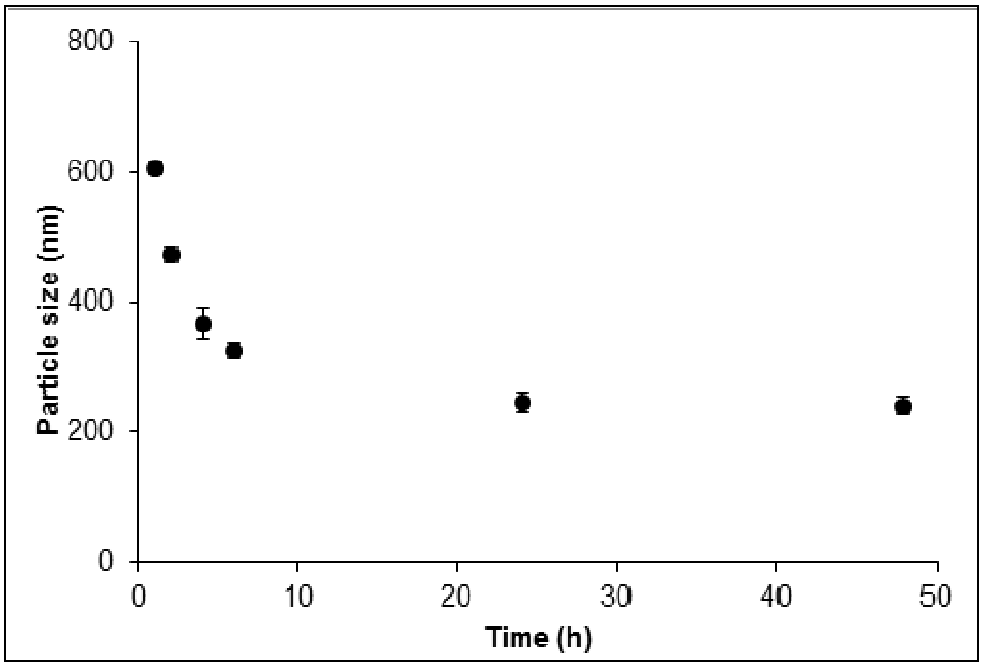

Figure 8 Dependent of Particle Size (nm) on the Milling Time (h), (n=3).

4.1.2. Central Composite Design (CCD)

In CCD study, particle size and zeta potential were considered as the responses of our nanosuspensions. This is because particle size influences not only the bio-distribution but also cellular uptake efficiency of nanosuspensions (Jani P et al. 1990). Zeta potential reflects the stability of colloidal drug delivery systems, such as nanosuspension. The concentration of CZ48, T-80/CZ48 ratio, and F-108/CZ48 ratio were chosen as the variables, since they were important factors affecting the particle size and zeta potential, as discussed above.

According to CCD design (Table 3), nanosuspensions were prepared with the three factors (at five different levels) which were indicated for each experimental run. The experiments at the center points at (0, 0, 0) (n=6) were performed to estimate the coefficient of variation (or reproducibility of experiment), which was less than 5%.

Table 3 Levels of Critical Influencing Factors and Coded Correspondent Values

Factor	Level				
	-α	**-1**	**0**	**1**	**+α**
X_1 (CZ48 concentration, wt%)	2	4	6	8	10
X_2 (T-80/CZ48 ratio)	0.02:1	0.22:1	0.51:1	0.80:1	1:1
X_3 (F-108/CZ48 ratio)	0.02:1	0.22:1	0.51:1	0.80:1	1:1

Factor levels of each experimental run and values of each nanosuspension properties were shown in Table 4. The particle size ranged from 215 to 484 nm (~ 2-fold), indicating that with a fine control of the selected factors, nanosuspensions of the optimum particle size could be acquired. The obtained data were fitted to the quadratic model (Eqation 1) to describe the relationships between the critical influencing factors and responses.

The following second-order polynomial equations of particle size (Y_1) and zeta potential (Y_2) were generated from the statistical analysis using the quadratic model:

$$Y_1(nm) = 535.338 - 101.26X_1 - 2.776X_2 - 2.705X_3 + 7.661X_1^2 + 0.018X_2^2 + 0.031X_3^2 + 0.617X_1X_2 - 0.027X_2X_3 + 0.016X_1X_3$$

---------- (7)

$$Y_3(mV) = 14.644 - 9.682X_1 - 0.952X_2 + 0.140X_3 + 0.418X_1^2 + 0.002X_2^2 - 0.001X_3^2 + 0.118X_1X_2 + 0.003X_2X_3 - 0.036X_1X_3$$

---------- (8)

The quadratic model was significant with F values of 148 and 79.9 ($p < 0.0001$), respectively, for particle size and zeta potential, which indicated that response variables of particle size and zetapotential Y were significantly related to the three of selected X variables. Moreover, the high regression coefficients (R^2) of these equations, 0.959 and 0.895, indicated a good correlation between the selected factors and resulting responses. The results were shown as Table 5.

Among the three factors, CZ48 concentration and F-108/CZ48 ratio had considerable impacts on the mean particle size with a p value less than 0.05, but T-80/CZ48 ratio did not. This might be due to the fact that T-80 only played a role as a wetting agent in the formulation; therefore, its effect on particle size is minimal. There was no correlation between seleted factors and PI.

Table 4 Experimental Responses and Results of CCD

Formulation NO.	(X_1, X_2, X_3)	Y_1: Particle size (nm)	Y_2: PI	Y_3: Zeta potential (mV)
1	(+1, +1, +1)	409.60	0.076	-11.20
2	(+1, +1, -1)	465.30	0.160	-13.79
3	(+1, -1, +1)	304.03	0.143	-28.25
4	(+1, -1, -1)	394.87	0.171	-28.40
5	(-1, +1, +1)	251.00	0.114	-23.00
6	(-1, +1, -1)	269.70	0.098	-38.25
7	(-1, -1, +1)	273.07	0.180	-17.00
8	(-1, -1, -1)	217.90	0.130	-21.18
9	(+α, 0, 0)	483.50	0.146	-24.40
10	(-α, 0, 0)	215.03	0.175	-23.62
11	(0, +α, 0)	286.20	0.122	-26.02
12	(0, -α, 0)	242.33	0.149	-28.98
13	(0, 0, +α)	298.03	0.143	-31.24
14	(0, 0, -α)	294.70	0.142	-30.75
15	(0, 0, 0)	221.90	0.159	-31.80
16	(0, 0, 0)	223.0	0.110	-27.46
17	(0, 0, 0)	220.9	0.124	-28.45
18	(0, 0, 0)	213.8	0.106	-28.22
19	(0, 0, 0)	218.5	0.138	-27.81
20	(0, 0, 0)	225.4	0.114	-27.21

Table 5 Summary of CCD Fitting Parameters

Regression Coefficient	Y_1 (Particle Size, nm)		Y_2 (PI)	Y_3 (Zeta Potential, mV)	
	Estimate	p-level		Estimate	p-level
b0	535.338	**0.006**		14.644	0.152
b1	-101.260	**0.005**		-9.682	**0.012**
b2	-2.776	0.934		-0.952	**0.0001**
b3	-2.705	**0.010**		0.140	0.214
b4	7.661	**0.002**	N/A	0.418	0.085
b5	0.018	0.423		0.002	0.621
b6	0.031	0.055		-0.001	0.269
b7	0.617	0.049		0.118	**0.0001**
b8	-0.027	0.768		0.003	0.168
b9	0.166	0.313		-0.036	0.091
F value (p<0.0001)	**148**			**79.9**	
R^2	**0.959**			**0.895**	

The dependence of particle size on the drug and F-108 concentration was plotted and shown in Figure 9, based on the regression equation (Equation 7) by fixing T-80/CZ48 ratio at 0.1:1. The minimum particle size of 190 nm could be achieved by operating the experiment under the following conditions: CZ48 concentration (X_1) = 5.9 wt%, T-80/CZ48 ratio (X_2) = 0.1:1 (i.e. 0.59 wt%: 5.9 wt%), F-108/CZ48 ratio (X_3) = 0.28:1 (i.e. 1.28 wt%: 5.9 wt%).

The dependence of zeta potential on the concentration of CZ48 and F-108/CZ48 ratio was also established (Figure 10), based on the regression Equation 8. The zeta potential value for a stable nanosuspension requires in the range of -15 to -35 mV. No minimum zeta potential value can be achieved. Moreover, the zeta potential values of the nanosuspensions, prepared by the optimized experimental conditions by particle size model, were all in the stable range. Therefore, the experimental conditions optimized by particle size model have been utilized empirically for the preparation of CZ48 nanosuspensions for further studies.

The model was proven to be valid since a fine agreement with < 3% of bias existed between the predicted and observed values (Table 6). Particle size, PI and Zeta potential were 197 ± 7 nm, - 26.5 ± 0.9 mV, and 0.11 ± 0.03, respectively.

To obtain a larger particle size nanosuspension (around 600 nm), the milling time was reduced from 24 hours to 2 hours by fixing the nanosuspension composition as the optimized formulation of 200 nm.

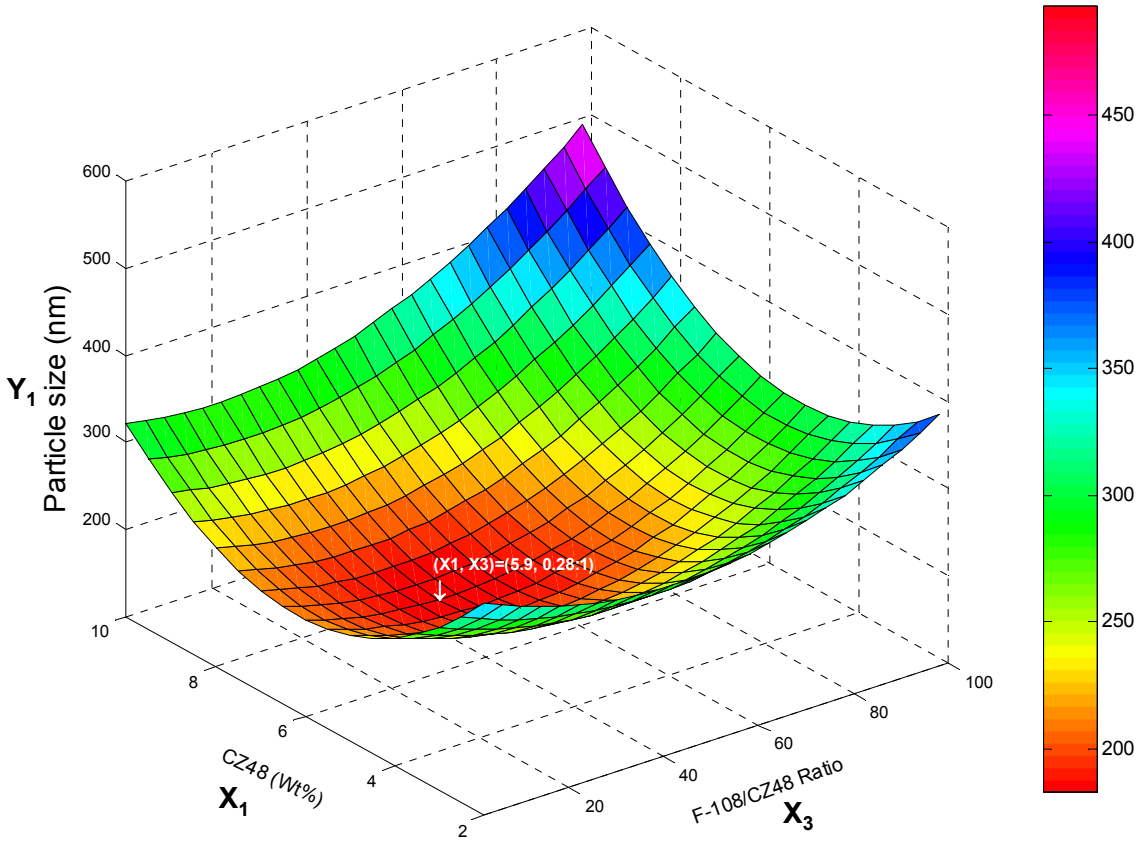

Figure 9 Surface Response Plot for Particle Size

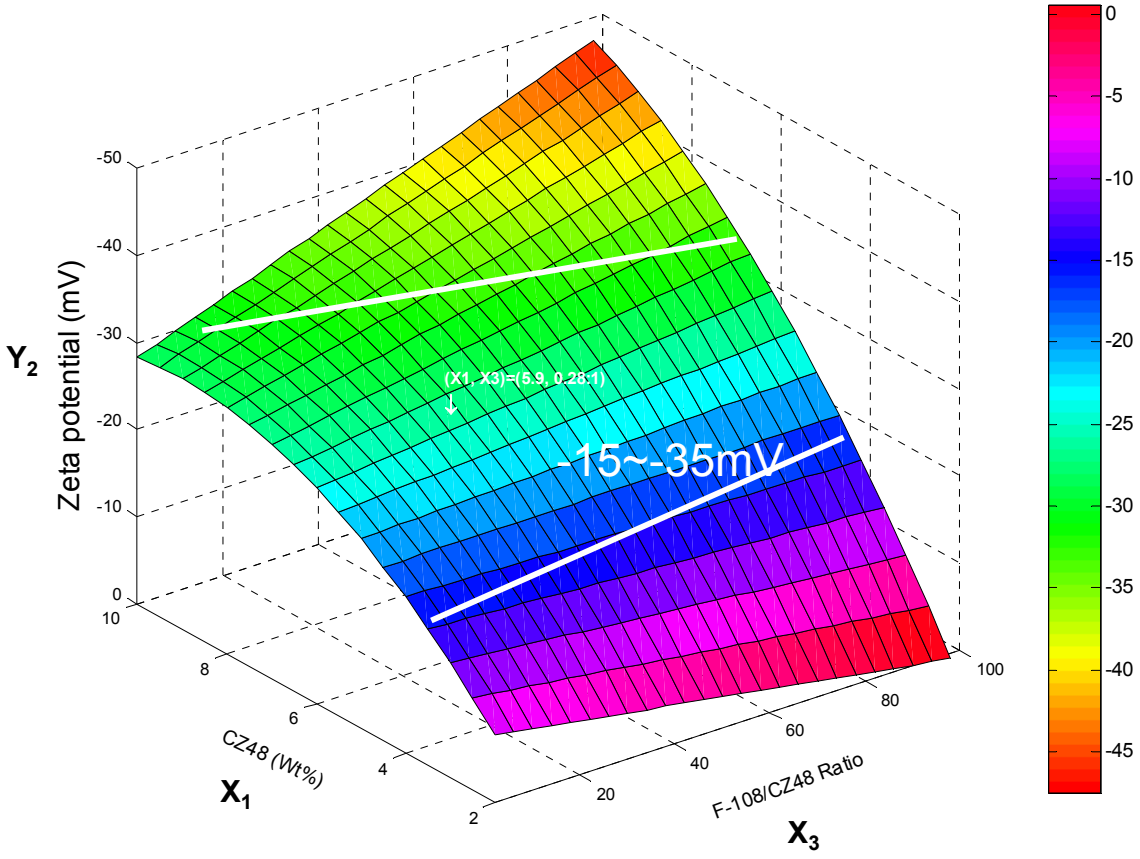

Figure 10 Surface Response Plot for Zeta Potential

Table 6 Predicted Values and Experimental Results of CZ48 Nanosuspensions Prepared under the Optimum Conditions (n=6)

Response	Predicted value	Experimental value	Bias (%)
Y1, particle size (nm)	190	197 ± 7	2.1
Y2, zeta potential (mV)	-25.8	-26.5 ± 0.9	2.7

4.1.3. CZ48 Nanosuspension Characterization

Two CZ48 nanosuspensions were developed by using wet milling technique where the drug was mixed with surfactants and ground in-between the sliding glass beads. The sizes of the nanosuspensions were about 200 nm (NS-S) and 600 nm (NS-L), respectively, depending the milling time. The single distribution population of the nanosuspensions indicated a narrow distribution of the particles diameter shown as Figure 11. The PI values of NS-S and NS-L were around 0.11 and 0.12, respectively, and they were considered within the stable range of nanosuspensions. In addition, the two nanosuspensions had similar negative zeta potential value of -26.5 ± 0.9 mV, and -27.9 ± 0.8 mV, respectively (Table 7).

4.1.4. CZ48 Nanosuspension Stability

The stability of the nanosuspensions was monitored for over 6 months by evaluating the size, PI and zeta potential of the formulations stored at 4 °C. The nanosuspensions were measured for the size of the fresh preparation (Day 0) and then on selected days as stored at 4 ^{o}C. No apparent changes were observed in sizes and size distributions. The physical stability could be attributed to the protection resulting from the well selected quantites and ratio of the stabilizers, as well as the homogeneous sizes of the nanoparticles. Long swinging hydrophilic PEO chains on the particle surface provide an excellent steric hindrance, which prevents the particles from aggregation. Moreover, the poorly soluble drugs and homogeneous particles hinder the dissolution of smaller particles and redeposit to grow into larger particles, i.e. Ostwald ripening.

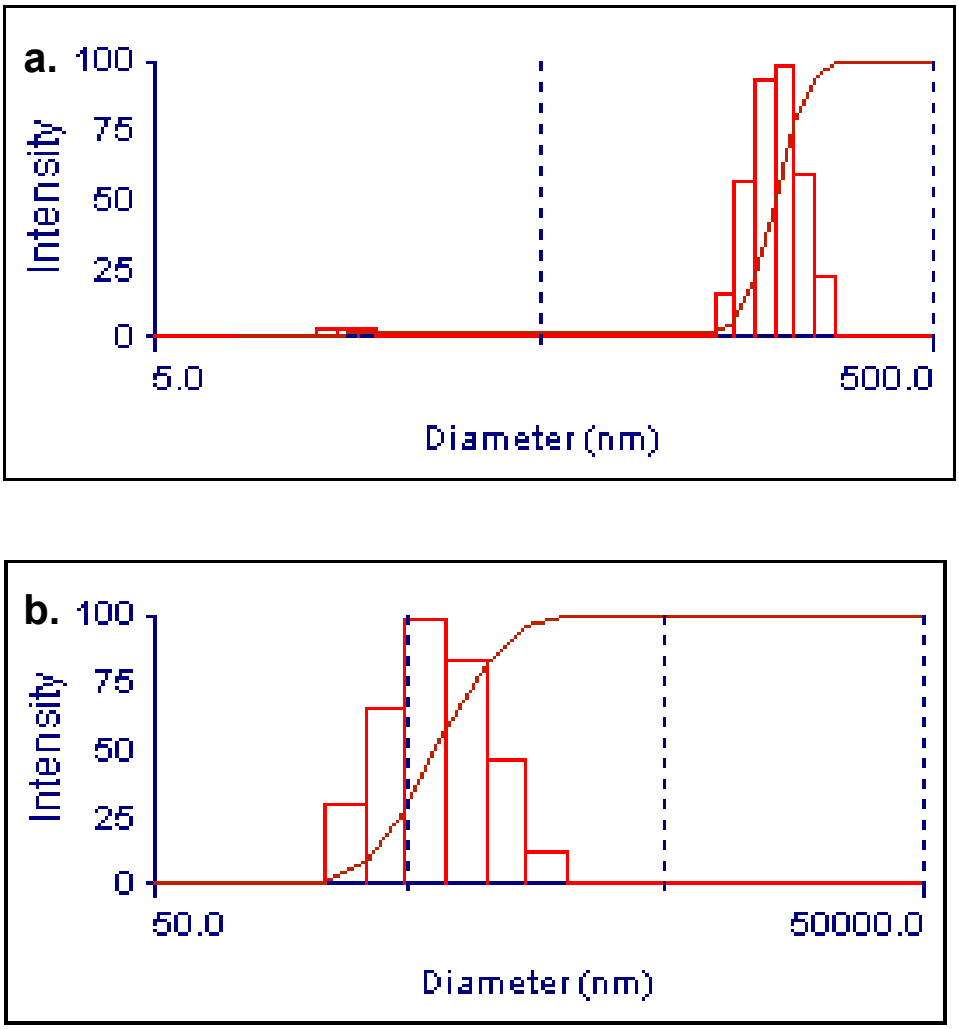

Figure 11 Particle Sizes Distribution [Intensity (%)] of (a) NS-S and (b) NS-L

Table 7 Physical Properties of CZ48 Nanosuspensions

Nanosuspensions	Particle Size (nm)	PI	Zeta Potential (mV)
NS-S	197 ± 7	0.11 ± 0.03	-26.5 ±0.9
NS-L	589 ± 22	0.12 ± 0.03	-27.9 ±0.8

4.1.5. In-vitro Drug Release Study

4.1.5.1 HPLC Assay for Simultaneous Quantifications of CZ48 and CPT in Aqueous Solution

The isocratic HPLC assay (Li XH, 2004) was adopted for simultaneous quantifications of CZ48 and CPT in aqueous solution, and CZ44 was used as IS. The assay was linear in the range of 12.5 ~ 200 ng/ml for both CZ48 and CPT. The CPT, CZ44 and CZ48 peaks were observed at the retention times of 5.03, 7.07 and 9.69 min, respectively (Figure 12 & Table 8). The assay was validated with the within-day variability (n = 3) of 1.82 and 1.59% for CZ48 and CPT, respectively, and the between-day variability (n = 6) of 2.52 and 2.30% for CZ48 and CPT, respectively (Table 9). Calibration curves for CZ48 and CPT were established in aqueous solution (Figure 13).

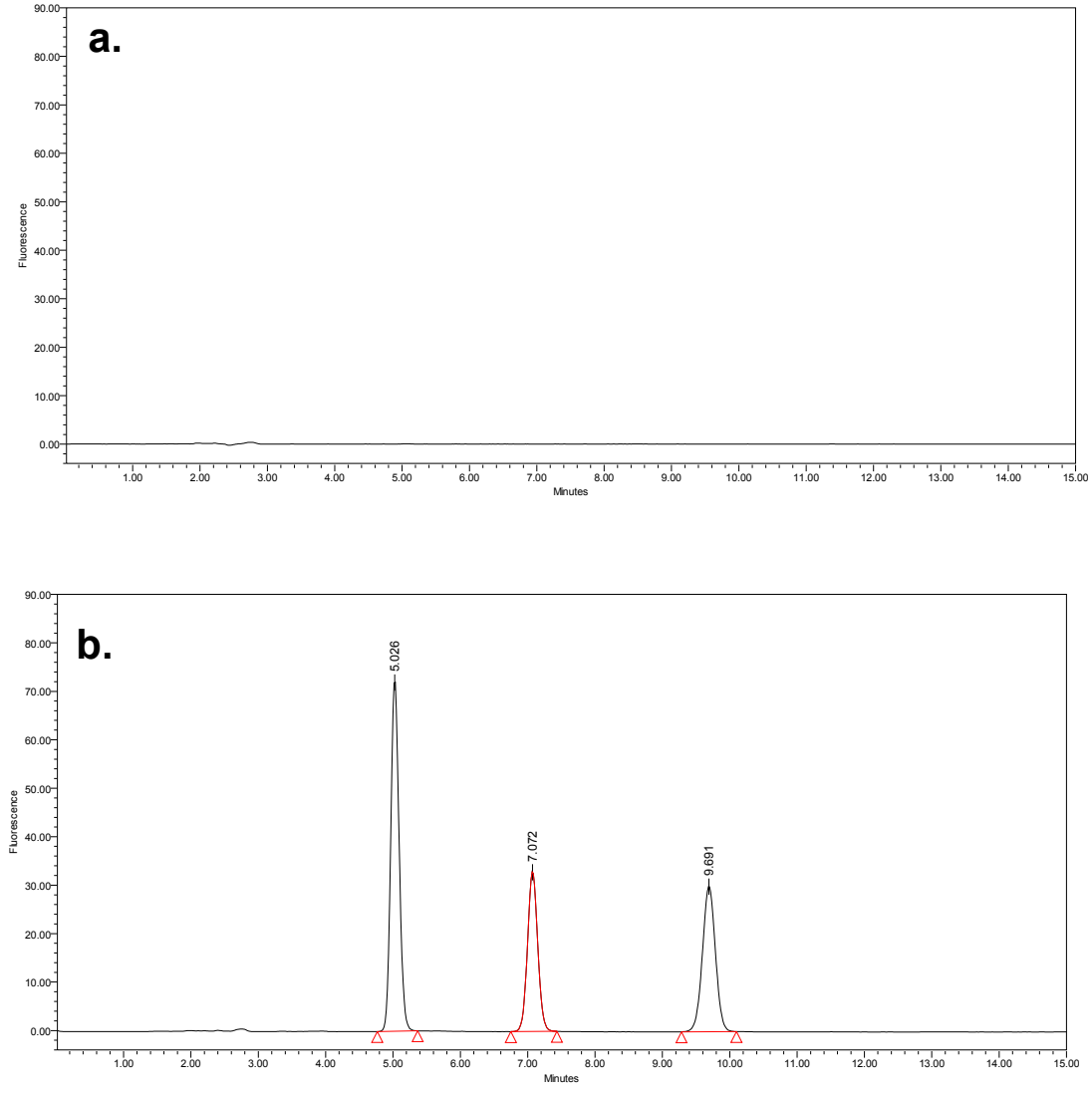

Figure 12 HPLC Chromatograms of (a) Blank Aqueous Solution, and (b) CZ48, and CPT (12.5 ng/ml) in Aqueous Solution

Table 8 HPLC Chromatogram Peak Identifications for CZ48, CPT, and CZ44 (IS)

Peak No.	Compound	Retention Time (min)
1	CPT-L	5.03
2	CZ44 (Internal Standard, 20 ng/ml)	7.07
3	CZ48-L	9.69

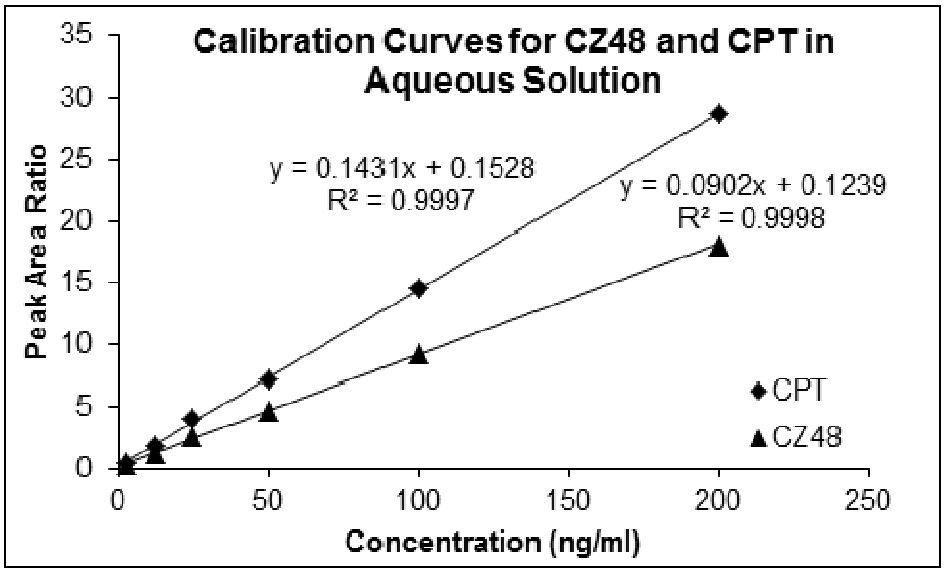

Figure 13 Calibration Curves for CZ48 and CPT in Aqueous Solution

Table 9 Linearity of HPLC Calibration Curves for CZ48 and CPT in Aqueous Solution

Parameters	CZ48	CPT
Conc. Range (ng/ml)	12.5 ~ 200	
Slope	0.09	0.14
Intercept	0.12	0.15
R^2 (correlation coefficient)	0.999	0.999
Within-day variability (%), n = 3	1.82	1.59
Between-day variability (%), n = 6	2.52	2.30

4.1.5.2 *In-vitro* Release of CZ48 from Cosolvent and Two Nanosuspensions (NS-S, and NS-L) in PBS (n=3)

In-vitro release of CZ48 from cosolvent, and nanosuspensions with different particle sizes (NS-S and NS-L) were evaluated in PBS at 37 °C. Due to the low water solubility of CZ48, 0.2 wt% T-80 was added in the PBS solution to maintain the sink condition.

The kinetics of CZ48 release were characterized by fitting with the equations of 1st-order, Higuchi, Peppas, Hixson-Crowell, and Weibull models, respectively, with cumulative release of CZ48 (Figure 14). The coefficient of determination was the criterion for the goodness of fit of the model to the data. Table 10 shows the fit criteria of the kinetic equations to the cumulative release of CZ48 from cosolvent, NS-S, and NS-L in PBS, respectively. Equations of 1st-order and Weibull had the best fit to the CZ48 cosolvent profile compared to the other models, but no significant difference between 1st-order and Weibull kinetics. All equations have equally good fit to the two CZ48 nanosuspensions. Based on the “parsimony principle of modeling”, the simplest 1st -order release kinetic model was selected to derive the release kinetic parameter, initial release rate, for all of the three formulations (Figure 15).

The initial release rate of CZ48 from nanosuspensions (about 30% /h) was significant slower compared to that from cosolvent (84.60 ± 2.76 %/h) (Table 11). Between CZ48 nanosuspensions of two different particle sizes, the initial release rate of CZ48 from larger size, NS-L, was significantly slower than that from the small-sized nanosuspension, NS-S at $P < 0.05$. The mean values of the initial release rate were

30.72 ± 3.72, and 21.36 ± 1.92 %/h, respectively. After 6 h, a complete release (> 98 %) was observed for all formulations.

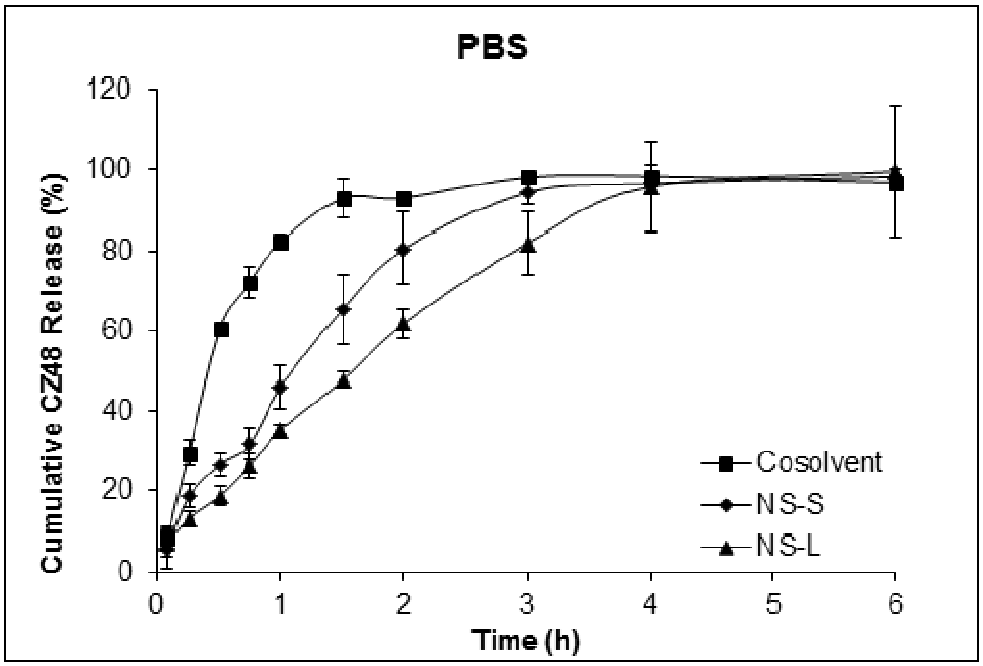

Figure 14 Release Profiles of CZ48 Cosolvent and Nanosuspensions of Different Sizes in PBS at 37 °C (n=3).

Table 10 Release Kinetics Criteria for CZ48 Cosolvent, NS-S, and NS-L in PBS (n=3)

Release Kinetic Model	Cosolvent			NS-S			NS-L		
	$R^2_{adjusted}$	MSE_{root}	AIC	$R^2_{adjusted}$	MSE_{root}	AIC	$R^2_{adjusted}$	MSE_{root}	AIC
1st-order	0.973	5.16	50.0	0.968	5.99	52.7	0.936	7.85	57.3
Higuchi	0.670	18.5	73.2	0.946	7.84	57.7	0.907	9.66	61.5
Peppas	0.829	13.3	68.0	0.946	7.72	58.0	0.952	6.25	53.0
Hixson-Crowell	0.820	13.6	67.7	0.975	5.21	50.1	0.947	6.89	54.0
Weibull	0.983	4.17	47.7	0.980	4.67	49.3	0.956	6.02	51.8

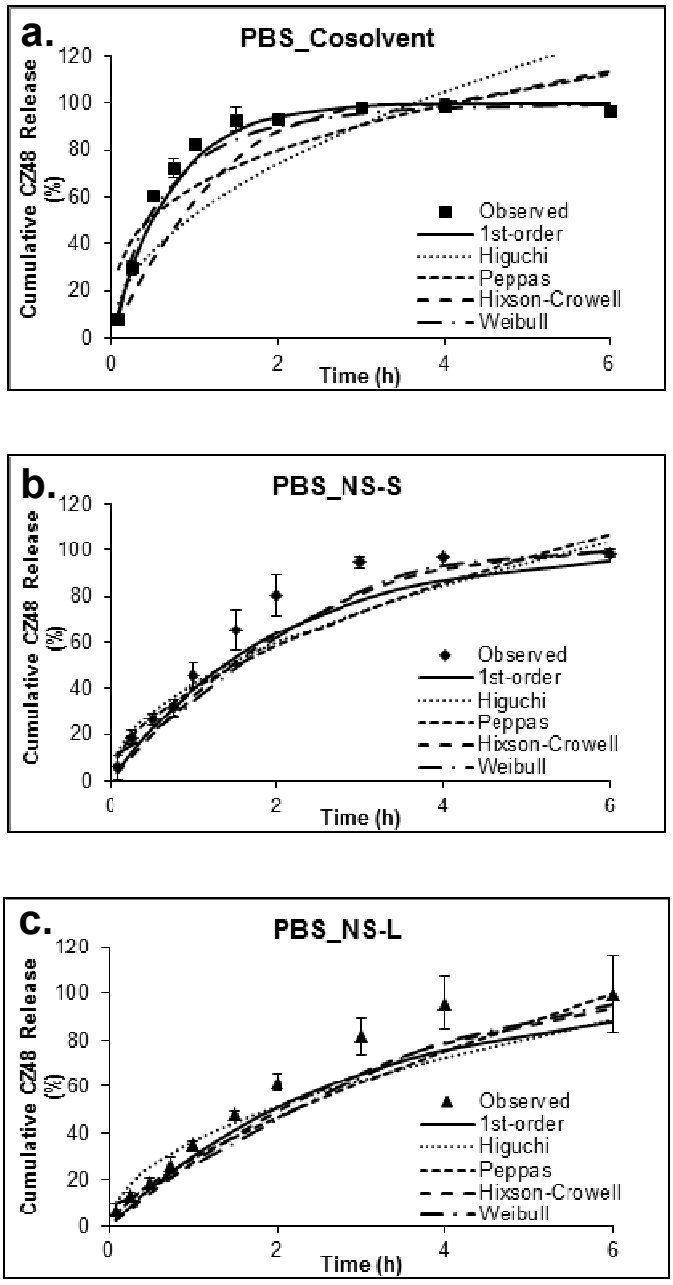

Figure 15 1st-order Release Kinetics from (a) CZ48 Cosolvent, (b) NS-S, and (c) NS-L in PBS.

Table 11 1st-order Release Kinetics parameters for CZ48 Cosolvent, NS-S, and NS-L in PBS (n=3)

Formulation	Extent of Release (%/6h)	1st-Order Release Rate Constant *k* (%/h)
Cosolvent	98.52 ± 8.40	84.60 ± 2.76
NS-S	98.40 ± 2.08	30.72 ± 3.72 *
NS-L	99.68 ± 1.99	21.36 ± 1.92 * #

Note:

* $p < 0.05$ compared to that of cosolvent

# $p < 0.05$ compared to that of NS-S

4.1.5.3 *In-vitro* Release of CZ48 from Cosolvent and Two Nanosuspensions (NS-S, and NS-L) in Human Plasma (n=3)

In vitro release of CZ48 from cosolvent and the nanosuspensions with different particle sizes were also evaluated in human plasma at 37 °C. Different from the CZ48 release study in PBS, 0.5 ml of human plasma mixed with CZ48 different formulations, respectively, were placed inside of dialysis bags. Similar to the release studies in PBS, 0.2 wt% T-80 was also added to the release media to maintain the condition. The release profiles were biphasic with an initial rapid release up to 2 h followed by a slow phase afterwards (Figure 16). The kinetics of CZ48 dissolution profiles were also characterized by fitting different equations. There was no single equation that had best fit to the profile compared to the other equations, because there was no significant difference among the fit to the release profiles to the kinetic equations (Table 12). Similar as the formulations dissolution in PBS, the 1st-order kinetic could adequately describe the release profiles (Figure 17).

Comparing the initial release rates of CZ48 from different formulations in human plasma, CZ48 nanosuspensions exhibited much slower initial release rates (0.60 %/h) than that of the cosolvent formulation (6.48 %/h) (Table 13). No statistical difference in the initial release rates was found between NS-S and NS-L. In addition, CZ 48 nanosuspensions showed a much lower extent of release (<40 % in 48 h) than that of the cosolvent with a complete release, 99% was observes at about 28 h. The extent of release of CZ48 nanosuspensions in human plasma was less than that in PBS by 60 %. This lower

extent can be explained by the strong binding of CZ48 to plasma protein inside the bag that yielded less available free CZ48 to be released to the media. CZ48 has a high plasma protein binding of ~ 82% (Pfuma E, 2009).

CZ48 in nanosuspensions exhibited sustained release characteristics when compared to cosolvent and this may be attributed to the fact that the solid status of CZ48 in nanosuspensions. This sustained release characteristics would be an advantage in cancer treatment since CZ48 levels in the systemic circulation would be sustained and yielded a prolonged exposure of CZ48 to cancer cells. In this way, the exposure of the active form of CPT to the cancer cells may also be increased and which is desirable.

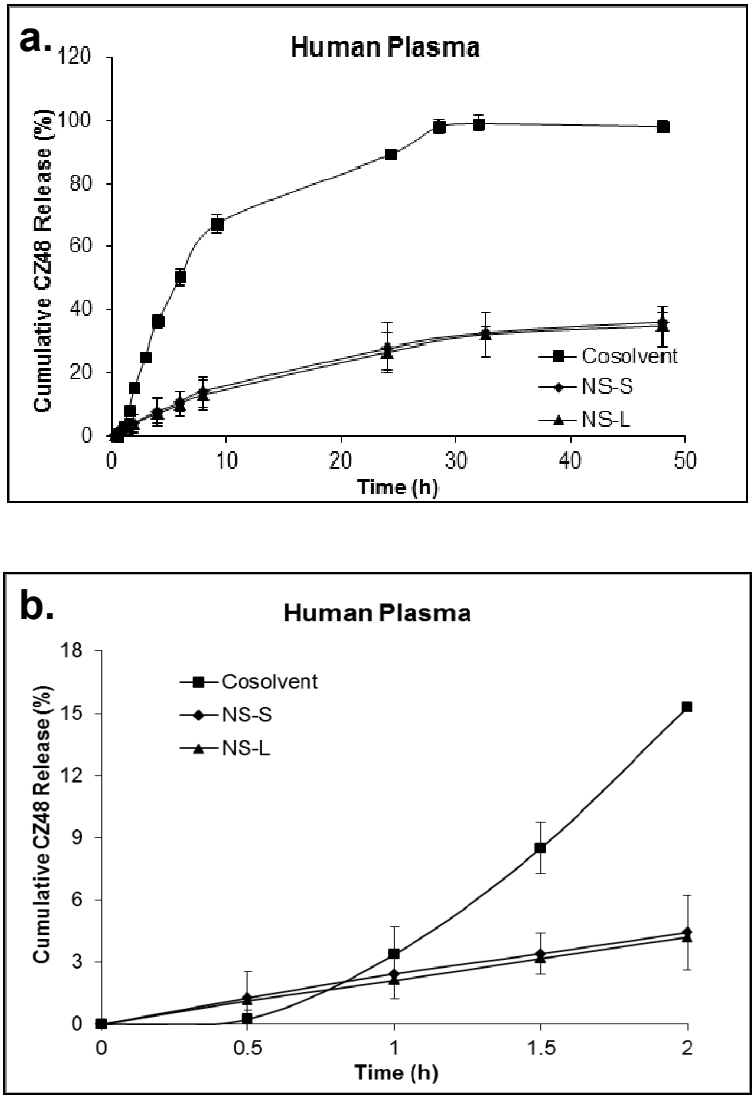

Figure 16 Release Profiles of CZ48 Cosolvent and Nanosuspensions of Different Sizes in Human Plasma at 37 °C for (a) 48 h and (b) the First 2 h (n=3).

Table 12 Release Kinetics Criteria for CZ48 Cosolvent, NS-S, and NS-L in PBS (n=3)

Release Kinetic Model	Cosolvent			NS-S			NS-L		
	$R^2_{adjusted}$	MSE_{root}	AIC	$R^2_{adjusted}$	MSE_{root}	AIC	$R^2_{adjusted}$	MSE_{root}	AIC
1^{st}-order	0.989	4.27	66.6	0.943	3.10	57.9	0.936	3.19	58.6
Higuchi	0.923	11.1	88.5	0.861	4.84	68.6	0.848	4.93	69.0
Peppas	0.915	11.6	90.4	0.939	3.20	59.6	0.936	3.33	60.5
Hixson-Crowell	0.983	5.23	70.5	0.941	3.16	58.4	0.935	3.23	58.9
Weibull	0.997	2.28	52.1	0.933	3.36	61.4	0.924	3.49	62.3

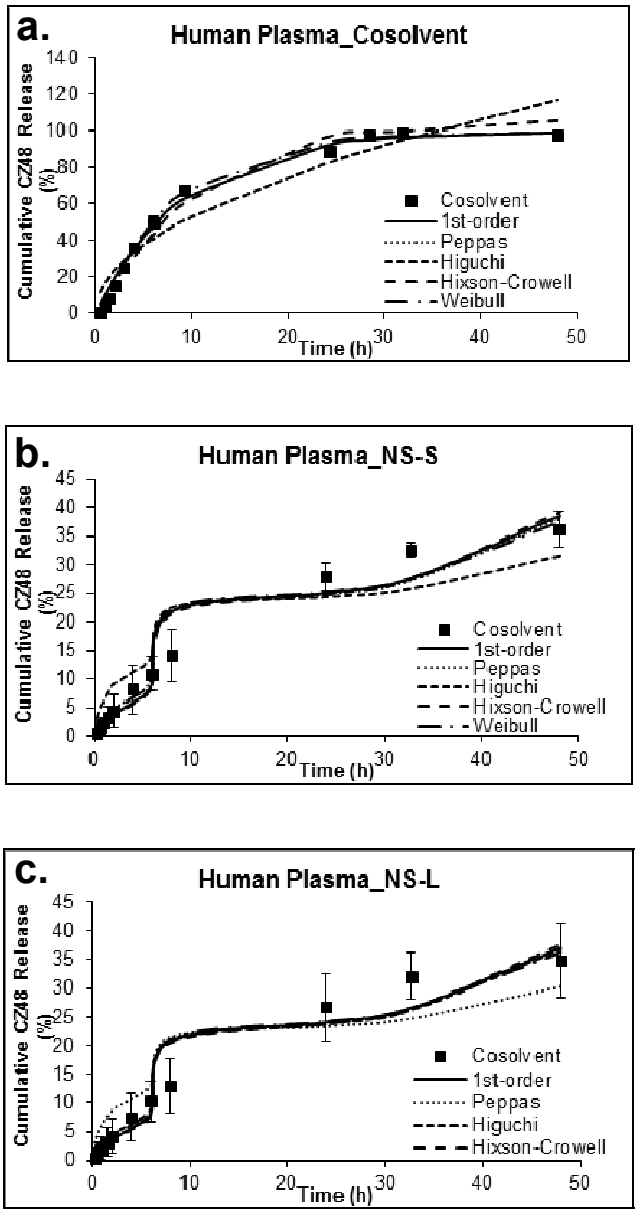

Figure 17 1st-order Release Kinetics from (a) CZ48 Cosolvent, (b) NS-S, and (c) NS-L in Human Plasma.

Table 13 1st-order Release Kinetics Parameters for CZ48 Cosolvent, NS-S, and NS-L in Human Plasma (n=3)

Formulation	Extent of Release (% / 48 h)	1st-Order Release Rate Constant *k* (%/h)
Cosolvent	98.96 ± 2.78	6.48 ± 0.90
NS-S	36.22 ± 2.49*	0.61 ± 0.12*
NS-L	34.89 ± 3.09*	0.60 ± 0.06*

Note: CZ48 Recovery = 98.37 ± 3.55%

* $p < 0.05$ compared to that of cosolvent

4.2. Plasma Pharmacokinetics and Biodistribution of CZ48 and CPT in Rats

4.2.1. HPLC Assay for Quantitative Analysis of CZ48 and CPT in Rat Plasma and Organ Samples

The reported HPLC assay is a rapid and convenient method for the simutaneous quantification of CZ48 and CPT in rat plasma and organs of liver, lungs, kidneys, spleen, heart and brain. The developed method was simple, using solvent extraction with acetonitrile. CZ44 was chosen as the internal standard for its chemical structure similarity to CZ48 and CPT.

For quantification of CZ48 and CPT in rat plasma, under described conditions (Section 3.2.6.5), the retention time was 15.13 min, 23.62 min, and 26.07 min for CPT, internal standard CZ44, and CZ48, respectively (Table 14). No interference peak was found from blank rat plasma (Figure 18). The calibration curves, each containing 6 concentration points, were constructed at the linearity range of 0.78 ~ 800 ng/ml with the correlation coefficients > 0.999 (Figure 19). The assay was validated with the within-day variability (n = 6) of 2.50 and 1.36% for CZ48 and CPT, respectively, and the between-day variability (n = 6) of 3.22 and 1.84% for CZ48 and CPT, respectively (Table 15). Plasma samples were prepared by precipitation with acetonitrile and the drug recovery of 96% for both CZ48 and CPT was achieved.

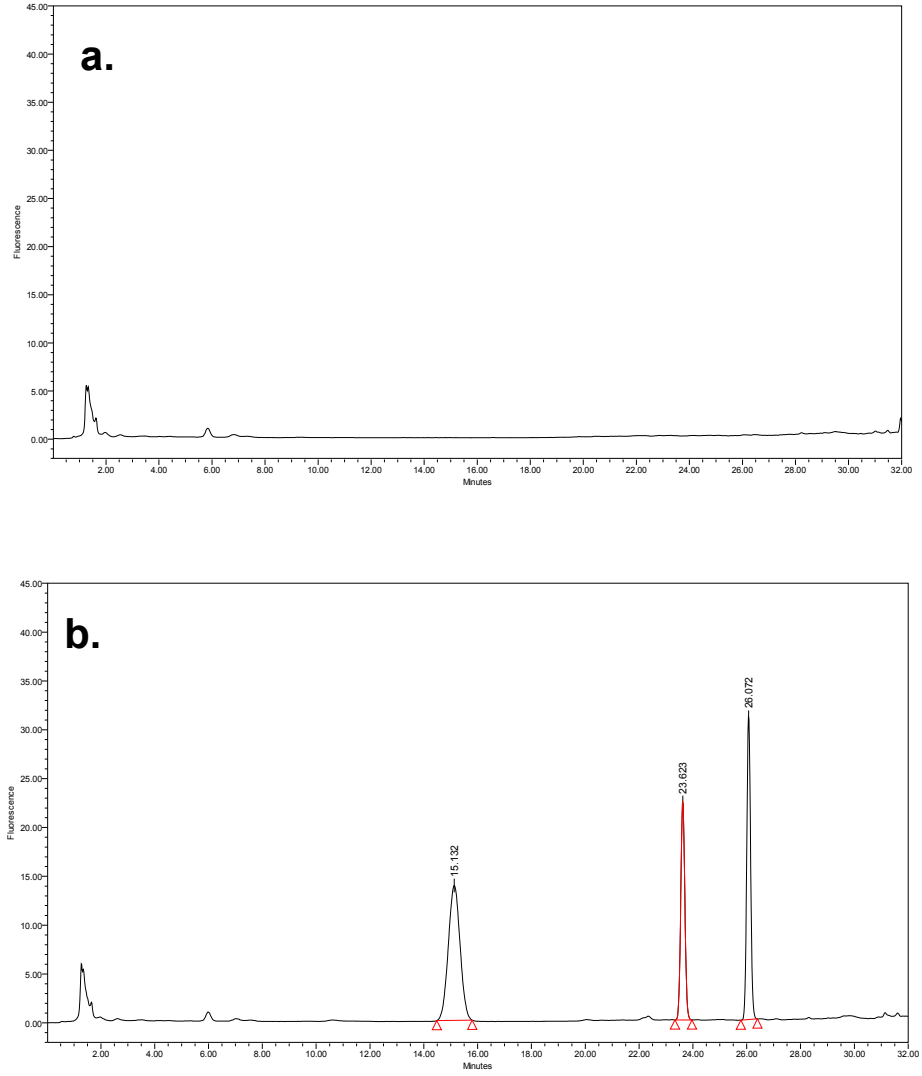

Figure 18 HPLC Chromatograms of (a) Rat Blank Plasma Sample and (b) CZ48 and CPT Spiked Rat Plasma Sample (50 ng/ml) with IS (40 ng/ml)

Table 14 HPLC Chromatogram Peak Identifications for CZ48, CPT, and CZ44 (IS)

Peak No.	Compound	Retention Time (min)
1	CPT-L	15.13
2	CZ44 (Internal Standard, 20 ng/ml)	23.62
3	CZ48-L	26.07

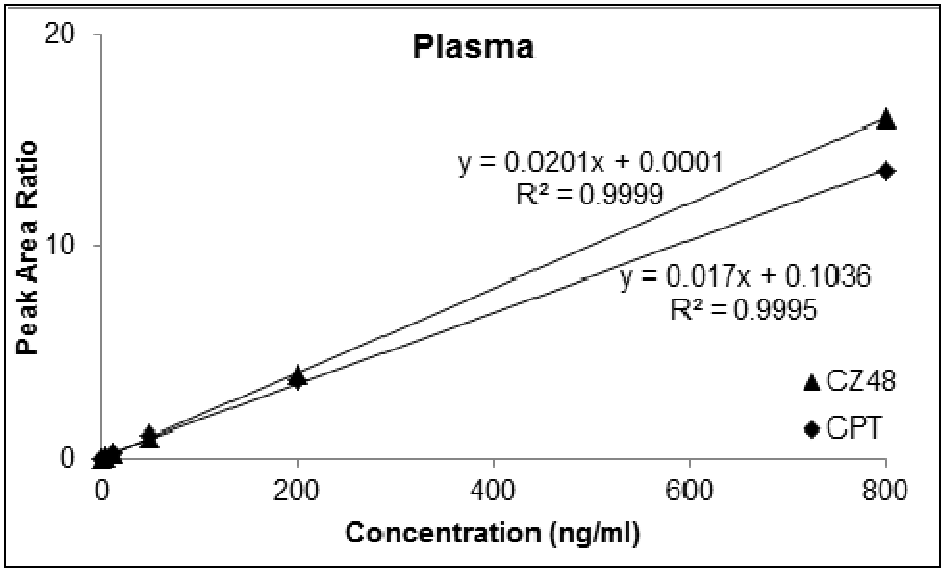

Figure 19 Calibration Curves of CZ48 and CPT in Rat Plasma Samples

Table 15 Linearity of HPLC Calibration Curves for CZ48 and CPT in Rat Plasma Samples

Parameters	CZ48	CPT
Conc. Range (ng/ml)	0.78 ~ 800	
Slope	0.0201	0.0170
Intercept	0.0001	0.1036
R^2 (correlation coefficient)	0.9999	0.9995
Within-day variability (%), n = 3	2.50	1.36
Between-day variability (%), n = 6	3.22	1.84
Extraction Recovery (%)	96	

For quantification of CZ48 and CPT in rat six organs, heart, liver, spleen, lung, kidney and brain, the analysis was also under the described conditions (Section 3.2.6.5). The HPLC chromatograms for each organ were shown, and no interference peak was found from individual six blank organs (Figure 20~ Figure 25). The calibration curves, each containing 6 concentration points, were constructed at the linearity range of 0.78 ~ 800 ng/ml with the correlation coefficients > 0.999 for all organs (Figure 26).

The assay was validated for each organ with the within-day variability (n = 3) of 1.01 ~ 5.62% and 1.30 ~ 5.76% for CZ48 and CPT, respectively, and the between-day variability (n = 6) of 2.32 ~ 6.61% and 1.85 ~ 5.92% for CZ48 and CPT, respectively (Table 16). The recoveries of CZ48 and CPT ranged from 83.64 to 98.97%. All of these recoveries were acceptable. The linear regression equations of peak area ratios (Y) versus concentrations were used to determine CZ48 and CPT concentrations in respective organ samples for the biodistribution studies in rats.

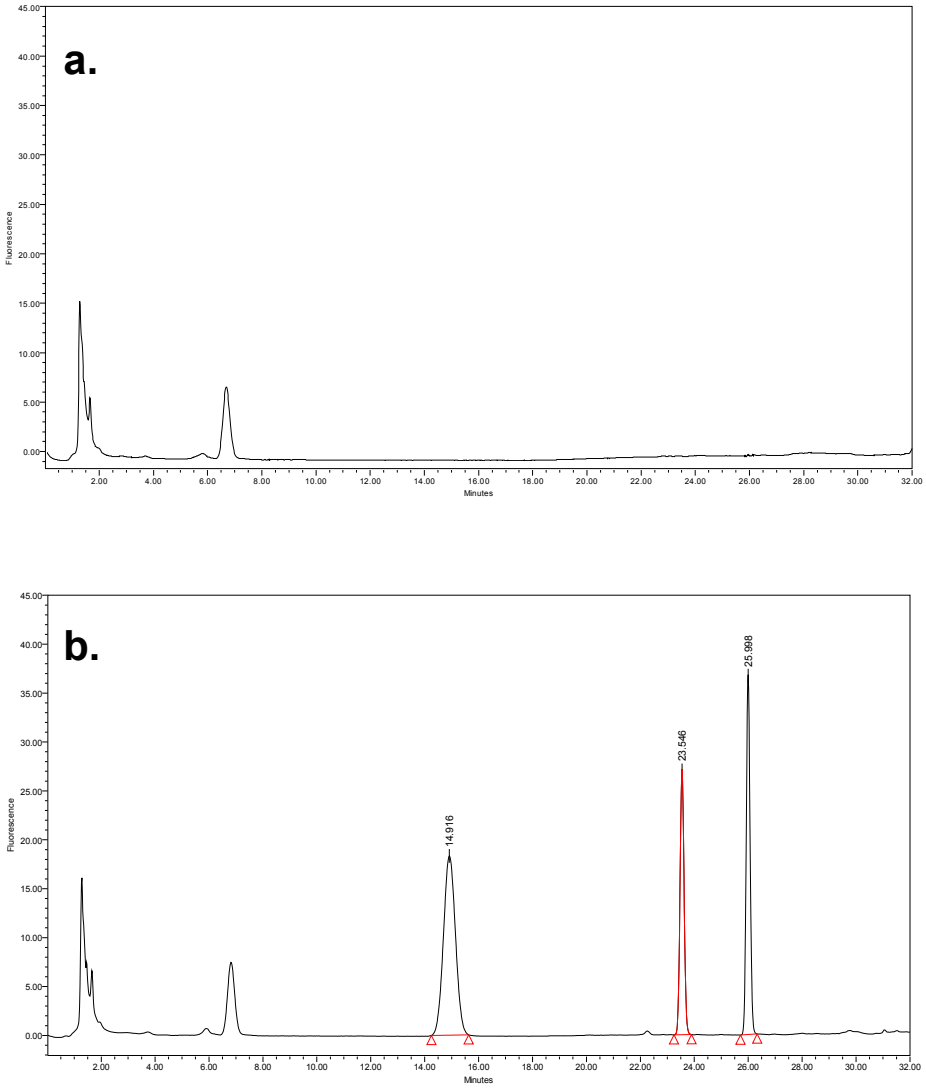

Figure 20 HPLC Chromatograms of CZ48 and CPT in Rat (a) Blank Heart Sample and (b) Spiked Heart Sample at 50 ng/ml (CZ44, 40 ng/ml)

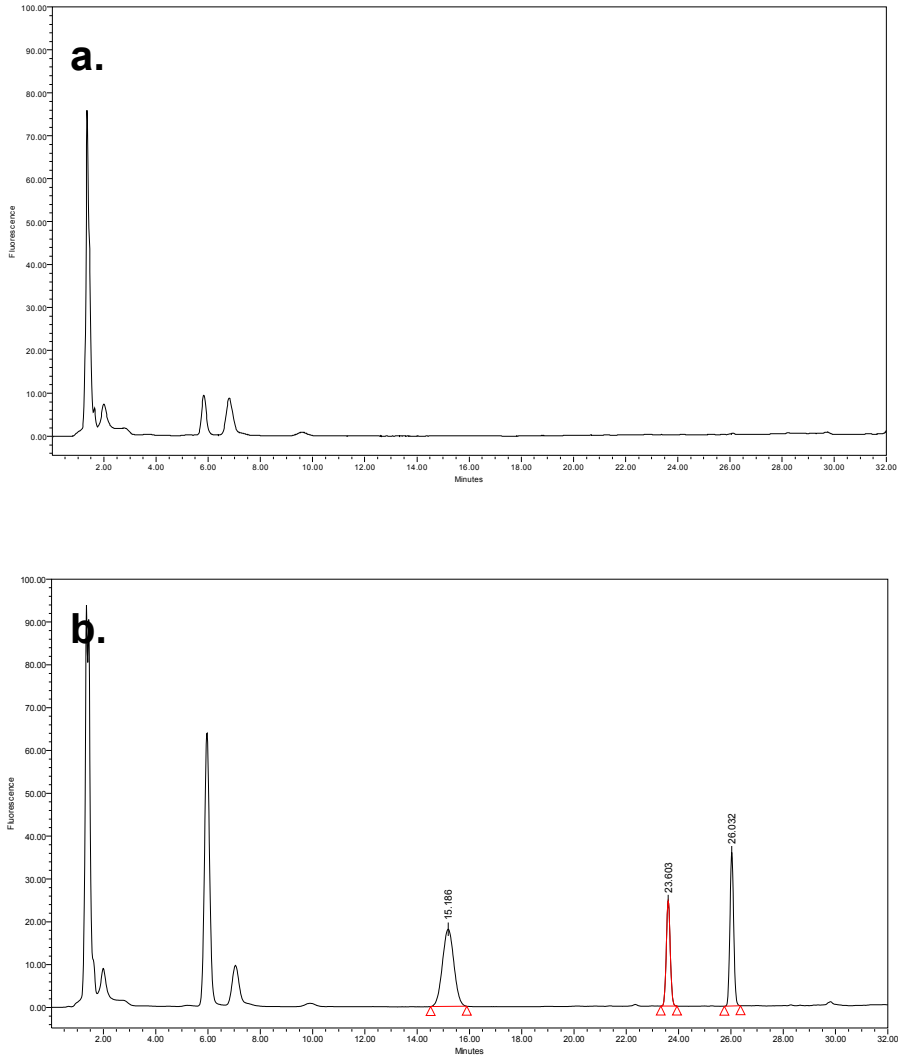

Figure 21 HPLC Chromatograms of CZ48 and CPT in Rat (a) Blank Liver Sample and (b) Spiked Liver Sample at 50 ng/ml (CZ44, 40 ng/ml)

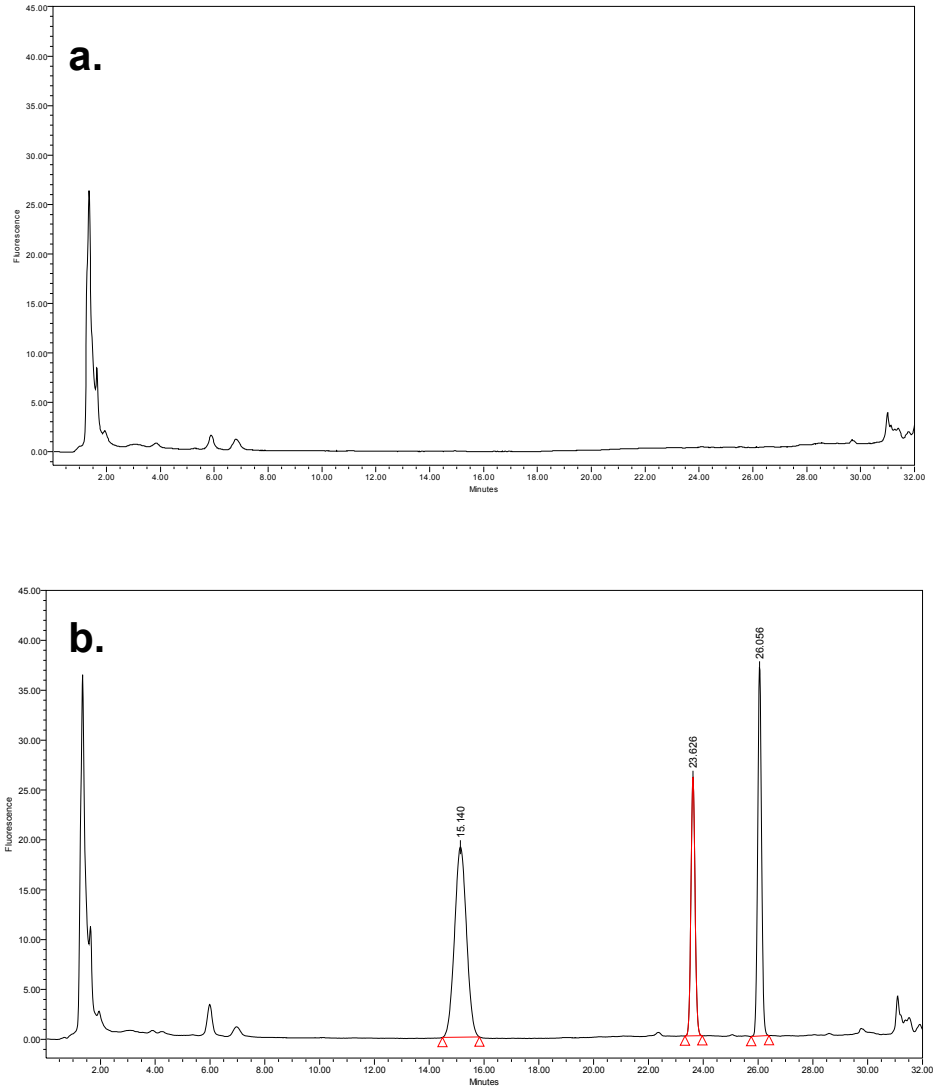

Figure 22 HPLC Chromatograms of CZ48 and CPT in Rat (a) Blank Spleen Sample and (b) Spiked Spleen Sample at 50 ng/ml (CZ44, 40 ng/ml)

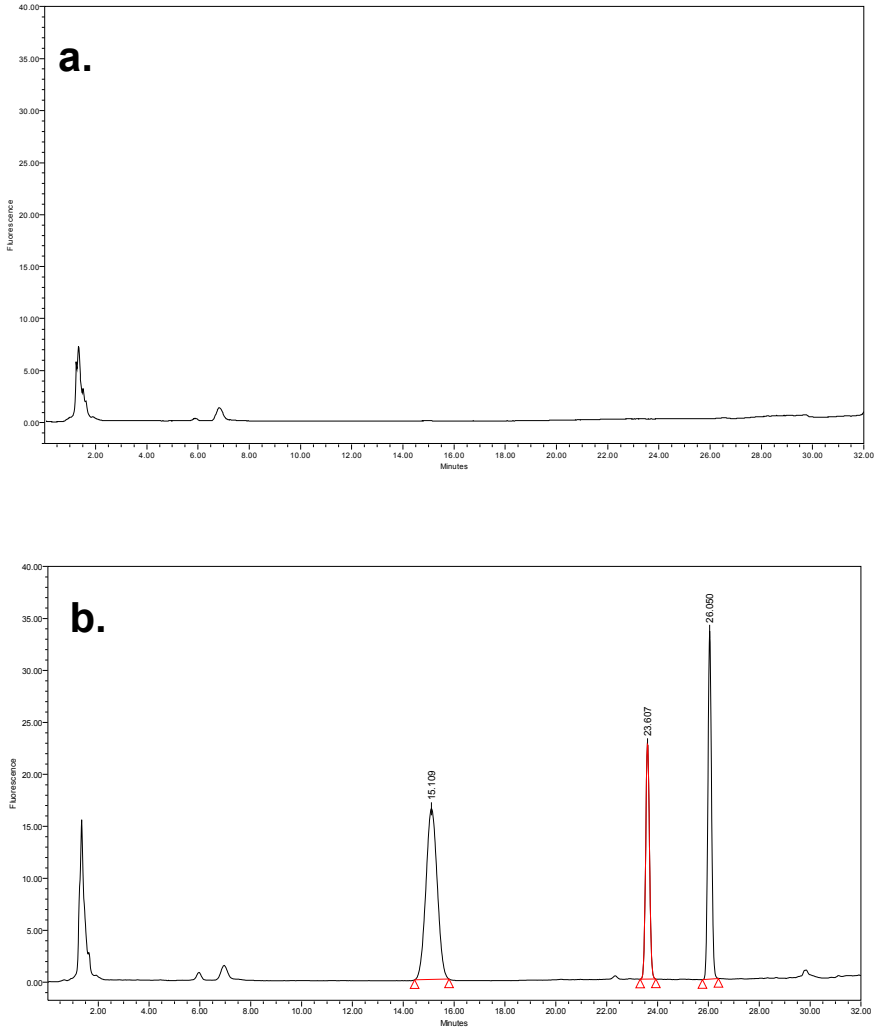

Figure 23 HPLC Chromatograms of CZ48 and CPT in Rat (a) Blank Lung Sample and (b) Spiked Lung Sample at 50 ng/ml (CZ44, 40 ng/ml)

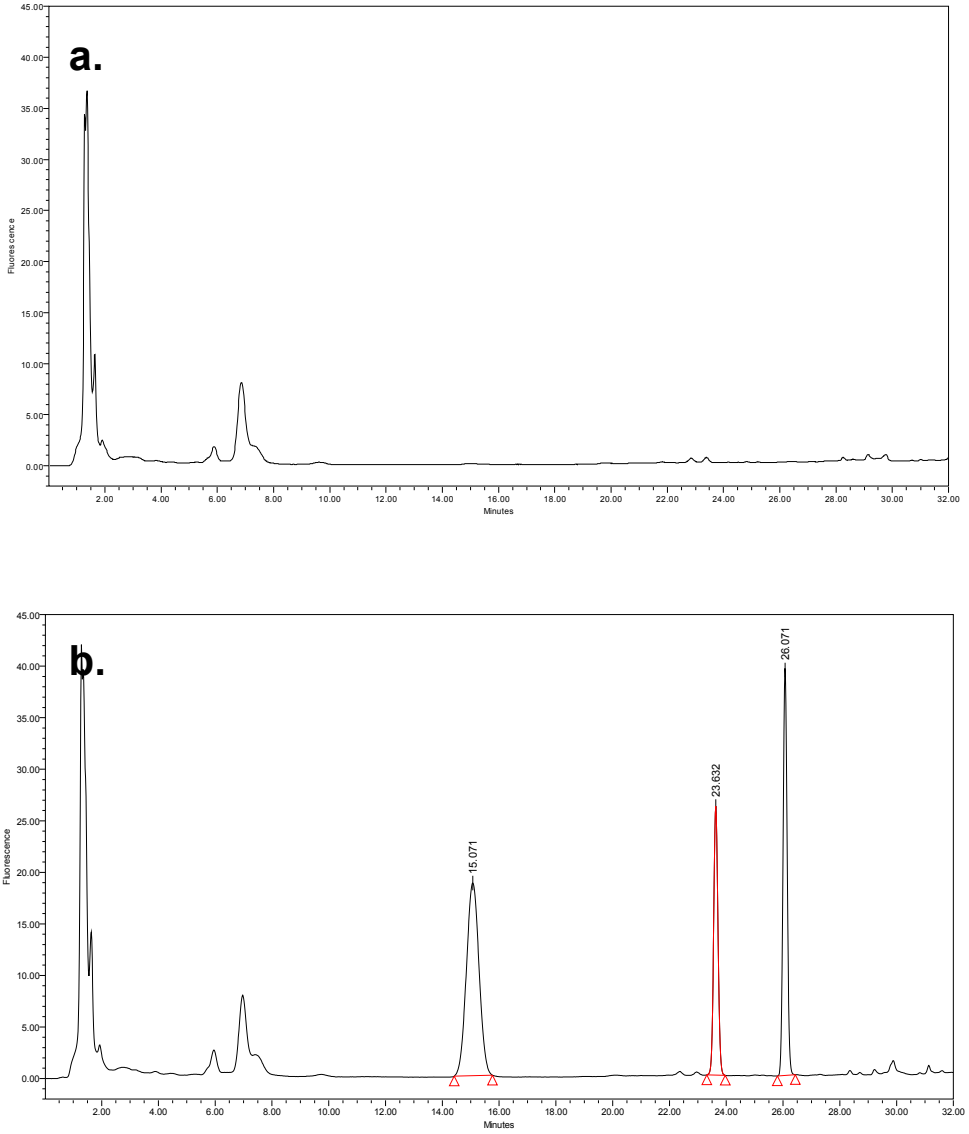

Figure 24 HPLC Chromatograms of CZ48 and CPT in Rat (a) Blank Kidney Sample and (b) Spiked Kidney Sample at 50 ng/ml (CZ44, 40 ng/ml)

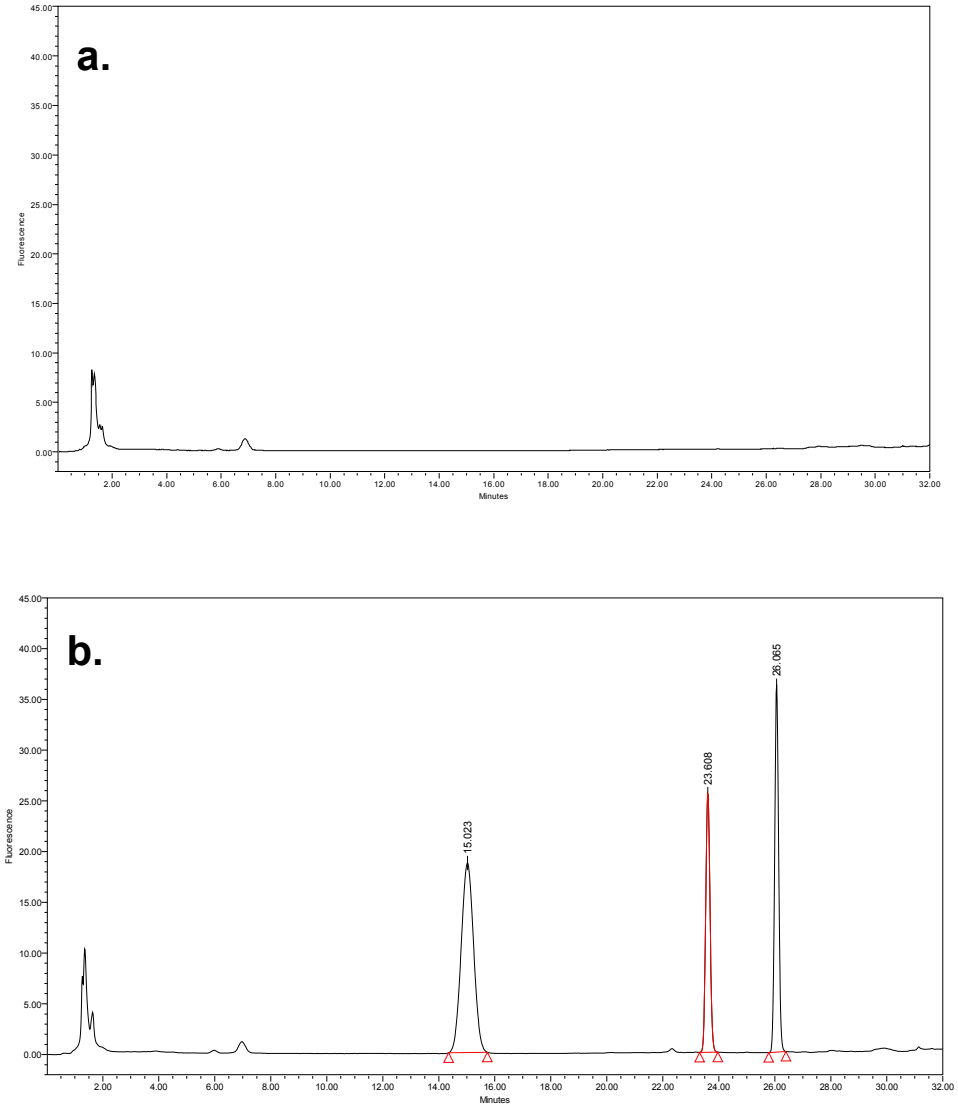

Figure 25 HPLC Chromatograms of CZ48 and CPT in Rat (a) Blank Brain Sample and (b) Spiked Brain Sample at 50 ng/ml (CZ44, 40 ng/ml)

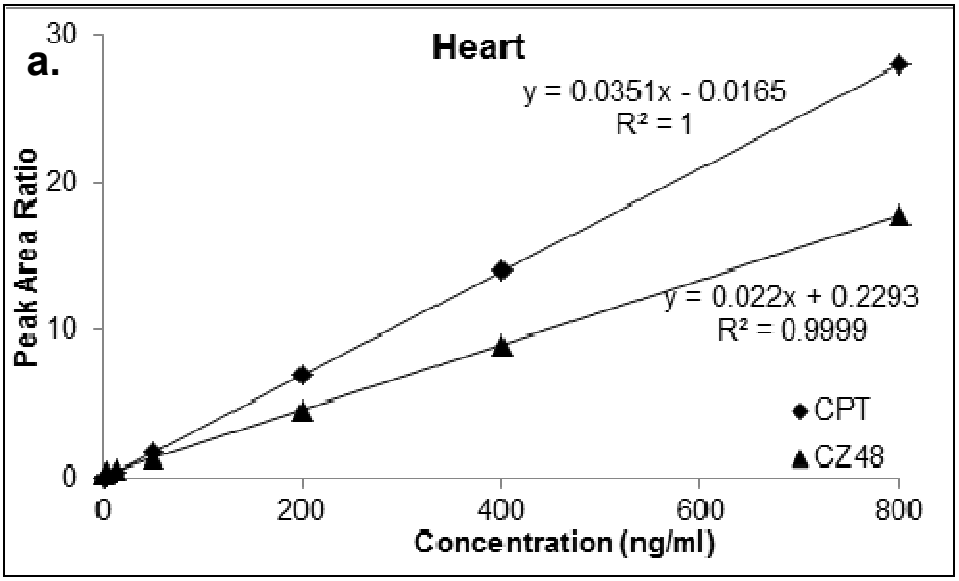

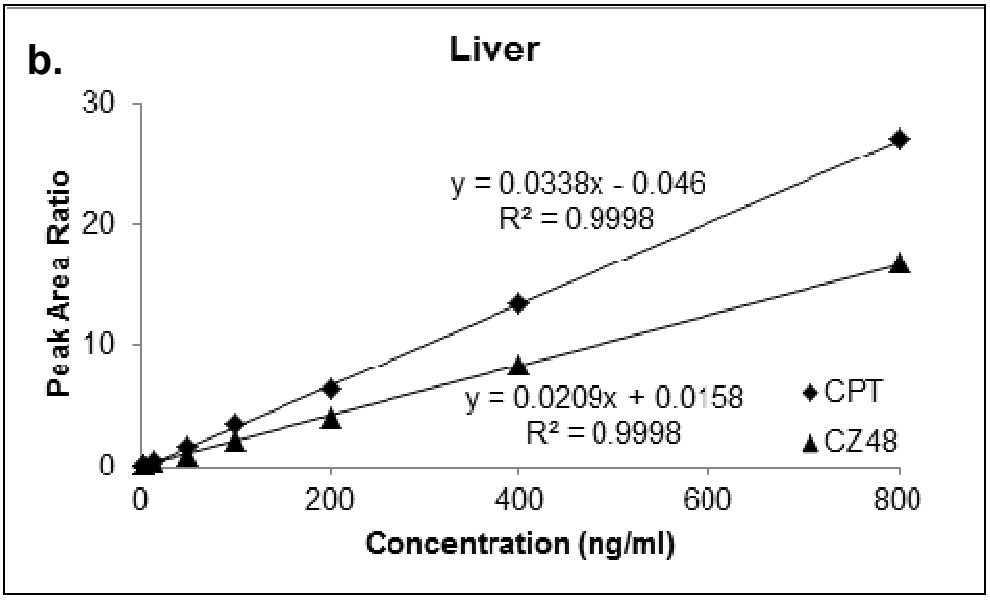

Figure 26 Calibration Curves of CZ48 and CPT in Rat (a) Heart, (b) Liver, (c) Spleen, (d) Lung, (e) Kidney, (f) Brain Samples

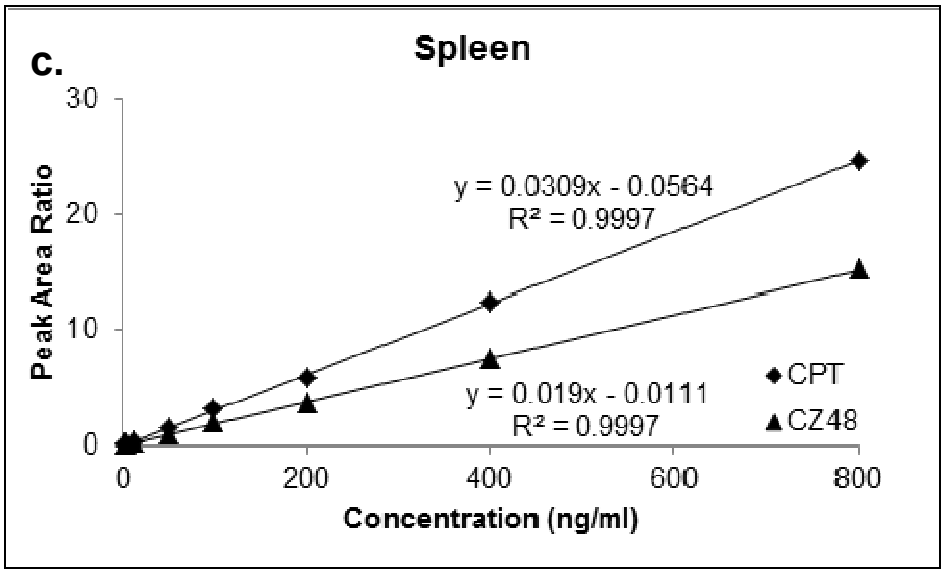

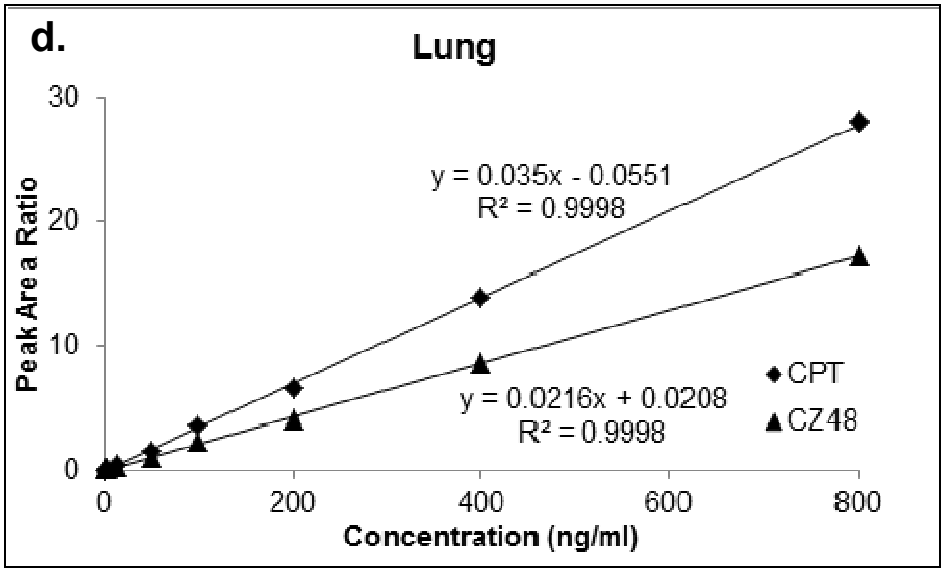

Figure 26 Calibration Curves of CZ48 and CPT in Rat (a) Heart, (b) Liver, (c) Spleen, (d) Lung, (e) Kidney, (f) Brain Samples (Cont's)

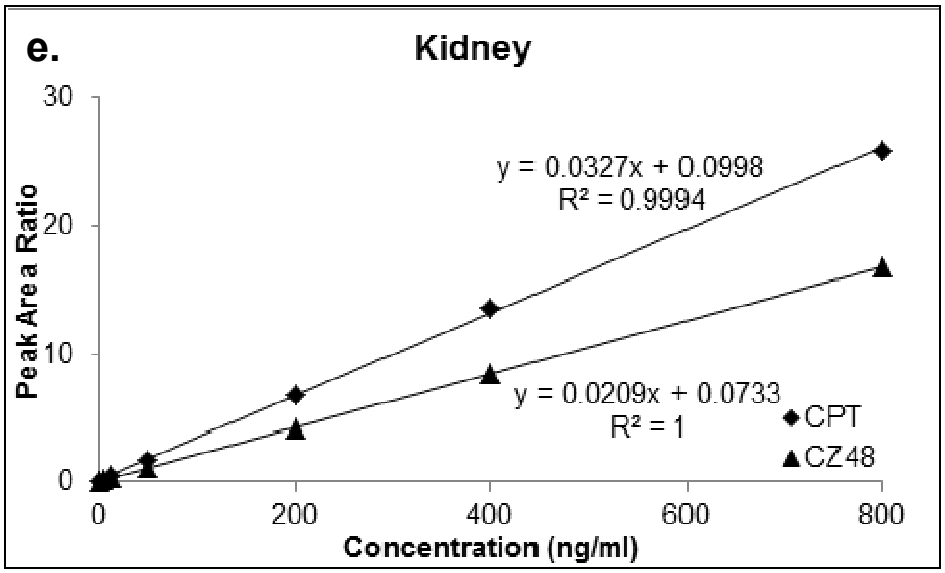

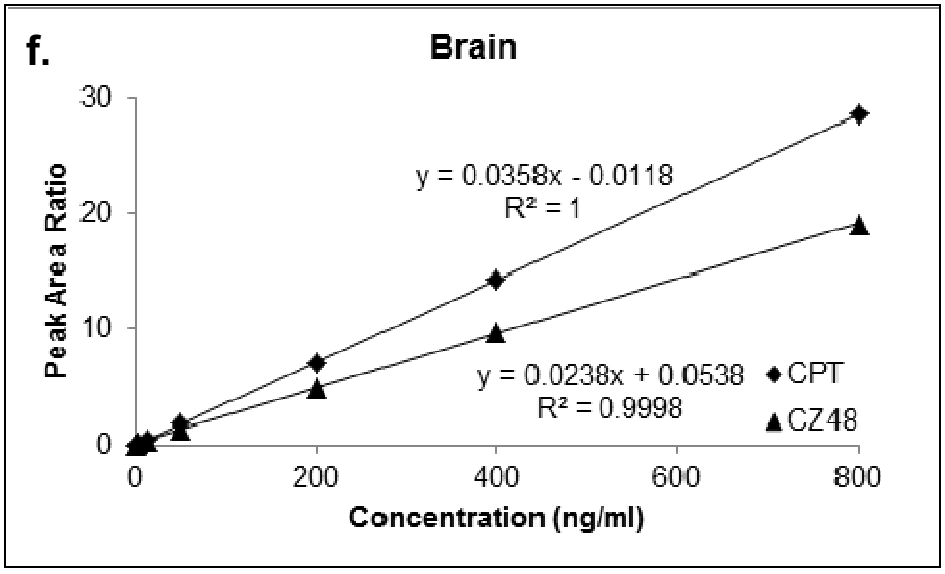

Figure 26 Calibration Curves of CZ48 and CPT in Rat (a) Heart, (b) Liver, (c) Spleen, (d) Lung, (e) Kidney, (f) Brain Samples (Cont's)

Table 16 Calibration Curve Parameters for CZ48 and CPT in Rat Organ Samples

Parameters	Heart		Liver		Spleen		Lung		Kidney		Brain	
	CZ48	CPT	CZ48	CPT	CZ48	CPT	CZ48	CPT	CZ48	CPT	CZ48	CPT
Conc. Range (ng/ml)	0.78 ~ 800											
Slope	0.0220	0.0350	0.0209	0.0338	0.019	0.0309	0.0216	0.035	0.0209	0.0327	0.0238	0.0358
Intercept	-0.0165	0.2293	-0.046	0.0158	-0.0564	-0.0111	-0.0551	0.0208	0.0733	0.0998	0.0538	-0.0118
R^2 (correlation coefficient)	1.0000	0.9999	0.9998	0.9998	0.9997	0.9997	0.9998	0.9998	0.9994	1.0000	0.9998	1.0000
Within-day variability (%), n = 3	1.58	1.30	1.01	2.25	2.34	2.83	5.62	5.76	2.55	3.17	3.79	3.01
Between-day variability (%), n = 6	2.66	1.85	2.32	4.11	3.49	3.74	6.61	5.92	4.30	3.96	4.05	3.88
Extraction Recovery (%)	96.86	93.62	97.56	90.56	98.97	95.07	90.18	83.64	98.91	95.28	91.21	94.68

4.2.2. Plasma Pharmacokinetics of CZ48 Cosolvent and Nanosuspensions (NS-S, and NS-L) in Rats

Plasma pharmacokinetics of CZ48 cosolvent and nanosuspensions (NS-S and NS-L) were studied in SD rats at a dose of 5 mg/kg, 25 mg/kg and 25mg/kg, respectively. The objective of the pharmacokinetic studies was to demonstrate any favorable pharmacokinetics of sustaining levels of CZ48 in plasma and consequently, those of the active moiety, CPT, which may offer potential therapeutic benefit from the nanosuspension formulations.

The formulations were given by i.v. injection and blood samples were collected for CZ48 and CPT quantifications by the validated HPLC assay. The mean concentration normalized by dose-time profiles of CZ48 and CPT were constructed (Figure 27). Compartmental modeling was used to desire the pharmacokinetic parameters of CZ48 and CPT for each rat (WinNonlin ver. 3.3). Then, each parameter was presented as mean value with the standard deviation, and statistical analysis was also performed (Table 17 & Table 18).

For all of these three formulations, the CZ48 plasma concentrations declined rapidly after the injection. After a rapid decline, CZ48 was slowly removed from the central compartment by nanosuspensions administration; however, CZ48 from cosolvent was undetectable 4 hours post dose. Similarly, the mean plasma concentrations of CPT converted from CZ48 nanosuspensions increased consistently to the peak concentrations and yielded sustained levels of CPT in the blood circulation for more than

24 h (NS-S) or 10 h (NS-L) compared with cosolvent of which the CPT was undetectable after 4 h (Figure 27). The plasma profiles of CPT were best described as 1-compartmental and 2-compartmental models from cosolvent and nanosuspensions, respectively.

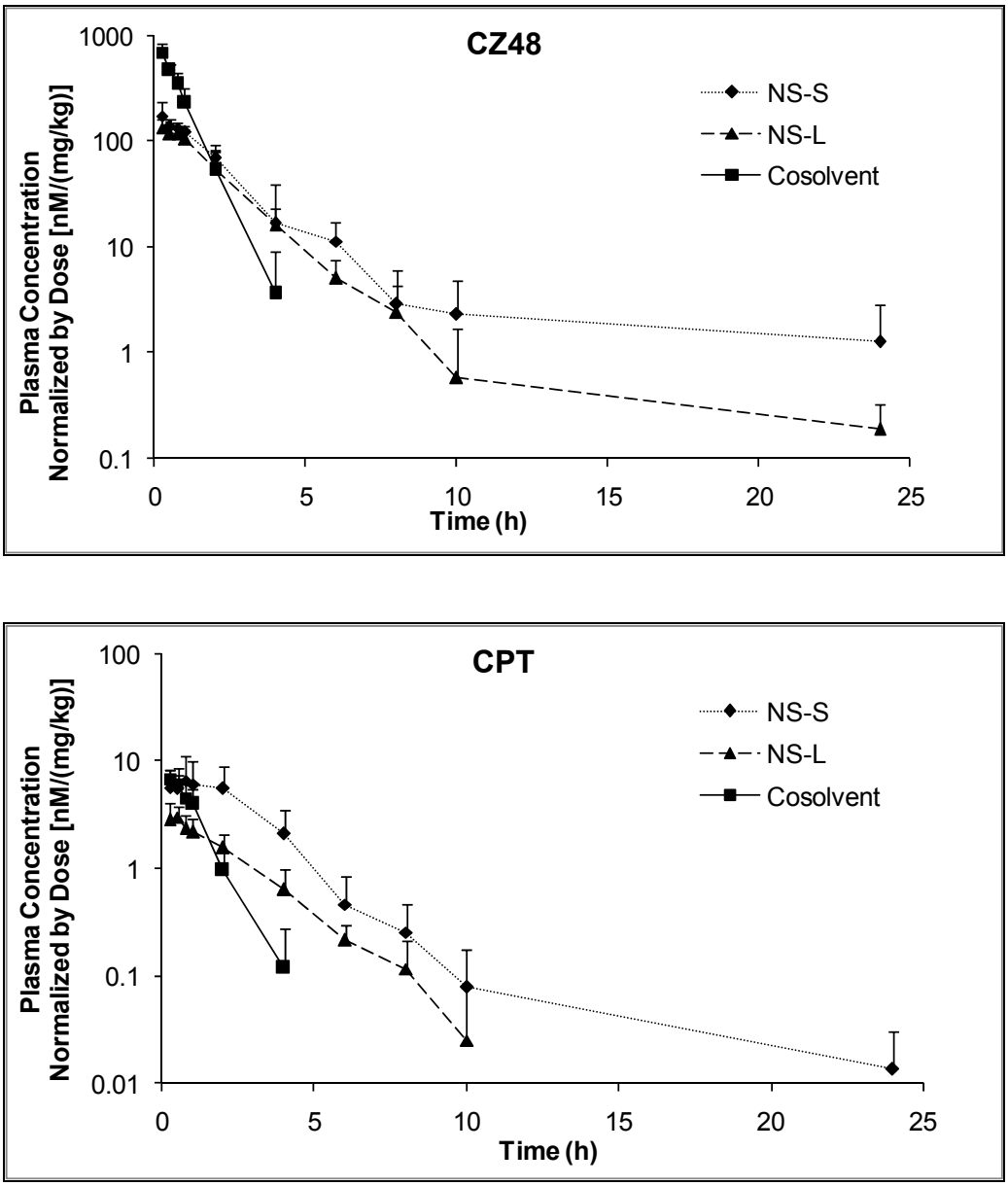

Figure 27 Mean Plasma Concentration Normalized by Dose verses Time Curves of CZ48 and CPT, after i.v. Administration of CZ48 Cosolvent (5 mg/kg), NS-200 nm (25 mg/kg) and NS-600 nm in SD rats (n = 6).

Table 17 Pharmacokinetic Parameters of CZ48 from Cosolvent, NS-S, and NS-L in SD Rat Plasma after i.v. Administration (n = 6).

Parameters	Unit	Cosolvent (5 mg/kg)	NS-S (25 mg/kg)	NS-L (25 mg/kg)
A	nM		65569.77 ± 19407.75	11484.35 ± 2046.37$^{\#}$
α	h^{-1}		51.49 ± 26.31	38.94 ± 7.35
B	nM		3774.39 ± 451.52	2986.89 ± 735.92$^{\#}$
β	h^{-1}		0.99 ± 0.35	1.00 ± 0.71
C	nM		236.06 ± 93.78	294.98 ± 142.51
γ	h^{-1}		0.02 ± 0.01	0.10 ± 0.04$^{\#}$
k_{10}	h^{-1}	1.44 ± 0.52	4.78 ± 2.30*	2.31 ± 1.21*$^{\#}$
k_{12}	h^{-1}		35.87 ± 26.31	26.64 ± 17.16
k_{21}	h^{-1}		3.86 ± 2.63	9.37 ± 4.23$^{\#}$
k_{13}	h^{-1}		7.93 ± 2.49	1.54 ± 0.32$^{\#}$
k_{31}	h^{-1}		0.07 ± 0.03	0.17 ± 0.05$^{\#}$
$t_{1/2\alpha}$	h		0.01 ± 0.00	0.02 ± 0.01$^{\#}$
$t_{1/2\beta}$	h		0.70 ± 0.24	0.70 ± 0.42
$t_{1/2\gamma}$	h	0.48 ± 0.13	27.74 ± 10.34*	7.27 ± 1.20*
C_0/Dose	nM/(mg/kg)	991.38 ± 316.52	738.21 ± 283.14	590.65 ± 110.98*
V_1	L/kg	2.49 ± 1.06	0.89 ± 0.15*	4.18 ± 1.50*$^{\#}$
CL_1	L/kg*h	3.59 ± 1.02	4.25 ± 1.19*	9.67 ± 1.86*$^{\#}$
V_2	L/kg		8.26 ± 2.68	11.89 ± 3.20$^{\#}$
CL_2	L/kg*h		31.85 ± 10.85	111.46 ± 39.61$^{\#}$
V_3	L/kg		102.35 ± 31.66	37.70 ± 16.42$^{\#}$
CL_3	L/kg*h		7.04 ± 1.45	6.44 ± 1.61
AUC_{0-t}/Dose	nM*h/(mg/kg)	686.12 ± 135.15	374.51 ± 55.49*	242.89 ± 46.44*$^{\#}$
$AUC_{0-\infty}$/Dose	nM*h/(mg/kg)	688.18 ± 146.21	581.94 ± 71.54	255.47 ± 44.71*$^{\#}$
F			0.85	0.37
AUMC	$nM*h^2$	2388.55 ± 451.24	381937.68 ± 23218.42*	35500.06 ± 8042.37*$^{\#}$
MRT	h	0.69 ± 0.35	26.25 ± 10.34*	5.56 ± 0.80*$^{\#}$
V_{ss}	L/kg	2.49 ± 1.64	111.49 ± 32.00*	53.77 ± 21.61*$^{\#}$

Note: * $p < 0.05$, compared to that of cosolvent; $^{\#}$ $p < 0.05$, compare to that of NS-S

Table 18 Pharmacokinetic Parameters of CPT from Cosolvent, NS-S, and NS-L in SD Rat Plasma after i.v. Administration (n = 6).

Parameters	Unit	Cosolvent (5 mg/kg)	NS-S (25 mg/kg)	NS-L (25 mg/kg)
A	nM	55.97 ± 14.31	534.44 ± 71.54*	301.76 ± 88.42*#
α	h^{-1}		0.55 ± 0.13	0.58 ± 0.20
B	nM		47.29 ± 17.46	89.40 ± 28.65
β	h^{-1}		0.11 ± 0.03	0.58 ± 0.17#
k_a	h^{-1}	7.76 ± 2.86	3.36 ± 0.85*	3.22 ± 0.61*
k_{10}	h^{-1}	1.13 ± 0.32	0.40 ± 0.07*	0.58 ± 0.20*
k_{12}	h^{-1}		0.11 ± 0.03	
k_{21}	h^{-1}		0.15 ± 0.06	
$t_{1/2\alpha}$	h		1.27 ± 0.39	
$t_{1/2\beta}$	h	0.62 ± 0.16	6.34 ± 1.45*	1.19 ± 0.35*#
$t_{1/2ka}$	h	0.09 ± 0.05	0.21 ± 0.17	0.22 ± 0.10
V_1	L/kg	299.94 ± 55.49	145.44 ± 83.43*	290.44 ± 59.44#
CL_1	L/kg*h	337.71 ± 73.10	57.88 ± 21.16*	169.61 ± 35.22*#
V_2	L/kg		103.78 ± 31.65	
CL_2	L/kg*h		15.53 ± 2.06	
T_{max}	h	0.29 ± 0.06	0.67 ± 0.10*	0.65 ± 0.15*
C_{max}/Dose	nM/(mg/kg)	6.90 ± 1.45	14.14 ± 3.82*	6.77 ± 1.68
AUC_{0-t}/Dose	nM*h/(mg/kg)	8.39 ± 2.86	48.33 ± 17.46*	16.73 ± 4.25*#
$AUC_{0-\infty}$/Dose	nM*h/(mg/kg)	8.50 ± 3.54	49.59 ± 17.54*	16.92 ± 2.06*#
F			5.83	1.99
AUMC	$nM*h^2$	43.22 ± 7.15	5707.35 ± 1502.04*	855.76 ± 202.98*#
MRT	h	1.02 ± 0.32	4.60 ± 0.72*	2.02 ± 0.55*#
Vss	L/kg	299.94 ± 55.49	249.22 ± 96.52	290.44 ± 59.44

Note: * $p < 0.05$, compared to that of cosolvent; # $p < 0.05$, compare to that of NS-S

4.2.2.1 Comparative Pharmacokinetics of CZ48 in Rats Following i.v. Administration of Cosolvent and Nanosuspensions (NS-S, and NS-L) of CZ48

The pharmacokinetic performances of CZ48 from NS-S and NS-L were significantly different from that of cosolvent with half-life of 60 and 15 fold longer (27.74 ± 10.34 h and 7.27 ± 1.20 h vs. 0.48 ± 0.13 h). The $AUC_{0-\infty}$ normalized by dose of CZ48 NS-S and NS-L were 85% and 37% of that of CZ48 cosolvent, respectively (581.94 ± 71.54 nM*h/(mg/kg), 255.47 ± 44.71 nM*h/(mg/kg) vs. 688.18 ± 146.21 nM*h/(mg/kg)). CZ48 from nanosuspensions were widely distributed to other tissues besides plasma, and had significantly larger V_{ss} compared to that from cosolvent (111.49 ± 32.00 L/kg and 53.77 ± 21.61 L/kg for NS-S and NS-L, respectively vs. 2.49 ± 1.64 L/kg for cosolvent).

4.2.2.2 Comparative Pharmacokinetics of CPT Following i.v. Administration of Cosolvent and Nanosuspensions (NS-S, and NS-L) of CZ48 in Rats

The dose-normalized $AUC_{0-\infty}$ values for NS-S and NS-L were significantly higher than that of cosolvent (48.33 ± 17.54 nM*h/(mg/kg), 16.92 ± 2.06 nM*h/(mg/kg) vs. 8.50 ± 3.54 nM*h/(mg/kg)). Nanosuspensions not only yielded larger systemic exposures of CPT, but also significantly longer half-lives compared to that from cosolvent, ~10.23 times longer for NS-S (6.34 ± 1.45 vs. 0.62 ± 0.16 h), and ~1.92 times longer for NS-L

(1.19 ± 0.35 vs. 0.62 ± 0.16 h) at $p < 0.05$. The V_{ss} of CPT were comparable among groups of cosolvent, NS-S and NS-L.

4.2.3. Organ Distribution of CZ48 and Metabolite, CPT, from Cosolvent and Nanosuspensions (NS-S, and NS-L) in Rats (n=4)

The biodistribution study in rats was comparatively evaluated for the CZ48 cosolvent, NS-S and NS-L. Different tissue distribution patterns of CZ48 and CPT from cosolvent, NS-S and NS-L were observed (Figure 28 ~ Figure 30) which were anticipated based on their plasma pharmacokinetic profiles. The mean organ parameters were derived from the mean concentration-time profiles for each formulation by WinNonlin (Table 19 ~ Table 21).

4.2.3.1 Organ Distributions of CZ48 and CPT from Cosolvent in Rats

CZ48 from cosolvent was cleared within 8 h in most of the organs with half-lives less than 1 hour (Table 19), except in lung and heart which can be detected more than 24 h (Figure 28). The observation of high substantial distribution of CZ48 in lung from cosolvent was not anticipated. This might be due to the CZ48 precipitation from the cosolvent. Similarly, the CPT concentrations in all the major organs and in plasma declined rapidly after reaching the peak concentrations (Figure 28).

CZ48 in cosolvent yielded the highest exposure in lung with and $AUC_{0-\infty}$/Dose of 25856.53 (ng/g*h)/(mg/kg), followed by liver of 721.49 (ng/g*h)/(mg/kg), kidney of 653.57

(ng/g*h)/(mg/kg), and spleen of 603.99 (ng/g*h)/(mg/kg) (Table 19). The elimination half-lives were all about 1 hour for heart, liver, spleen, lung, kidney, and brain (0.70 h, 1.14 h, 0.81 h, 1.05 h, 0.86 h, and 0.59 h, respectively). But only a very small portion of CZ48 in lung was transformed to CPT with a small $AUC_{0-\infty}$/Dose of 35.79 (ng/g*h)/(mg/kg) and low C_{max}/Dose 19.09 (ng/g)/(mg/kg) (Table 19).

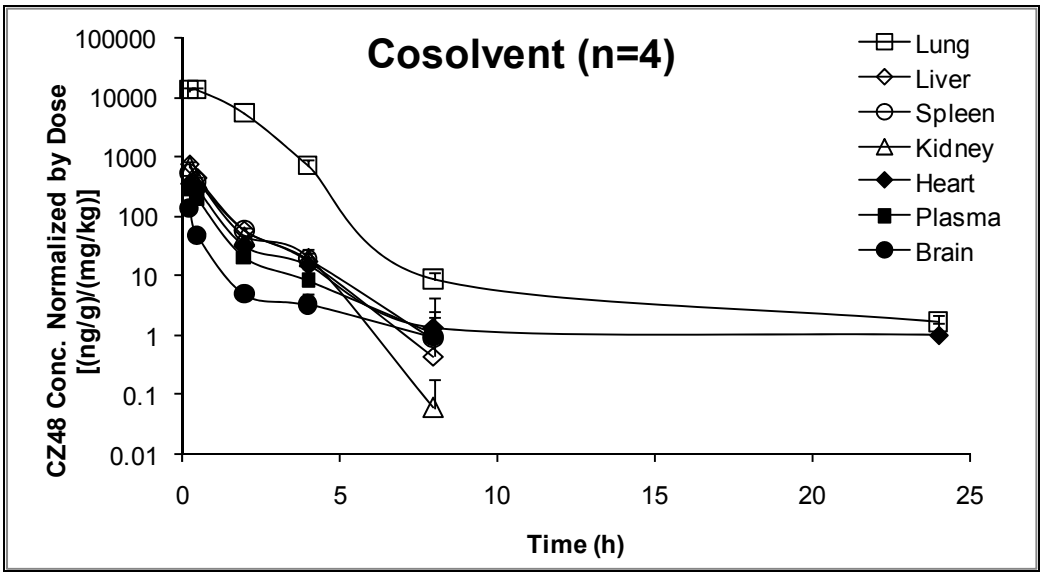

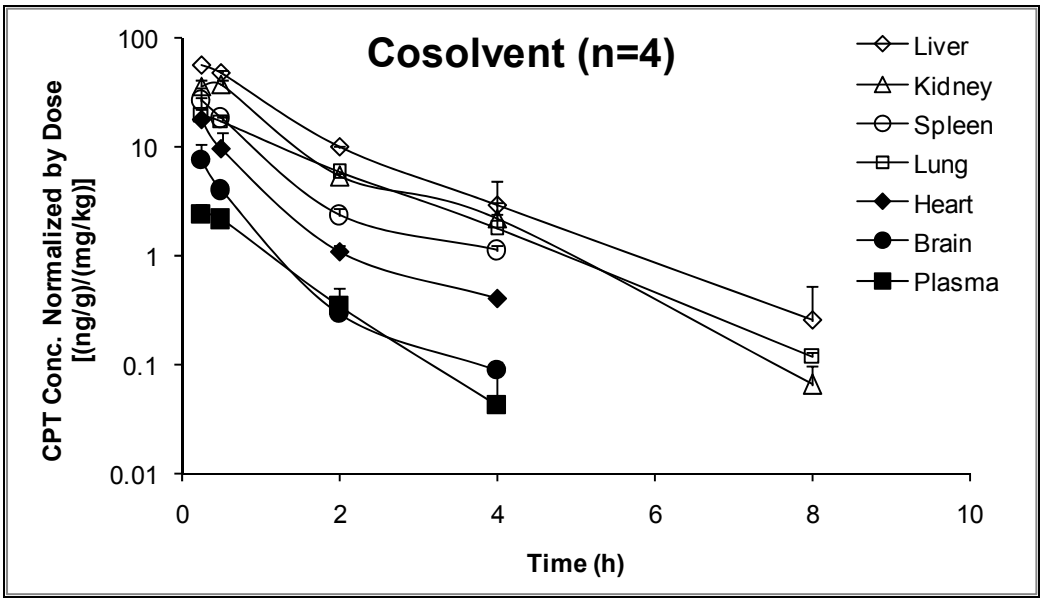

Figure 28 Organ Distribution Profiles of CZ48 and CPT from Cosolvent in Rats (n=4)

Note: The concentration unit for CZ48 and CPT in plasma is (ng/ml)/(mg/kg).

Table 19 CZ48 and CPT Organ Distribution Parameters from Cosolvent in Rats after i.v. Administration (n=4)

Parameters		Unit	Cosolvent						
			Heart	Liver	Spleen	Lung	Kidney	Brain	Plasma
CZ48	$AUC_{0-\infty}$/Dose	(ng/g*h)/(mg/kg)	447.95	721.49	603.99	25856.53	653.57	97.29	278.44
	C_{max}/Dose	(ng/g)/(mg/kg)	339.92	736.54	506.44	12873.34	658.76	133.29	268.94
	$t_{1/2}$	h	3.12	0.78	0.99	1.90	0.60	0.42	0.48
CPT	$AUC_{0-\infty}$/Dose	(ng/g*h)/(mg/kg)	15.56	82.74	29.02	35.79	57.34	6.06	2.96
	C_{max}/Dose	(ng/g)/(mg/kg)	17.96	56.61	26.23	19.09	36.98	7.61	2.39
	$t_{1/2}$	h	0.70	1.14	0.81	1.05	0.86	0.59	0.63

4.2.3.2 Organ Distributions of CZ48 and CPT from NS-S in Rats

For all the organs, the CZ48 concentrations declined rapidly after CZ48 NS-S injection, and then followed by a slow elimination with long half-lives of 11.18 h for heart, 7.88 h for liver, 1.76 h for spleen, 5.37 h for lung, 16.50 h for kidney, 5.13 h for brain (Table 19). The CZ48 could still be detected 24 h post injection in all the organs, except in brain (Figure 28). The RES rich organs obtained more CZ48 particles with the highest $AUC_{0-\infty}$/Dose of 38697.93 (ng/g*h)/(mg/kg) in spleen, followed by 26501.08 (ng/g*h)/(mg/kg) in liver, and 3299.46 (ng/g*h)/(mg/kg) in lung (Table 19).

Similar to CZ48, CPT exposures were high in RES rich organs, and yielded the highest exposure in liver with the $AUC_{0-\infty}$/Dose of 58.26 (ng/g*h)/(mg/kg), followed by spleen of 35.04 (ng/g*h)/(mg/kg), and lung of 15.60 (ng/g*h)/(mg/kg). Except brain heart and kidney, CPT can be retained more than 24 hours in all the other organs (Figure 28).

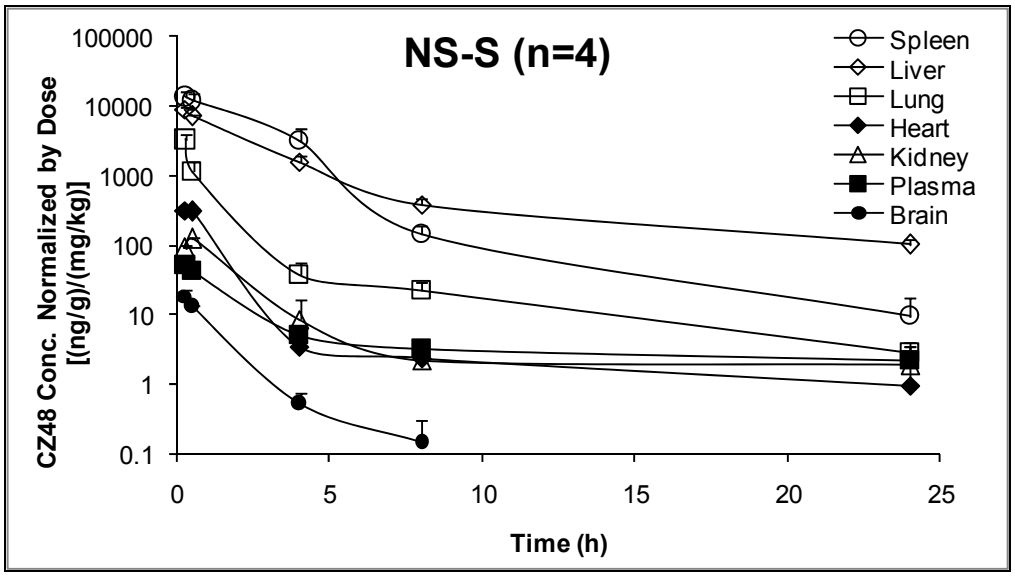

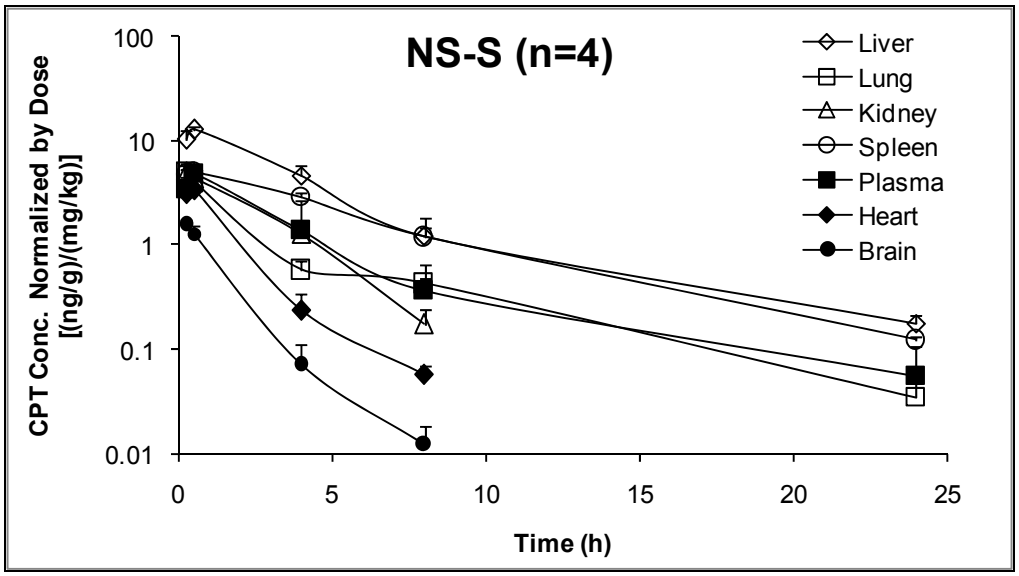

Figure 29 Organ Distribution Profiles of CZ48 and CPT from NS-S in Rats (n=4)

Note: The concentration unit for CZ48 and CPT in plasma is (ng/ml)/(mg/kg).

Table 20 CZ48 and CPT Organ Distribution Parameters from NS-S in Rats after i.v. Administration (n=4)

Parameters		Unit	NS-S						
			Heart	Liver	Spleen	Lung	Kidney	Brain	Plasma
CZ48	$AUC_{0-\infty}$/Dose	(ng/g*h)/(mg/kg)	701.60	26501.08	38697.93	3299.46	330.37	30.78	235.45
	C_{max}/Dose	(ng/g)/(mg/kg)	310.74	8867.73	13515.22	3242.30	120.50	18.31	50.70
	$t_{1/2}$	h	11.18	7.88	1.76	5.37	16.50	5.13	13.33
CPT	$AUC_{0-\infty}$/Dose	(ng/g*h)/(mg/kg)	8.15	58.26	35.04	15.60	15.81	3.08	17.28
	C_{max}/Dose	(ng/g)/(mg/kg)	3.36	12.65	5.05	4.97	4.88	1.55	4.77
	$t_{1/2}$	h	1.28	5.59	4.30	4.10	2.48	1.08	3.77

4.2.3.3 Organ Distributions of CZ48 and CPT from NS-L in Rats

Similarly, the CZ48 could still be detected 24 h post injection in all the organs with long half-lives of 5.21 h for heart, 8.25 h for liver, 2.88 h for spleen, 7.97 h for lung, 2.57 h for kidney, 9.49 h for brain. The RES rich organs obtained more CZ48 particles with the highest $AUC_{0-\infty}$/Dose of 50336.22 (ng/g*h)/(mg/kg) in liver, followed by 35172.84 (ng/g*h)/(mg/kg) in spleen, and 8221.77 (ng/g*h)/(mg/kg) in lung (Table 19).

Except heart, CPT could be retained more than 24 hours after CZ48 NS-L injection in all the other organs. In liver, CPT showed the highest C_{max}/Dose of 23.86 (ng/g)/(mg/kg), and $AUC_{0-\infty}$/Dose of 124.59 (ng/g*h)/(mg/kg) (Table 19).

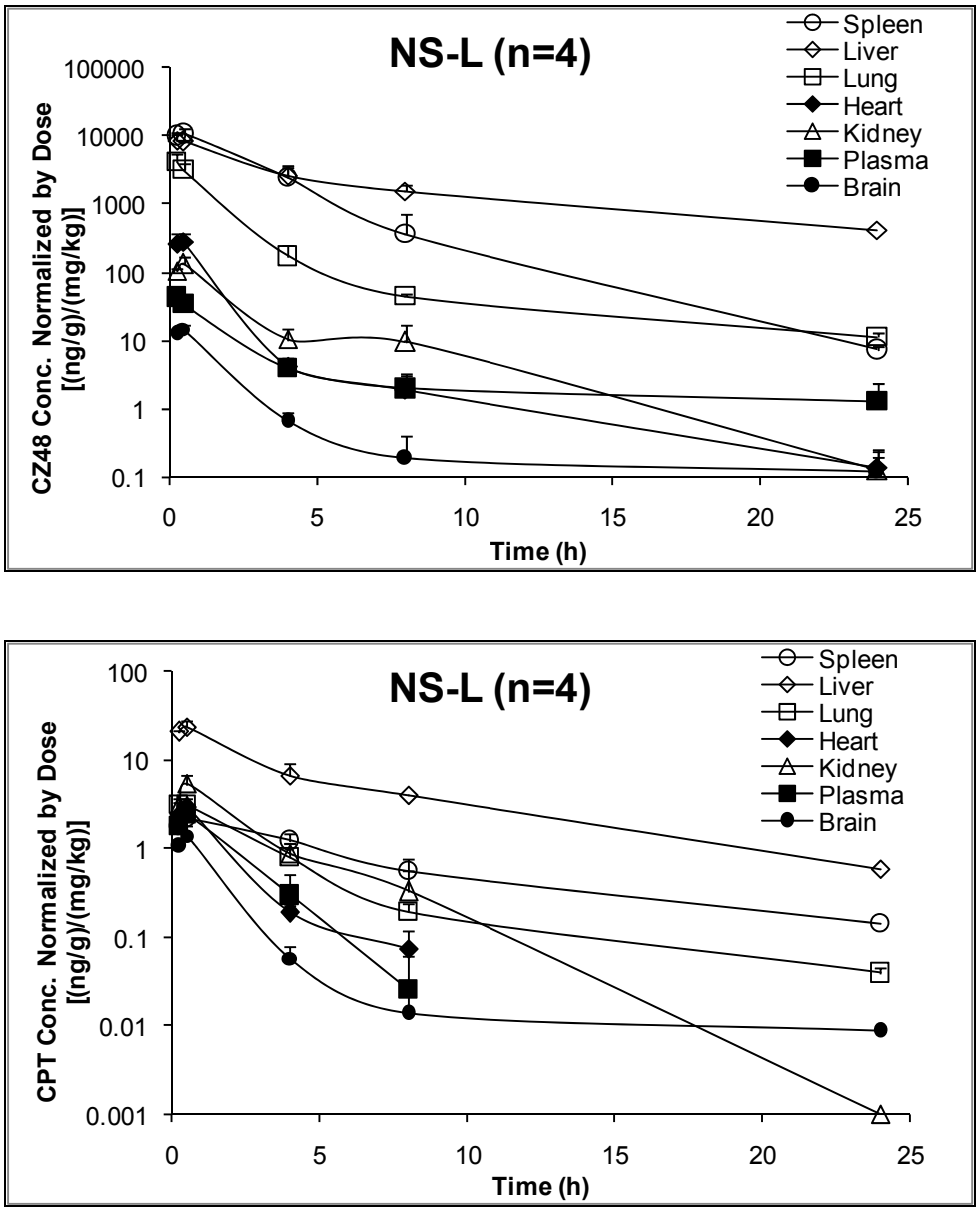

Figure 30 Organ Distribution Profiles of CZ48 and CPT from NS-L in Rats (n=4)

Note: The concentration unit for CZ48 and CPT in plasma is (ng/ml)/(mg/kg).

Table 21 CZ48 and CPT Organ Distribution Parameters from NS-L in Rats after i.v. Administration (n=4)

Parameters		Unit	NS-L						
			Heart	Liver	Spleen	Lung	Kidney	Brain	Plasma
CZ48	$AUC_{0-\infty}$/Dose	(ng/g*h)/(mg/kg)	619.18	50336.22	35172.84	8221.77	400.85	36.49	103.36
	C_{max}/Dose	(ng/g)/(mg/kg)	276.00	8532.57	10519.72	4120.52	128.89	14.62	42.36
	$t_{1/2}$	h	5.21	8.25	2.88	7.97	2.57	9.49	3.96
CPT	$AUC_{0-\infty}$/Dose	(ng/g*h)/(mg/kg)	7.00	124.59	17.05	12.13	15.69	3.34	6.84
	C_{max}/Dose	(ng/g)/(mg/kg)	2.87	23.86	2.15	3.12	5.35	1.39	2.44
	$t_{1/2}$	h	1.44	5.63	7.00	5.11	1.65	4.16	1.95

4.2.3.4 Comparative Organ Distributions of CZ48 and CPT Following i.v. Administration of Cosolvent and Nanosuspensions (NS-S, and NS-L) of CZ48 in Rats

Based on the areas under the curve normalized by the dose, biodistribution patterns of CZ48 nanosuspensions were distinct from those from cosolvent, but followed a similar trend between the NS-S and NS-L, with significantly high CZ48 exposures of 3299.46 ~ 50336.22 (ng/g*h)/(mg/kg) in liver, spleen and lung, due to RES uptake (Table 22). The exposure ranking of CZ48 after nanosuspensions administration was Spleen, Liver >> Lung >> Heart >> Kidney > Plasma > Brain. CZ48 from cosolvent was relatively evenly distributed among organs (difference is within one log scale), except in the lung. One possibility of the exception is potential precipitation of CZ48 in the lung and subsequent entrapment of the precipitate following tail vein injection. However, the change of nanosuspension particle sizes within 200 nm to 600 nm range does not have significant effect on the distribution patterns of CZ48. Similar exposure of CPT from all three formulations were observed with the exposure ranking of Liver > Spleen, Kidney, Lung > Heart, Brain.

CZ48 from nanosuspensions were eliminated much slowly from all the organs and plasma, with longer elimination half-lives of 1.76 h ~ 16.05 h, compared to those from cosolvent of 0.42 h ~ 3.12 h, with 2 to 25 times increase (Table 23). More importantly, both nanosuspensions provided 2 ~ 9 times prolonged exposures of active CPT in all 6 major organs (heart, liver, spleen, lung, kidney, and brain) and in plasma, compared to

those from cosolvent (Table 23). However, the change of nanosuspension particle sizes within 200 nm to 600 nm range does not have significant effects on the half-lives of CZ48 and CPT.

4.2.3.5 Comparative Organ/Plasma Partition Coefficient of CZ48 and CPT Following i.v. Administration of Cosolvent and Nanosuspensions (NS-S, and NS-L) of CZ48 in Rats

The organ/plasma partition coefficient (Kp) of CZ48 and CPT for the heart, liver, spleen, lung, kidney and brain were derived experimentally from the Organ AUC/Plasma AUC ratios toward the end of the study (Figure 31 ~ Figure 33). The Kp values of CZ48 in organs from nanosuspensions were several times to hundred times higher than those from cosolvent, except in kidney and brain, which may indicate that the nanoparticles were easily trapped by heart, liver, spleen, lung. On the contrary, the partition coefficients (Kp) of CPT from nanosuspensions were significantly lower in all organs, except in spleen. The uptake of CZ48 was in nanosuspension form, while only dissolved CZ48 could be converted to CPT and provided the reservoir effect in the organs.

Table 22 Exposure (AUC_{0-t}/Dose) of CZ48 and CPT from Cosolvent, NS-S and NS-L in Different Organs

Organs	$AUC_{0-\infty}$/Dose [(ng/g)/(mg/g)]					
	CZ48			**CPT**		
	Cosolvent	NS-S	NS-L	Cosolvent	NS-S	NS-L
Heart	447.95	701.60	619.18	15.56	8.15	7.00
Liver	721.49	26501.08	50336.22	82.74	58.26	124.59
Spleen	603.99	38697.93	35172.84	29.02	35.04	17.05
Lung	25856.53	3299.46	8221.77	35.79	15.60	12.13
Kidney	653.57	330.37	400.85	57.34	15.81	15.69
Brain	97.29	30.78	36.49	6.06	3.08	3.34
Plasma	278.44	235.45	103.36	2.96	17.28	6.84

Table 23 Half-lives of CZ48 and CPT from Cosolvent, NS-S and NS-L in Different Organs

Organs	$t_{1/2}$ (h)					
	CZ48			CPT		
	Cosolvent	NS-S	NS-L	Cosolvent	NS-S	NS-L
Heart	3.12	11.18	5.21	0.70	1.28	1.44
Liver	0.78	7.88	8.25	1.14	5.59	5.63
Spleen	0.99	1.76	2.88	0.81	4.30	7.00
Lung	1.90	5.37	7.97	1.05	4.10	5.11
Kidney	0.60	16.05	2.57	0.86	2.48	1.65
Brain	0.42	5.13	9.49	0.59	1.08	4.16
Plasma	0.48	13.33	3.96	0.63	3.77	1.95

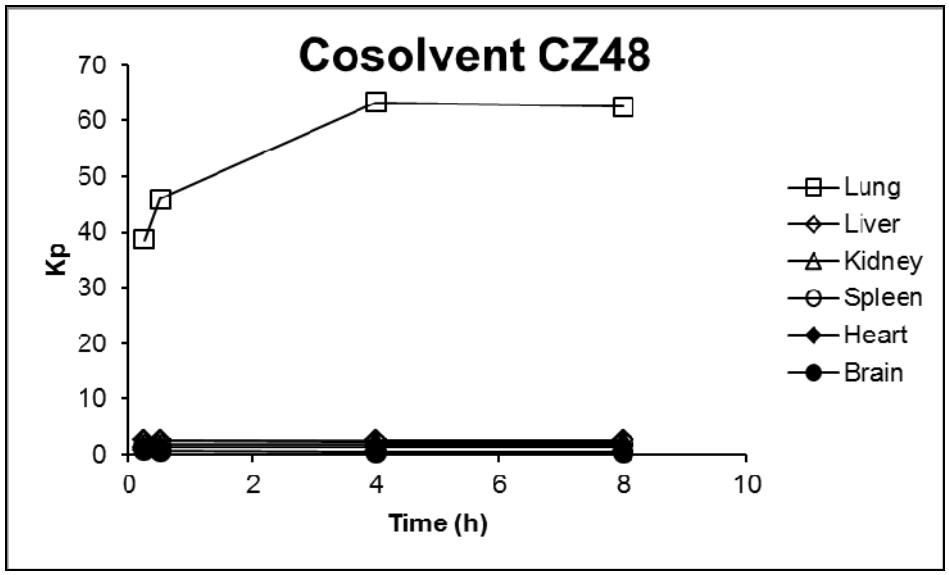

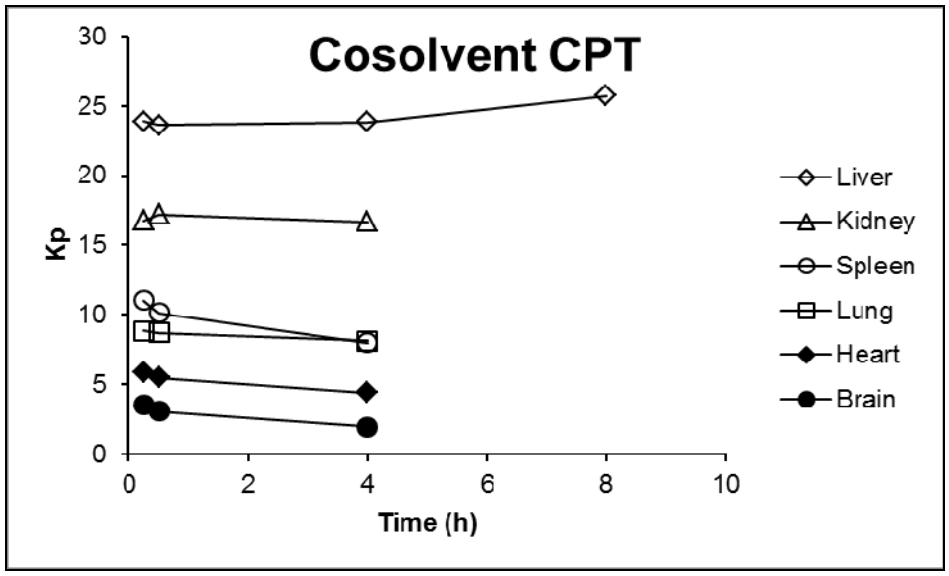

Figure 31 Profiles of Partition Coefficient (Kp) of CZ48 and CPT from Cosolvent

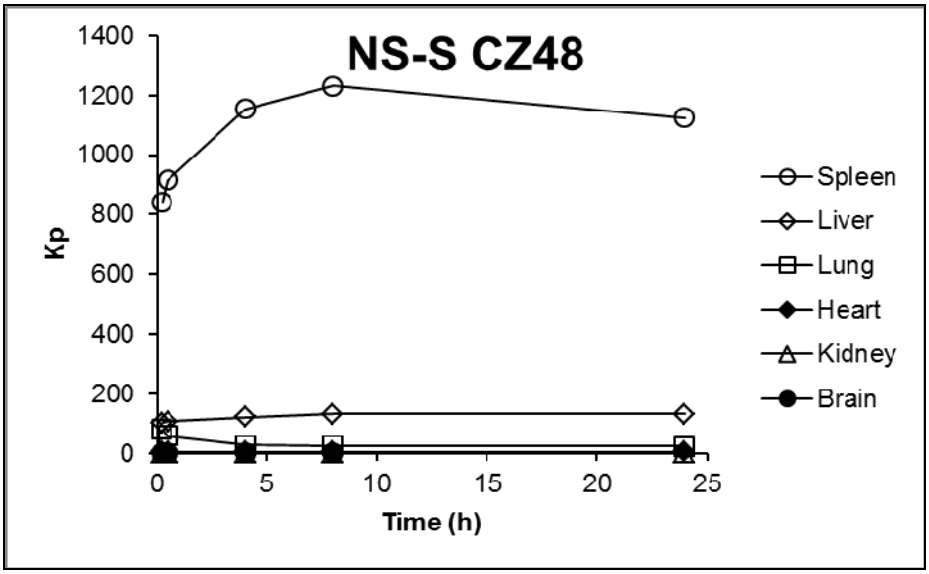

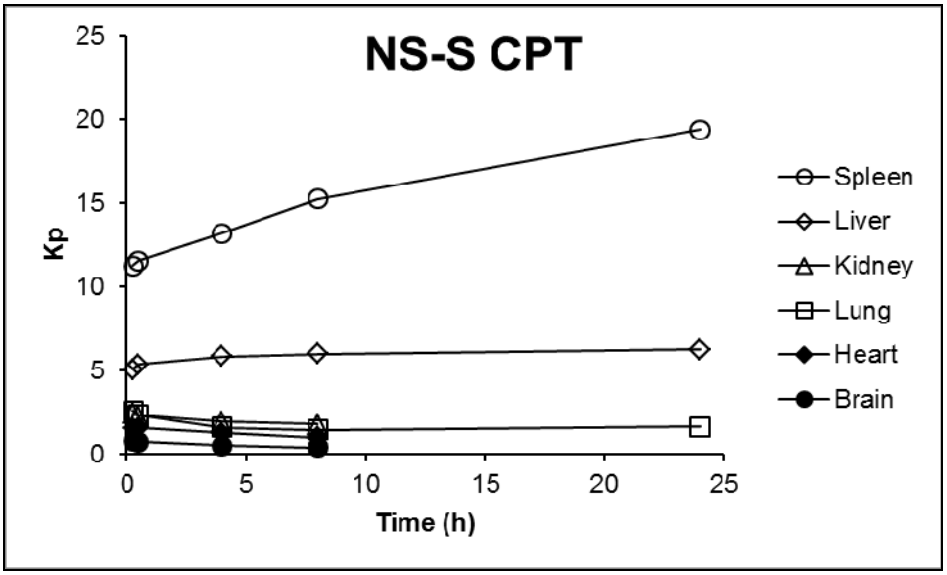

Figure 32 Profiles of Partition Coefficient (Kp) of CZ48 and CPT from NS-S

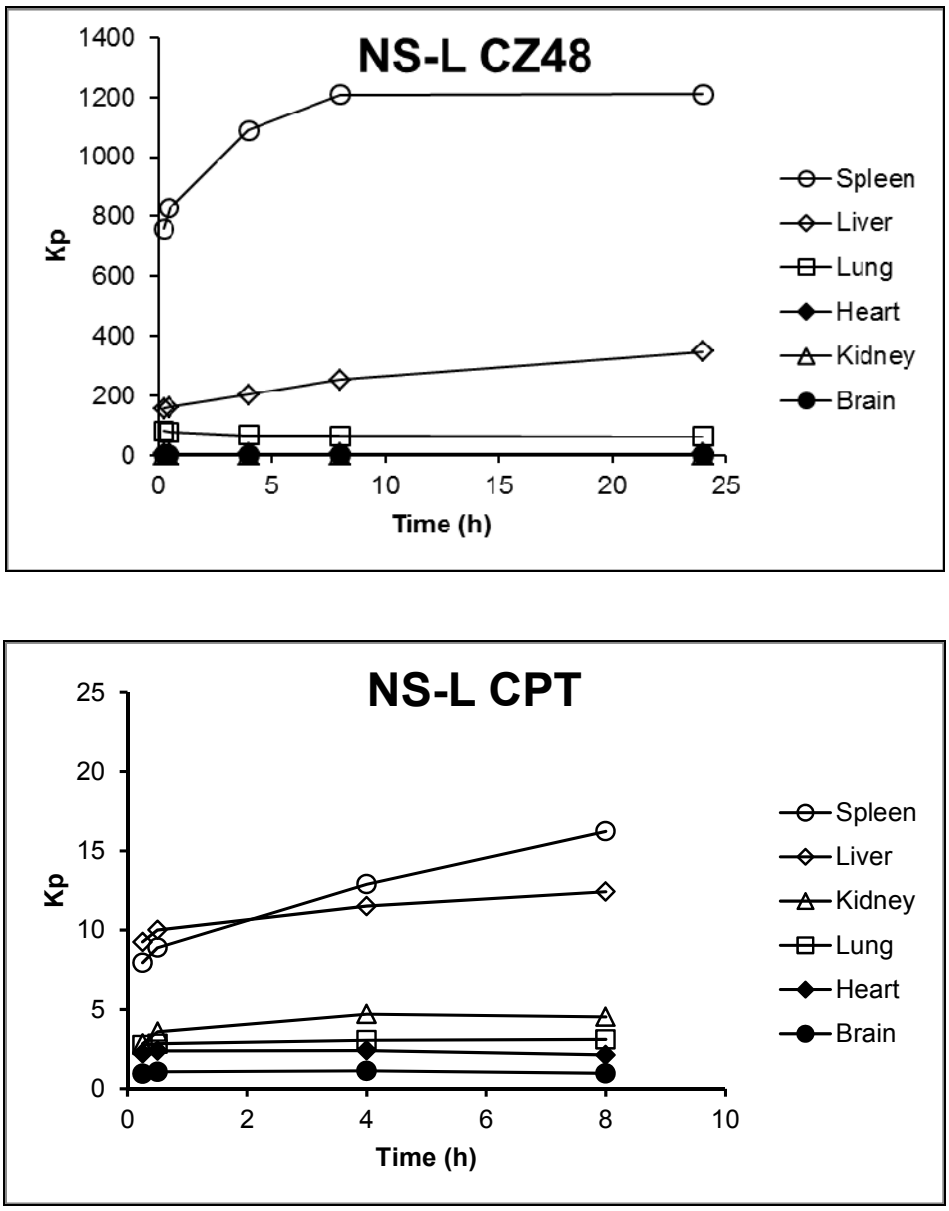

Figure 33 Profiles of Partition Coefficient (Kp) of CZ48 and CPT from NS-L

4.3. Plasma Pharmacokinetics and Biodistribution of CZ48 and CPT in Mice

4.3.1. HPLC Assay for Quantitative Analysis of CZ48 and CPT in Mice Plasma and Organ Samples

For quantifications of CZ48 and CPT in mouse plasma, under described conditions (Section 3.2.6.5), the retention time was 15.13 min, 23.62 min, and 26.07 min for CPT, internal standard CZ44, and CZ48, respectively. No interference peak was found from blank mouse plasma. The calibration curves, each containing 6 concentration points, were constructed at the linearity range of 0.78 ~ 800 ng/ml with the correlation coefficients > 0.999. The assay was also validated with the within-day variability (n = 6) of 3.26 and 1.58% for CZ48 and CPT, respectively, and the between-day variability (n = 6) of 3.86 and 2.48% for CZ48 and CPT, respectively. Plasma samples were prepared by precipitation with acetonitrile and high recoveries of 96% for both CZ48 and CPT drug was achieved.

For quantifications of CZ48 and CPT in mouse six organs, heart, liver, spleen, lung, kidney and brain, the analysis was also performed under the described conditions (Section 3.2.6.5). No interference peak was found from all six blank organs. The calibration curves, each containing 6 concentration points, were also constructed at the linearity range of 0.78 ~ 800 ng/ml with the correlation coefficients > 0.999 for all organs.

The assay was also validated for each organ with the within-day variability (n = 3) of 1.86 ~ 5.17% and 1.21 ~ 4.56% for CZ48 and CPT, respectively, and the between-day variability (n = 6) of 2.43 ~ 6.52% and 1.82 ~ 4.95% for CZ48 and CPT, respectively. The recoveries of CZ48 and CPT were ranged from 84.25 to 97.32%. All of these recoveries were acceptable according to FDA Guidance for Industry - Bioanalytical Method Validation. The linear regression equations of peak area ratios (Y) versus concentrations (X) were used to determine CZ48 and CPT concentrations in respective organs of biodistribution studies in mice.

4.3.2. Plasma Pharmacokinetics of CZ48 Cosolvent and Nanosuspensions (NS-S, and NS-L) in Mice (n=4)

Plasma pharmacokinetics for CZ48 and its active metabolite, CPT, from cosolvent and nanosuspensions (NS-S and NS-L) in Swiss nude mice have also been studied. Different doses of CZ48 cosolvent, and CZ48 nanosuspensions were selected due to the toxicity of the cosolvent formulation to mice and for the consistency to the *in vivo* study in rats. The formulations were given by i.v. injection and blood samples were collected for CZ48 and CPT quantifications by the HPLC assay. The plasma concentration-time profiles were constructed using sparse sampling approach. The mean concentration-time profiles were generated by calculating the mean concentration at each time point from samples collected from four mice that were sacrificed at the given time point as described in Section 3.2.7.2.

The profiles of nanosuspensions were distinct from that of cosolvent for both CZ48 and CPT, especially the slower elimination phase (Figure 34). Compartmental models by WinNonlin Professional 3.0 were fitted to the mean plasma concentration profiles to derive the pharmacokinetics parameters. The pharmacokinetics parameters were presented as the means without the standard deviations (Table 24 & Table 25).

4.3.2.1 Comparative Pharmacokinetics of CZ48 Following i.v. Administration of Cosolvent and Nanosuspensions (NS-S, and NS-L) of CZ48 in Mice

The pharmacokinetic performances of CZ48 from NS-S and NS-L were different from those of cosolvent with half-lives of 11 and 8 fold longer (8.00 h and 5.58 h vs. 0.70 h) (Table 26). CZ48 from NS-S and NS-L were widely distributed to other organs besides plasma, and had larger V_{ss} compared to that from cosolvent (41.12 and 30.61 L/kg vs. 6.48 L/kg, respectively). At the same time, NS-S and NS-L had lower C_0 normalized by the dose of CZ48 than that from the cosolvent (122.29 and 172.48 nM/(mg/kg) vs. 381.66 nM/(mg/kg)). The $AUC_{0-\infty}$/Dose values of CZ48 were comparable among groups of cosolvent, NS-S and NS-L.

4.3.2.2 Comparative Pharmacokinetics of CPT Following i.v. Administration of Cosolvent and Nanosuspensions (NS-S, and NS-L) of CZ48 in Mice

The dose-normalized $AUC_{0-\infty}$ values for NS-S was higher than those of NS-L and cosolvent (19.78 nM*h/(mg/kg), 10.95 nM*h/(mg/kg) vs. 8.29 nM*h/(mg/kg)). NS-S and NS-L not only showed larger systemic exposure of CPT, but also longer half-lives compared to cosolvent (12.51, and 5.81 h vs. 0.40 h). The V_{ss} of CPT were comparable among groups of cosolvent, NS-S and NS-L (Table 26).

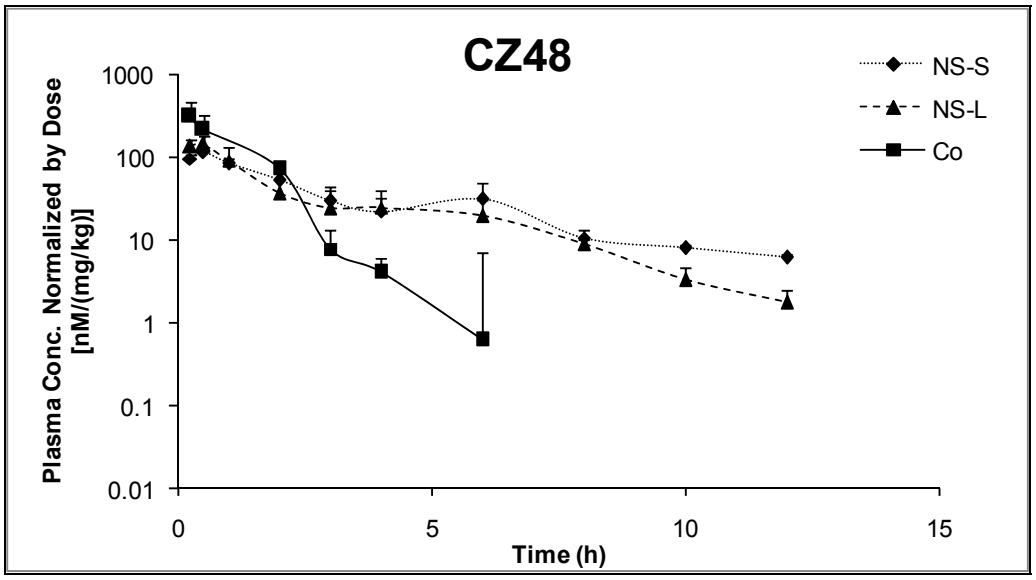

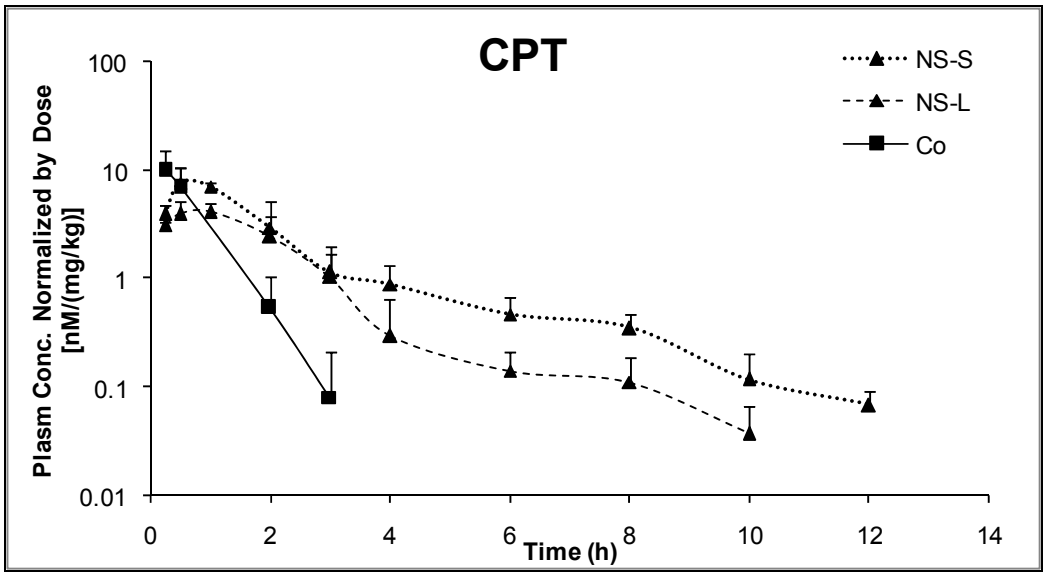

Figure 34 Mean Plasma Concentration Normalized by Dose verses Time Curves of CZ48 and CPT after i.v. Administration of CZ48 Cosolvent (5 mg/kg), NS-S (25 mg/kg) and NS-L (25 mg/kg) in Mice (n = 4).

Table 24 Pharmacokinetic Parameters of CZ48 from Cosolvent, NS-S, and NS-L in Mouse Plasma after i.v. Administration (n = 4).

Parameters		Unit	Cosolvent	NS-S	NS-L
			5 mg/kg	25 mg/kg	25 mg/kg
CZ48	A	nM		2521.58	3774.76
	α	h^{-1}		0.52	0.79
	B	nM		535.64	537.16
	β	h^{-1}		0.09	0.12
	k_{10}	h^{-1}	0.99	0.28	0.48
	k_{12}	h^{-1}		0.17	0.24
	k_{21}	h^{-1}		0.16	0.21
	$t_{1/2\alpha}$	h		1.33	0.87
	$t_{1/2\beta}$	h	0.70	8.00	5.58
	V_1	L/kg	6.48	20.21	14.33
	CL_1	L/kg*h	6.41	5.62	6.81
	V_2	L/kg		20.91	16.28
	CL_2	L/kg*h		3.41	3.38
	C_0/Dose	nM/(mg/kg)	381.66	122.29	172.48
	AUC_{0-t}/Dose	nM*h/(mg/kg)	384.68	352.31	323.98
	$AUC_{0-\infty}$/Dose	nM*h/(mg/kg)	385.70	440.08	362.95
	F			1.14	0.94
	AUMC	$nM*h^2$	1948.90	80551.07	40783.45
	MRT	h	1.01	7.32	4.49
	V_{ss}	L/kg	6.48	41.12	30.61

Table 25 Pharmacokinetic Parameters of CPT from Cosolvent, NS-S, and NS-L in Mouse Plasma after i.v. Administration (n = 4).

	Parameters	Unit	Cosolvent	NS-S	NS-L
			5 mg/kg	25 mg/kg	25 mg/kg
CPT	A	nM	84.19	10732.96	7970.13
	α	h^{-1}		1.42	1.33
	B	nM		9.25	7.69
	β	h^{-1}		0.06	0.12
	k_a	h^{-1}	11.12	1.49	1.38
	k_{10}	h^{-1}	1.72	0.98	1.07
	k_{12}	h^{-1}		0.42	0.23
	k_{21}	h^{-1}		0.08	0.15
	$t_{1/2\alpha}$	h		0.49	0.52
	$t_{1/2\beta}$	h	0.40	12.51	5.81
	$t_{1/2ka}$	h	0.06	0.47	0.50
	V_1	L/kg	11587.84	1703.65	2814.09
	CL_1	L/kg*h	19893.92	1668.12	3015.03
	V_2	L/kg		8867.19	4394.96
	CL_2	L/kg*h		714.67	652.55
	T_{max}	h	0.20	0.70	0.75
	C_{max}/Dose	nM/(mg/kg)	10.12	7.38	4.46
	AUC_{0-t}/Dose	nM*h/(mg/kg)	8.24	16.35	10.16
	$AUC_{0-\infty}$/Dose	nM*h/(mg/kg)	8.29	19.78	10.95
	F			2.39	1.32
	AUMC	$nM*h^2$	27.88	3466.05	852.25
	MRT	h	0.67	7.01	3.11
	V_{ss}	L/kg	11587.84	10570.84	7209.05

4.3.3. Organ Distributions of CZ48 and Metabolite, CPT, from Cosolvent and Nanosuspensions (NS-S, and NS-L) in Mice (n=4)

The biodistribution study in mice was also comparatively evaluated for the CZ48 from cosolvent, NS-S and NS-L. Different organ distribution patterns of CZ48 and CPT among cosolvent, NS-S and NS-L were observed (Figure 35 ~ Figure 37). The mean organ parameters were derived from the mean concentration-time profiles for each formulation by WinNonlin (Table 26 ~ Table 28). The drug concentrations in different organs showed similar trends as that in plasma. The profiles of nanosuspensions were distinct from those of cosolvent for both CZ48 and CPT, especially the slower elimination phase.

4.3.3.1 Organ Distributions of CZ48 and CPT from Cosolvent in Mice

Both CZ48 and CPT can be characterized as one-compartment model.

The concentrations decreased very fast after CZ48 cosolvent administration with the half-lives of about 1 hour (Table 26). The organ peak concentrations were reached before the collection at the first time point. CZ48 uptake (C_{max}/dose) from the cosolvent was comparable among the lung, liver, kidney, spleen and heart (200.65 ~ 543.24 (ng/g)/(mg/kg)), but lower by the brain, 49.63 (ng/g)/(mg/kg) (Figure 35 & Table 26)). The exposure (AUC) normalized by the dose of the lung from CZ48 cosolvent was 1038.38 (ng*h/g)/(mg/kg), the highest among the organs. The exposures of CZ48 in the liver, and kidney were comparable (690.54 and 604.57 (ng*h/g)/(mg/kg)) and higher than those of

the heart, spleen and brain (296.14, 282.28 and 59.59 (ng*h/g)/(mg/kg), respectively) (Table 26).

The highest CPT exposure from cosolvent was in the liver followed by kidney, 99.03, and 57.25 (ng*h/g)/(mg/kg), respectively. The CPT exposure was comparable in spleen and lung (34.34, and 34.18 (ng*h/g)/(mg/kg)). The smallest exposure was in the brain (8.25 (ng*h/g)/(mg/kg)). The elimination half-lives were all about 1 hour for heart, liver, spleen, lung, kidney, and brain; 0.99 h, 1.17 h, 0.81 h, 0.77 h, 1.48 h, and 0.68 h, respectively (Table 26).

4.3.3.2 Organ Distributions of CZ48 and CPT from NS-S in Mice

Both CZ48 and CPT can be characterized by two-compartment model.

The distribution pattern from CZ48 NS-S was different from that of the cosolvent (Figure 35. The highest uptake was in the liver with the highest C_{max}/Dose (5521.13 (ng/g)/(mg/kg)) followed by the spleen/lung, kidney/heart, and brain; 3230.42/1689.83, 194.71/148.24, and 9.99 (ng/g)/(mg/kg), respectively. The CZ48 exposures ($AUC_{0-\infty}$/Dose) among the organs from NS-S followed the same ranking in patterns of C_{max}/Dose. The highest CZ48 exposure from NS-S was in the liver followed by spleen and lung; 13686.92, 5374.30 and 5374.30 (ng*h/g)/(mg/kg), respectively. The smallest exposure from NS-S was in the brain of 34.61 (ng*h/g)/(mg/kg)). The $t_{1/2}$ of CZ48 in the lung was 38.21 h, the longest among the organs. The $t_{1/2}$ in the heart (8.29 h) was longer than that in the brain and kidney (4.45 and 3.20 h). The $t_{1/2}$ of CZ48 in the liver (1.96 h)

was comparable to that in the spleen (1.64 h) which was the shortest among the organs (Table 29).

CPT yielded the highest exposure in liver with the $AUC_{0-\infty}$/Dose of 191.38 (ng/g*h)/(mg/kg), followed by kidney of 57.35 (ng/g*h)/(mg/kg), spleen of 48.51 (ng/g*h)/(mg/kg) and lung of 55.18 (ng/g*h)/(mg/kg). CPT can be retained more than 12 hours in all the six major organs (Table 29).

4.3.3.3 Organ Distributions of CZ48 and CPT from NS-L in Mice

Both CZ48 and CPT can be characterized by two-compartment model.

The distribution pattern of CZ48 from NS-L was different from that of the cosolvent but similar to that of NS-S (Figure 35 & Figure 35). The highest uptake (C_{max}/Dose) was observed in the liver, 86253.18 (ng/g)/(mg/kg), while the other organs were in the following rank: spleen > lung > kidneys > heart > brain (3350.07, 1612.12, 355.41, 169.97 and 34.14 (ng/g)/(mg/kg), respectively. The liver exposure was the highest among the organs of 23288.49 (ng*h/g)/(mg/kg), about 10 times higher than the second high organ spleen of 3350.07 (ng*h/g)/(mg/kg). The half-lives were comparable among all the organs, 2.74 ~ 4.77 h, except that in spleen, 1.92 h. (Table 29)

CPT could be detectable more than 12 hours after CZ48 NS-L injection in all the major organs with the half-lives of 3.81 h ~ 8.24 h (Figure 35). In liver, CPT showed the highest C_{max}/Dose of 31.03 (ng/g)/(mg/kg), followed by lung (20.95 (ng/g)/(mg/kg)), kidney (15.85 (ng/g)/(mg/kg)) and spleen (14.40 (ng/g)/(mg/kg)); and CPT also showed the

largest $AUC_{0-\infty}$/Dose of 189.48 (ng/g*h)/(mg/kg), followed by kidney (59.94 (ng/g*h)/(mg/kg)), spleen (54.90 (ng/g*h)/(mg/kg)), and lung (39.55 (ng/g*h)/(mg/kg)).

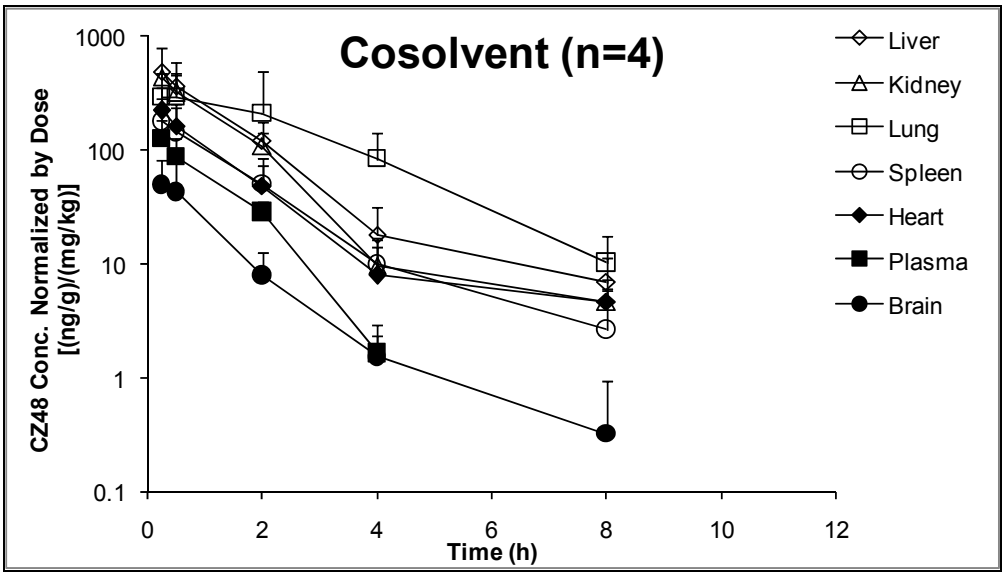

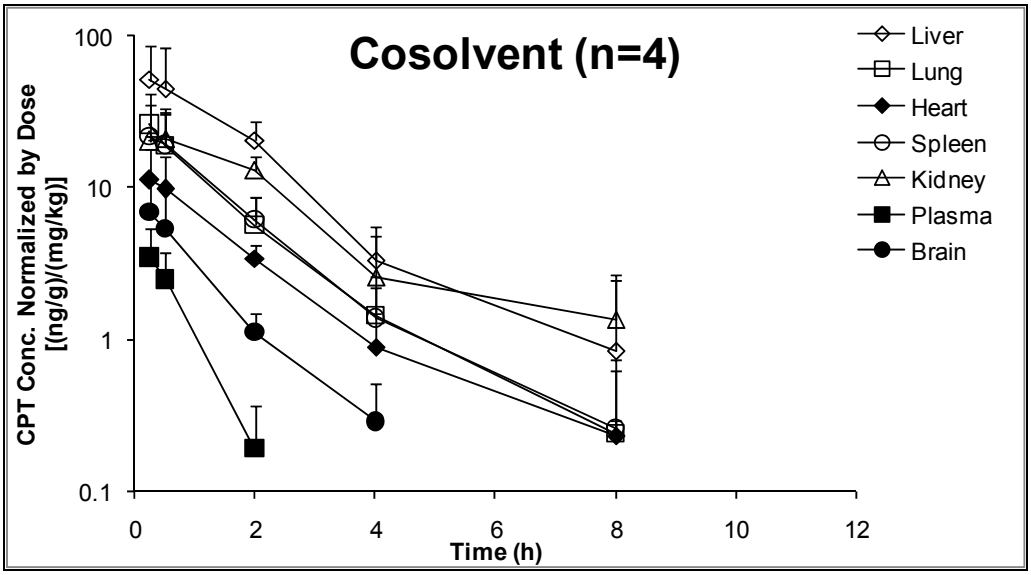

Figure 35 Organ Distribution Profiles of CZ48 and CPT from Cosolvent in Mice (n=4)

Table 26 CZ48 and CPT Organ Distribution Parameters from Cosolvent in Mice after i.v. Administration (n=4)

Parameters		Unit	Cosolvent						
			Heart	Liver	Spleen	Lung	Kidney	Brain	Plasma
CZ48	$AUC_{0-\infty}$/Dose	(ng/g*h)/(mg/kg)	296.14	690.54	282.28	1038.38	604.57	59.59	156.05
	C_{max}/Dose	(ng/g)/(mg/kg)	263.04	543.24	200.65	309.97	488.36	49.63	154.42
	$t_{1/2}$	h	0.76	0.84	0.93	2.00	0.81	0.62	0.70
CPT	$AUC_{0-\infty}$/Dose	(ng/g*h)/(mg/kg)	18.75	99.03	34.34	34.18	57.25	8.25	2.89
	C_{max}/Dose	(ng/g)/(mg/kg)	11.18	50.99	21.46	29.26	21.78	7.28	3.53
	$t_{1/2}$	h	0.99	1.17	0.81	0.77	1.48	0.68	0.40

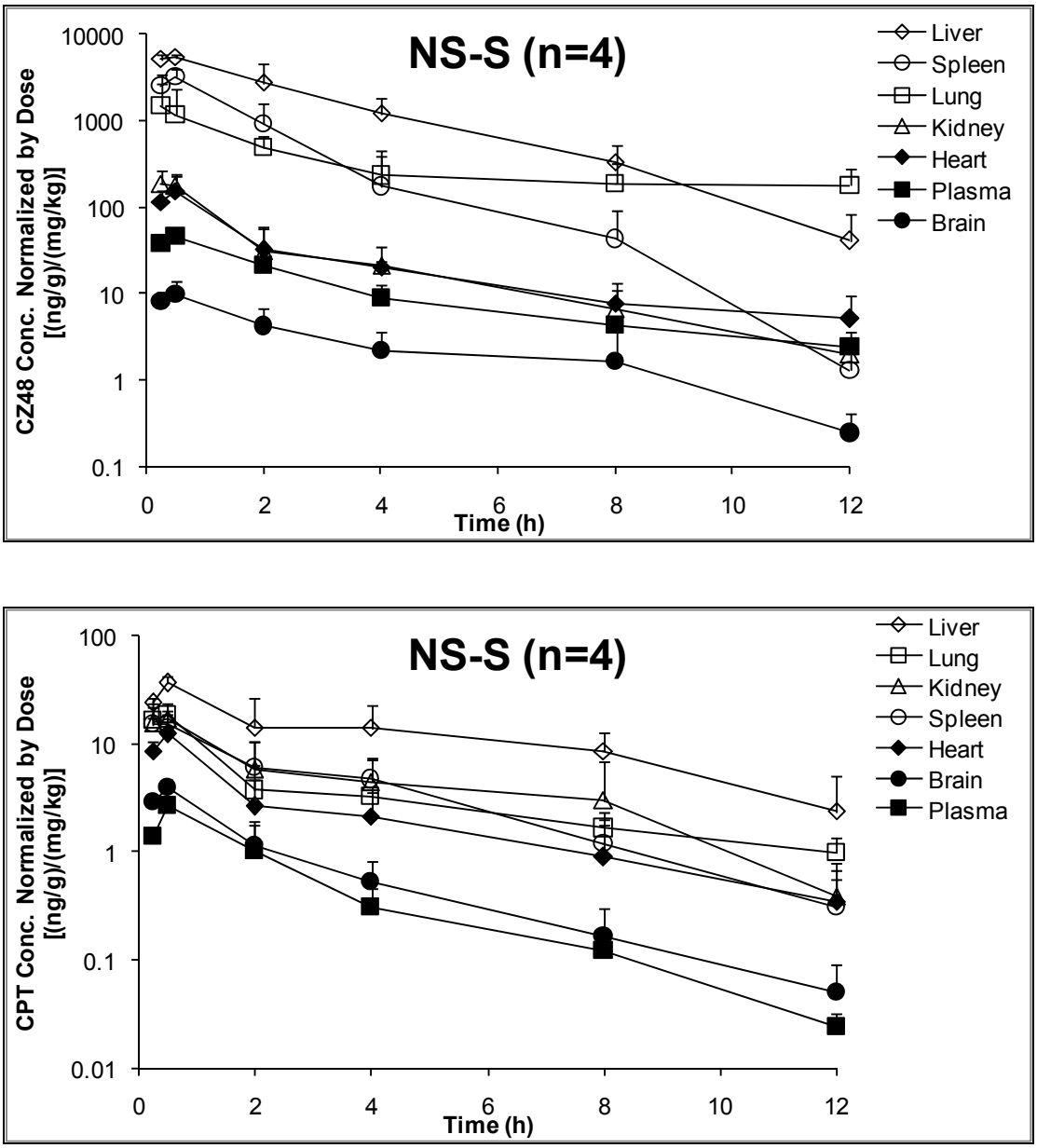

Figure 36 Organ Distribution Profiles of CZ48 and CPT from NS-S in Mice (n=4)

Table 27 CZ48 and CPT Organ Distribution Parameters from NS-S in Mice after i.v. Administration (n=4)

Parameters		Unit	NS-S						
			Heart	Liver	Spleen	Lung	Kidney	Brain	Plasma
CZ48	$AUC_{0-\infty}$/Dose	(ng/g*h)/(mg/kg)	378.34	15324.07	5374.30	13686.92	332.13	34.61	178.06
	C_{max}/Dose	(ng/g)/(mg/kg)	148.24	5521.13	3230.42	1689.83	194.71	9.99	49.48
	$t_{1/2}$	h	8.29	1.96	1.64	38.21	3.20	4.45	8.00
CPT	$AUC_{0-\infty}$/Dose	(ng/g*h)/(mg/kg)	32.93	181.38	48.51	55.18	57.35	8.91	6.89
	C_{max}/Dose	(ng/g)/(mg/kg)	11.55	34.22	16.15	18.71	17.38	3.91	2.51
	$t_{1/2}$	h	7.13	6.31	2.99	7.28	4.16	4.02	12.51

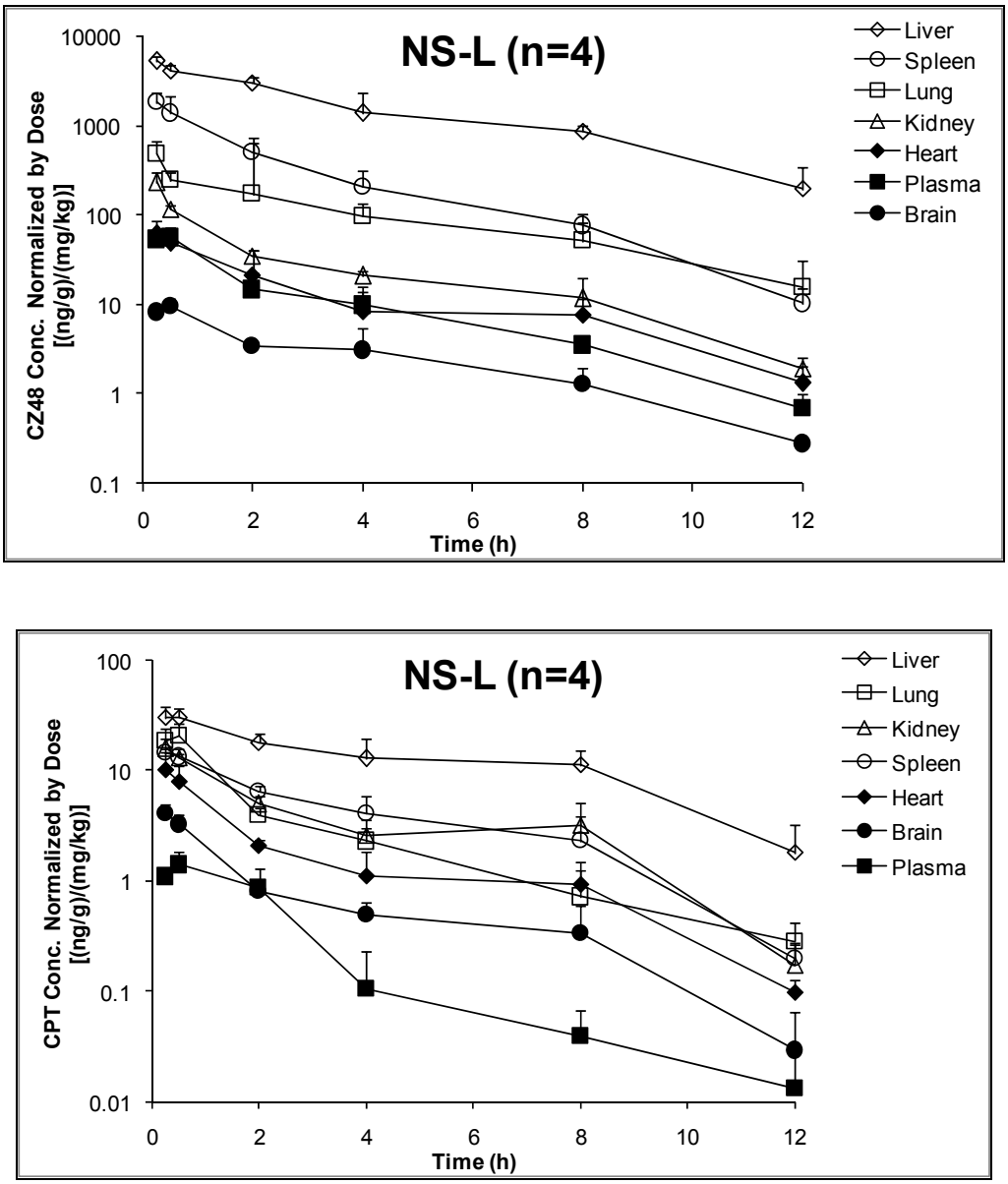

Figure 37 Organ Distribution Profiles of CZ48 and CPT from NS-L in Mice (n=4)

Table 28 CZ48 and CPT Organ Distribution Parameters from NS-L in Mice after i.v. Administration (n=4)

Parameters		Unit	NS-L						
			Heart	Liver	Spleen	Lung	Kidney	Brain	Plasma
CZ48	$AUC_{0-\infty}$/Dose	(ng/g*h)/(mg/kg)	169.67	23288.49	3350.07	1612.12	355.41	34.14	146.85
	C_{max}/Dose	(ng/g)/(mg/kg)	70.91	86253.18	2014.29	5036.33	386.09	9.41	69.79
	$t_{1/2}$	h	4.77	2.74	1.92	3.07	3.17	4.16	5.58
CPT	$AUC_{0-\infty}$/Dose	(ng/g*h)/(mg/kg)	23.16	189.48	54.90	39.55	59.94	8.24	3.81
	C_{max}/Dose	(ng/g)/(mg/kg)	10.73	31.03	14.40	20.95	15.85	4.15	1.55
	$t_{1/2}$	h	6.49	5.99	4.58	3.81	8.24	4.04	5.81

4.3.3.4 Comparative Organ Distributions of CZ48 and CPT Following i.v. Administration of Cosolvent and Nanosuspensions (NS-S, and NS-L) of CZ48 in Mice

The distribution patterns of CZ48 from nanosuspensions were different from that of the cosolvent. The exposures of CZ48 from both nanosuspensions were higher than that from the cosolvent in the RES rich system such as liver, spleen and lung (Table 29). On the contrary, the exposures of CZ48 in kidney, and brain from CZ48 of both nanosuspensions were lower than that from cosolvent. In addition, CZ48 from NS-S distributed more in spleen and lung (5374.30 vs. 3350.07 (ng*h/g)/(mg/kg), 13686.92 vs. 1612.12 (ng*h/g)/(mg/kg), respectively), compare to NS-L from which CZ48 distributed more in liver (15123.00 vs. 22408.20 (ng*h/g)/(mg/kg)) (Table 30). The half-lives of CZ48 from nanosuspensions were longer than those from cosolvent in all the organs (Table 30). By comparing the biodistribution patterns of CPT among the three formulations, nanosuspensions had the highest exposure in liver, spleen, and lung, with long half-lives in all organs. The exposures of CPT in all the organs from NS-S were comparable to those from NS-L.

4.3.3.5 Comparative Organ/Plasma Partition Coefficients of CZ48 and CPT Following i.v. Administration of Cosolvent and Nanosuspensions (NS-S, and NS-L) of CZ48 in Mice

The organg/plasma partition coefficient (Kp) of CZ48 and CPT for the heart, liver, spleen, lung, kidney and brain were obtained experimentally from the Organ AUC/Plasma AUC

ratios toward the end of the study (Figure 38 ~ Figure 40). The Kp values of CZ48 in different organs were lower than those of CPT by cosolvent administration, which may be due to instabilities of CPT in plasma. Similar results were found in nanosuspensions administration except in RES rich organs, liver, spleen, and lung. This due to the super uptake of nanoparticles by RES systems, and only free CZ48 can be biotranformed to CPT by CEs.

Table 29 Exposure (AUC0-t/Dose) of CZ48 and CPT from Cosolvent, NS-S and NS-L in Different Organs

Organs	$AUC_{0-\infty}$/Dose [(ng/g)/(mg/g)]					
	CZ48			**CPT**		
	Cosolvent	NS-S	NS-L	Cosolvent	NS-S	NS-L
Heart	296.14	378.34	169.67	18.75	32.93	23.16
Liver	690.54	15324.07	23288.49	99.03	181.38	189.48
Spleen	282.28	5374.30	3350.07	34.34	48.51	54.90
Lung	1038.38	13686.92	1612.12	34.18	55.18	39.55
Kidney	604.57	332.13	355.41	57.25	57.35	59.94
Brain	59.59	34.61	34.14	8.25	8.91	8.24
Plasma	156.05	178.06	146.85	2.89	6.89	3.81

Table 30 Half-lives of CZ48 and CPT from Cosolvent, NS-S and NS-L in Different Organs

Organs	$t_{1/2}$ (h)					
	CZ48			CPT		
	Cosolvent	NS-S	NS-L	Cosolvent	NS-S	NS-L
Heart	0.76	8.29	4.77	0.99	7.13	6.49
Liver	0.84	1.96	2.74	1.17	6.31	5.99
Spleen	0.93	1.64	1.92	0.81	2.99	4.58
Lung	2.00	38.21	3.07	0.77	7.28	3.81
Kidney	0.81	3.20	3.17	1.48	4.16	8.24
Brain	0.62	4.45	4.16	0.68	4.02	4.04
Plasma	0.70	8.00	5.58	0.40	12.51	5.81

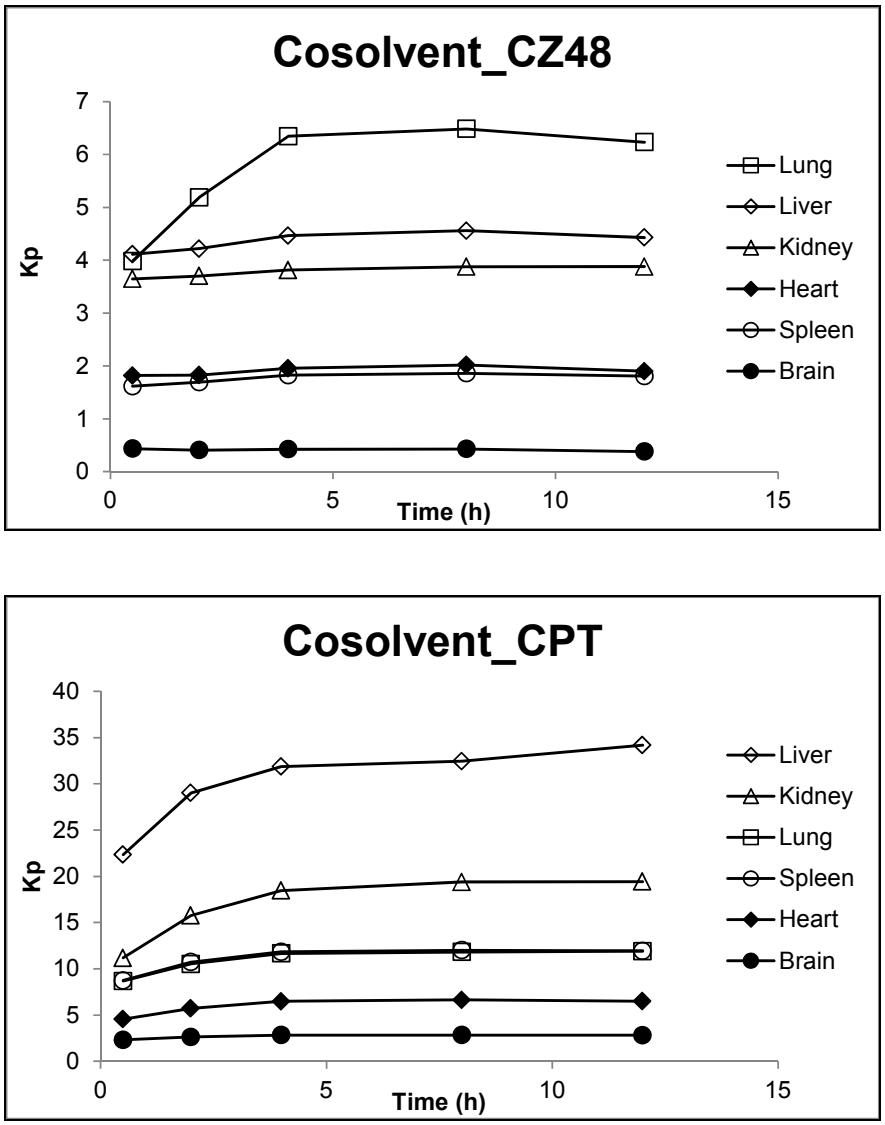

Figure 38 Profiles of Partition Coefficient (Kp) of CZ48 and CPT from Cosolvent in Mice

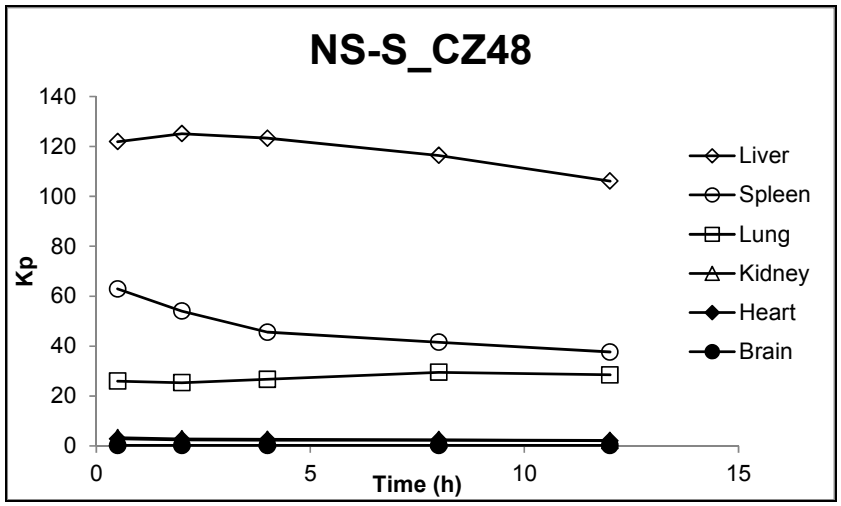

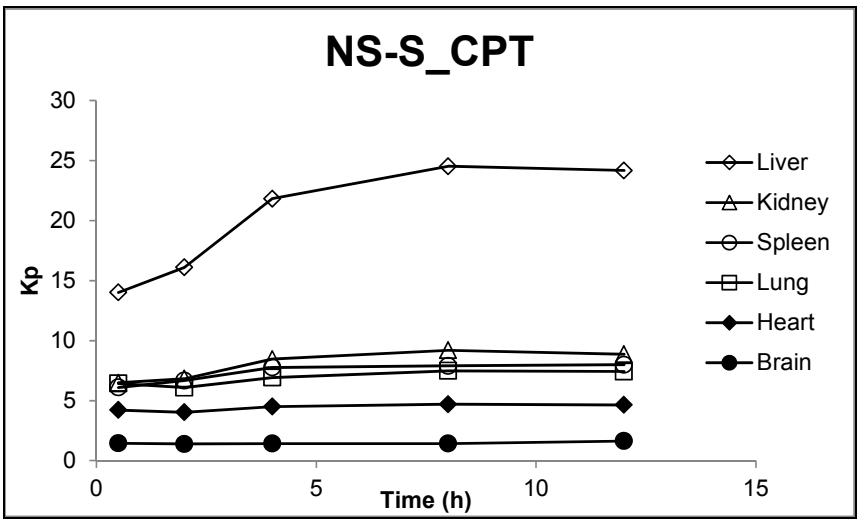

Figure 39 Profiles of Partition Coefficient (Kp) of CZ48 and CPT from NS-S in Mice

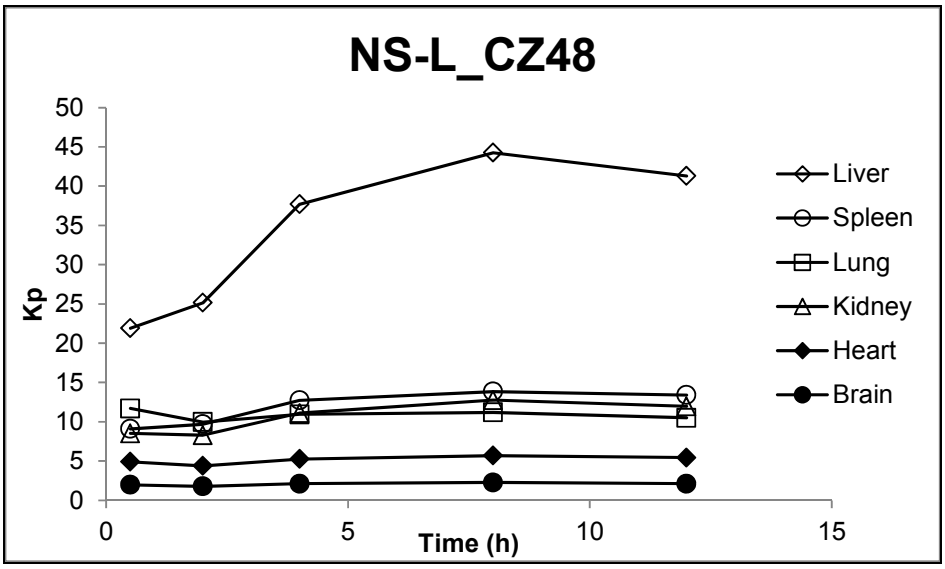

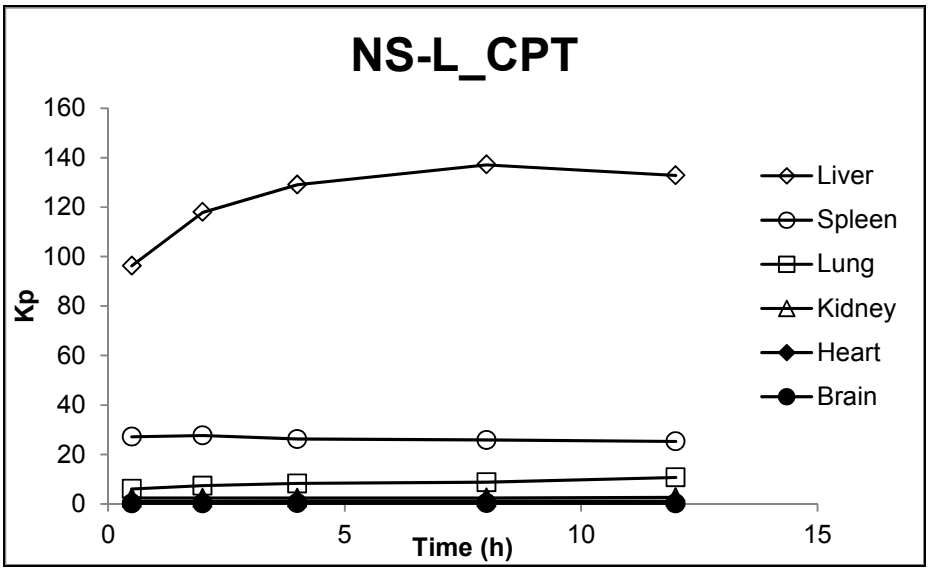

Figure 40 Profiles of Partition Coefficient (Kp) of CZ48 and CPT from NS-L in Mice

4.4. NS-S Efficacy Study

Based on the pharmacokinetic and organ distribution study in mice, NS-S was selected as the lead formulation to perform the efficacy study. Seven groups of tumor-bearing mice were used, receiving no treatment (NT), cosolvent placebo (CP), nanosuspension placebo (NP), CZ48 cosolvent (Co, 5 mg/kg), NS-S of low dose (NS-S-L, 5 mg/kg), NS-S of medium dose (NS-S-M, 25 mg/kg), and NS-S of high dose (NS-S-H, 50 mg/kg), respecting the same formulations used in the pharmacokinetic studies. Different doses between cosolvent and NS-S formulations were employed due to the toxicity of cosolvent formulation with 5 mg/kg as the maximum tolerable dose to the mice and the results of pharmacokinetic study in mice. The groups for NT, CP, and NP were used as control groups, and cosolvent as reference for comparison. The concentrations of CZ48 (50 mg/kg) in the nanosuspensions were diluted to the required concentrations, and the tail vein injection dose was limited up to 0.2 ml or less. The control groups received equal volumes of placebo formulations. The drugs were dosed twice weekly for a total of 8 doses.

The tumor size was measured before the first dose and then twice weekly for 29 days. The size was recorded as a volume (Volume = Lengeh * Width * Hight). The growth of the tumor was expressed as V/V_0, the ratio of the tumor volume on day of measurement to the initial volume on Day 1. The survival duration was expressed as the period between the day of sacrifice or death and the first day of dosing. The median survival was the time (expressed in days) when half the animals are expected to be alive. The

efficacy was definced as the suppression of tumor growth, the increase of survival duration and the median survial. The toxicity was expressed as the body weight loss. Mice were sacrificed if tumor volume was >7,000 mm^3 or the body weight loss was >15%.

Tumors were inoculated into 55 mice following the protocol described in Section 3.2.8.1. The tumor was allowed to grow for 10 days and when the tumor size was between 100 ~ 300 mm^3. The mice were randomized using Microsoft FoxPro 7.0 based on the tumor size and the body weight, into groups and given the first dose.

4.4.1. Tumor Growth Rate

The comparative tumor growth, V/V_0 ratio, versus the time from the first day of dosing to day 11 and day 29 of treatment period in days was shown in Figure 41 for different groups. In day 11, the mice in each control group (NT, CP, NP) and reference group (Co) started to be sacrificed due to the tumor size was larger than 7000 mm^3, the comparison to day 11 was more presice compared to the comparison to day 29 because of the observation number due to the animal death.

The growth rate /day for each group to day 11 treatment was calculated according to the exponential tumor growth model, as summarized in Table 31, and ANOVA followed by Tukey's post-hoc statistical analysis was conducted (Table 32). The growth rates were 0.157 ± 0.048 day^{-1} ~ 0.192 ± 0.049 day^{-1} for the three control groups, 0.181 ± 0.064 day^{-1} for cosolvent, 0.130 ± 0.030 day^{-1} for NS-S-L, 0.084 ± 0.030 day^{-1} for NS-S-M, and

0.010 ± 0.003 day^{-1} for NS-S-H, respectively. The tumor growth rate of NS-S-L group did not show significant difference from Co group; however, both NS-S-M and NS-S-H groups had statistically slower tumor growth rate as compared to that of all the control groups. Moreover, the tumor growth rate of NS-S-H group was statistically slower than that of NS-S-M group

4.4.2. Average Body Weight

Body weight loss was considered toxicity. The average body weights of groups versus the day post first dose were monitored (Figure 42). No statistical difference was observed in the body weights when among different groups except NS-S-H group.

4.4.3. Survival Rate

The survival rates of mice in three control groups, cosolvent reference group and three nanosuspension treatment groups were shown in Figure 43. The survival rate was expressed as percent of mice surviving from original number at time 0. The median survival was estimated as 8 ~ 15 days for three control groups, 18 days for cosolvent reference group, and 22 days for NS-S-L, more than 29 days for NS-S-M, and 15 days for NS-S-H (Table 33). CZ48 nanosuspensions of low and medium doses prolonged the animal survival. However, the high dose group did not show merits to the animal survival due to the toxicity.

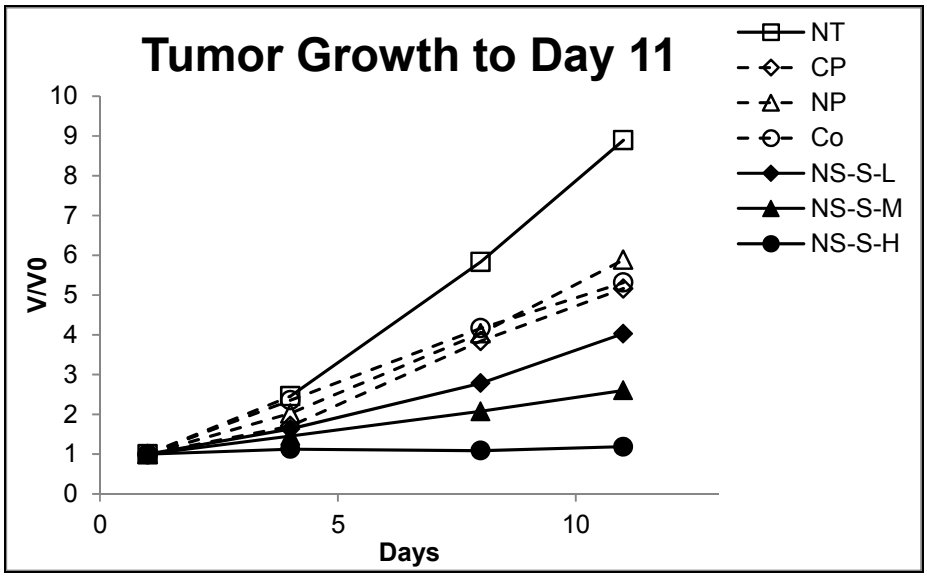

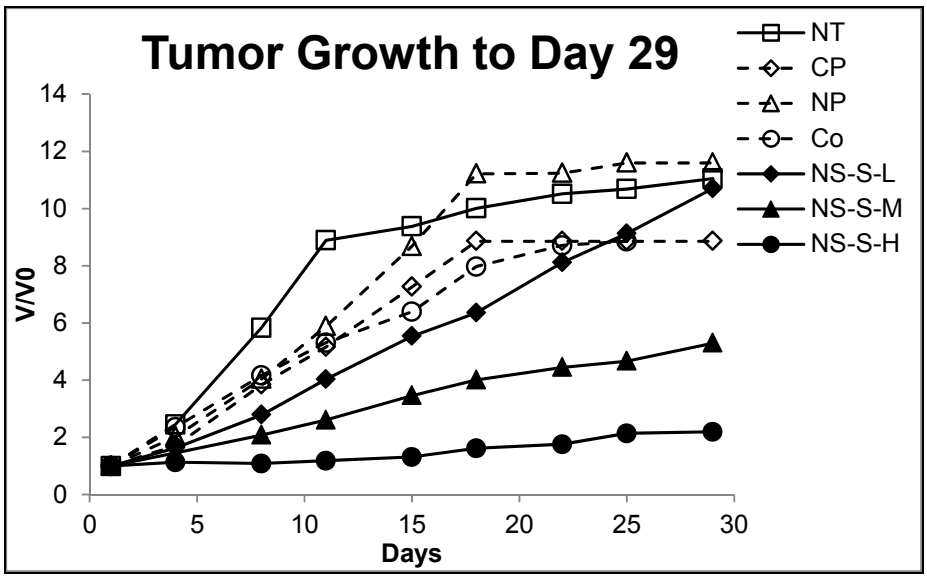

Figure 41 Tumor Growth versus Time from the First Day of Dosing to Day 11 and Day 29 of Treatment Period. n=7 in Blank, CP, NP Groups, n=10 in Co (5 mg/kg), NS-S-L (5 mg/kg), NS-S-M (25 mg/kg) and NS-S-H (50 mg/kg) groups.

Table 31 Tumor Growth Rate from the First Day of Dosing to Day 11 of Treatment

Groups	Day 11
NT (n=7)	0.192 ± 0.049
CP (n=7)	0.157 ± 0.048
NP (n=7)	0.191 ± 0.052
Co (n=10, 5 mg/kg)	0.181 ± 0.064
NS-S-L (n=10, 5 mg/kg)	0.130 ± 0.030
NS-S-M (n=10, 25 mg/kg)	0.084 ± 0.030
NS-S-H (n=10, 50 mg/kg)	0.010 ± 0.003

Table 32 ANOVA with Tukey's Post-hoc Analysis Testing for Tumor Growth Rate from the First Day of Dosing to Day 11 of Treatment

One-way analysis of variance	
P value	< 0.0001
P value summary	***
Are means significantly different? (P < 0.05)	Yes
Number of groups	7
F	14.20
R squared	0.6543

Table 32 ANOVA with Tukey's Post-hoc Analysis Testing for Tumor Growth Rate from the First Day of Dosing to Day 11 of Treatment (Cont'd)

Tukey's Multiple Comparison Test	Significant? P < 0.05?	Summary
NT vs CP	No	ns
NT vs NP	No	ns
NT vs Co	No	ns
NT vs NS-S-L	No	ns
NT vs NS-S-M	Yes	**
NT vs NS-S-H	Yes	***
CP vs NP	No	ns
CP vs Co	No	ns
CP vs NS-S-L	No	ns
CP vs NS-S-M	No	ns
CP vs NS-S-H	Yes	***
NP vs Co	No	ns
NP vs NS-S-L	No	ns
NP vs NS-S-M	Yes	**
NP vs NS-S-H	Yes	***
Co vs NS-S-L	No	ns
Co vs NS-S-M	Yes	**
Co vs NS-S-H	Yes	***
NS-S-L vs NS-S-M	No	ns
NS-S-L vs NS-S-H	Yes	***
NS-S-M vs NS-S-H	Yes	*

Note: "ns", no significant difference

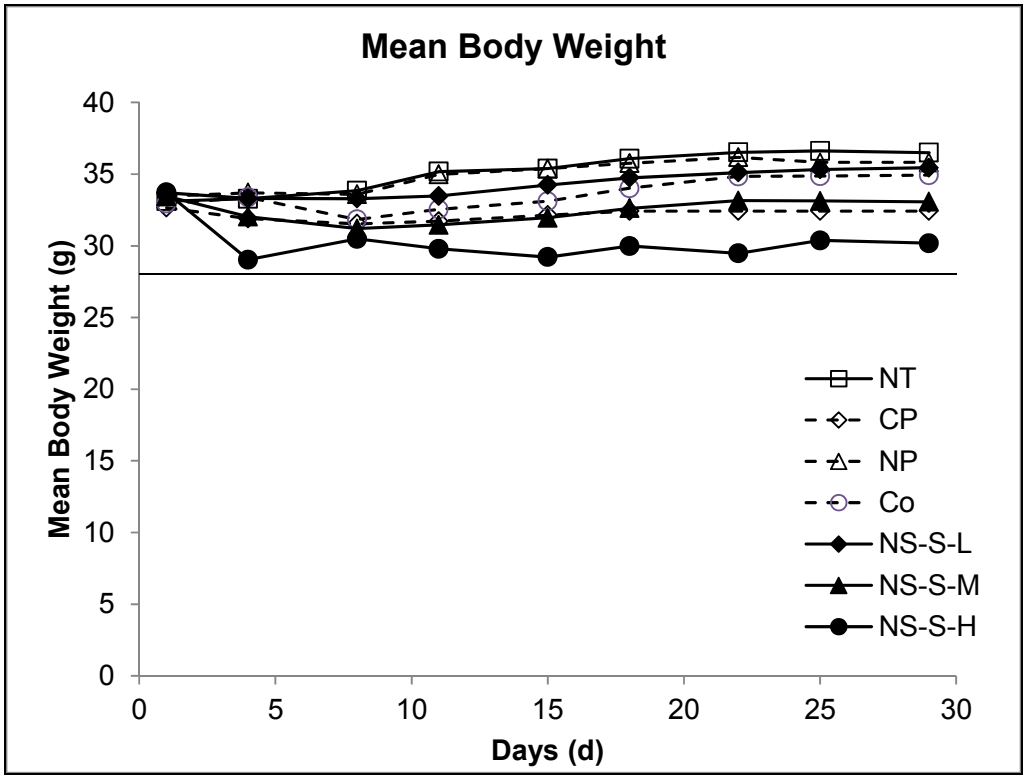

Figure 42 Average Body Weight of Each Group versus the Day after the First Dose. No Statistical Difference was Observed in the Body Weights among Different Groups (Co, 5 mg/kg, NS-S-L, 5 mg/kg, NS-S-M, 25 mg/kg, and NS-S-H, 50 mg/kg)

Table 33 Median Survival (Days)

Median Survival (Days)	
NT (n=7)	8
CP (n=7)	11
NP (n=7)	15
Co (n=10, 5 mg/kg)	18
NS-S-L (n=10, 5 mg/kg)	22
NS-S-M (n=10, 25 mg/kg)	>29
NS-S-H (n=10, 50 mg/kg)	15

The Kaplan-Meier plot was used for survival analysis comparison. The p-values for the 10-way comparison are summarized in Table 34. NS-S-M group was statistically different from all the control groups, cosolvent group and other treatment groups with a p-value of 0.0002 ~ 0.0029. The comparison survival plots among different groups were conducted (Figure 44 ~ Figure 46). There was no significant difference among these three control groups without CZ48 treatment (NT, CP and NP) with a p value of 0.3356 (Figure 44). Moreover, NS-S-M i.v. administration showed an improved survival compared to the no treatment control group and cosolvent reference group (p=0.0023, Figure 45). The high dose group showed significantly stronger tumor suppression compare to low and medium dose groups; however, the low survival rate indicated a high toxicity (p = 0.0230, Figure 46).

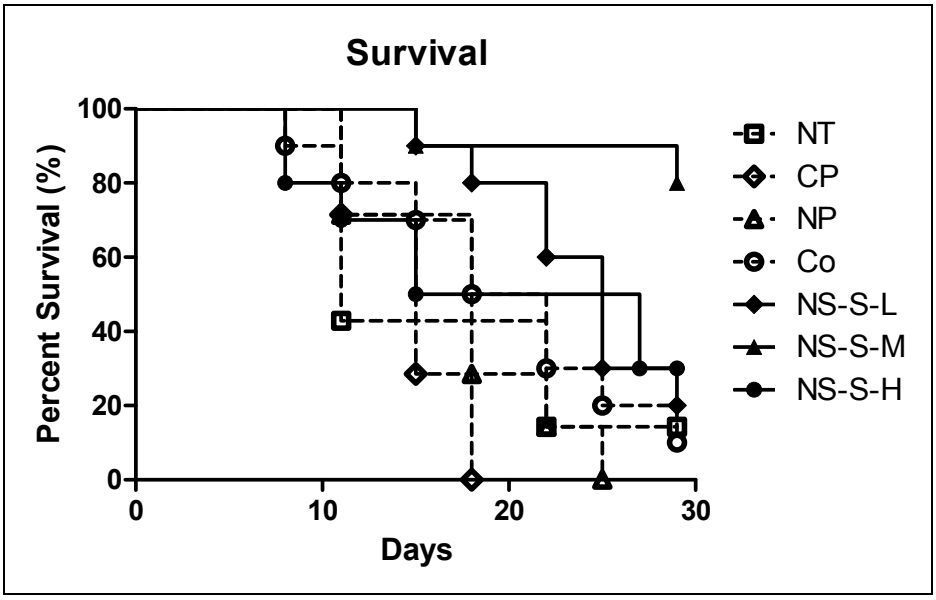

Figure 43 Percent Survival in Each Group over Time in Days. The Survival was Expressed as % Surviving from Original Number at Time 0. (Co, 5 mg/kg, NS-S-L, 5 mg/kg, NS-S-M, 25 mg/kg, and NS-S-H, 50 mg/kg)

Table 34 Summary of Kaplan-Meier Survival Analysis Significance Testing among Different Groups

	Survival Comparison			
	Co	NS-S-L	NS-S-M	NS-S-H
CP	0.0453	-	-	-
NP	-	0.0219	0.0002*	0.2046
Co	-	0.2309	0.0011*	0.4765
NS-S-L	-	-	0.0085	0.9646
NS-S-M	-	-	-	0.0167

* Indicated statistically significant differences in survival among the groups at $p < 0.005$ for a 10-way comparison in Kaplan-Meier Analysis.

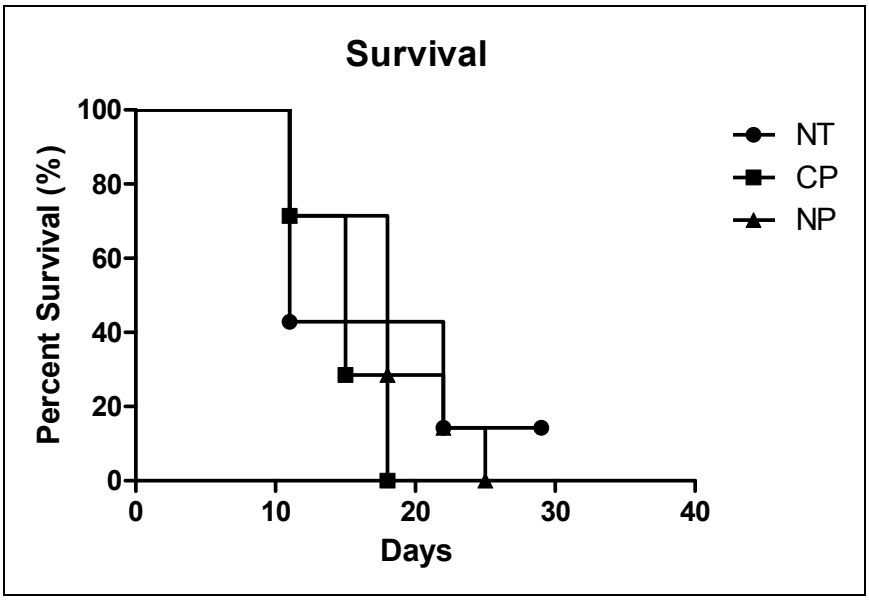

Figure 44 Kaplan-Meier Survival Plot among Control Groups (NT, CP and NP) with p value of 0.3356

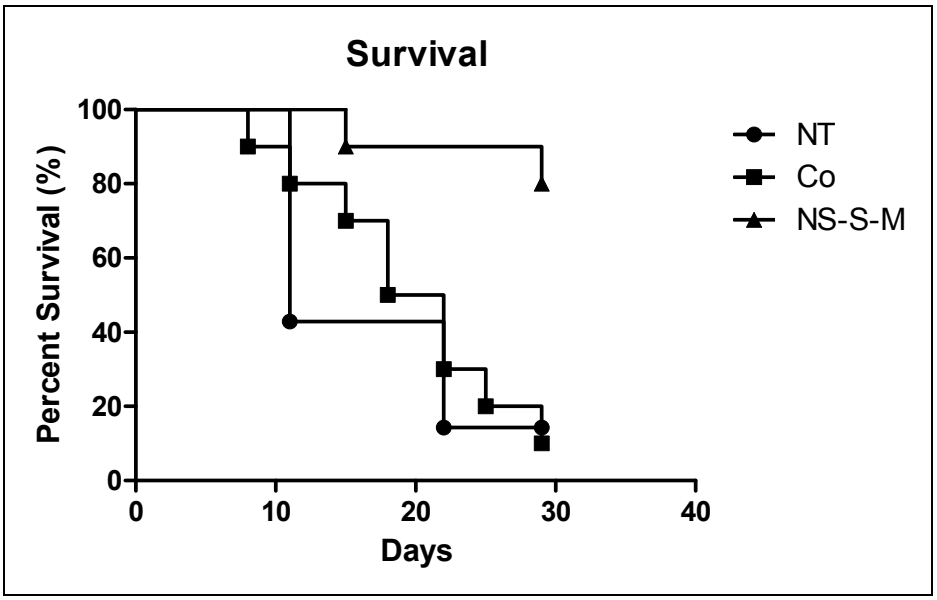

Figure 45 Kaplan-Meier Survival Plots among NT, Co and NS-S-M Groups with p value of 0.0023

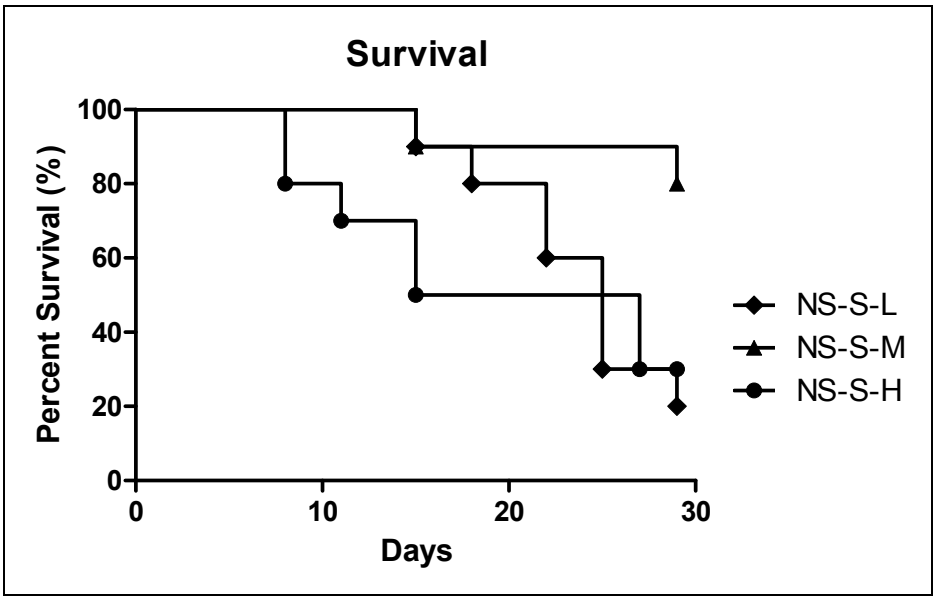

Figure 46 Kaplan-Meier Survival Plots among Nanosuspension Treatment Groups (NS-S-L, NS-S-M and NS-S-H) with p value of 0.023

Chapter 5 Discussion

CPT is naturally occurring anti-neoplastic agent that inhibits the nuclear enzyme Topo-I, which is overexpressed in certain tumor types including those of cervix and colon (McLeod HL et al., 1994; Giovanella BC et al., 1989). The lactone moiety of CPT is unstable *in vivo*, but essential for the anti-tumor efficacy. Cytotoxicity of Topo-I inhibitors is S-phase cell-cycle specific and *in vitro* and *in vivo* studies have suggested that prolonged exposure to low concentrations is more relevant for efficacy than a short-term exposure to high concentrations (Gerrits CJ et al., 1997). Poor aqueous solubility is a major chemical characteristics of CPT and the development of more water-soluble analogues is one of the two major approaches in CPT research, along with the development of more lactone-stable derivatives.

Currently, numerous CPT analogues are at different stages of drug development. At present, two water-soluble CPT analogues have been approved by FDA for clinical use in the U.S.: Topotecan (Hycamptin®), indicated as a second-line therapy for advanced ovarian and small cell lung cancers, and irinotecan (Camptosar®), indicated for the treatment of advanced colorectal cancer. However, the response rates of clinical anticancer activity of these two products were modest, 12-50% depending on the type of cancer being treated (Takimoto CH et al., 1998). This is modest efficacy due to the fact that at physiological pH, the equilibrium favors the inactive carboxylate form over the active lactone species.

CZ48, a novel propionate ester of CPT, demonstrated superior lactone stability over CPT both *in vitro* and *in vivo*. CZ48 exerts its anti-neoplastic activity after hydrolysis to CPT by the action of carboxyestrase (Liehr JG et al., 2000). However, the solubility of CZ48 is extremely low, which is only 57.22 ~ 63.20 ng/ml at physiology pH (Pfuma E, 2008). CZ48 is the C20-propinate derivative of CPT, an alkaloidal compound. This group of compounds has a weakly basic character. Therefore, it was not surprising to display a 2-fold increase in solubility at pH 1. Although the amide nitrogen in ring C of the molecule possesses very low basicity, the non-bonding electron pair on the quinoline nitrogen, ring B, is localized and available for protonation at this low pH (Chen HJ et al., 1971). Irrespective of that, CZ48 solubility of 116.02 ng/ml at pH=1 is still considered very low. In addition, any pharmaceutical preparation at this extreme pH is impractical. The low aqueous solubility of CZ48 clearly demonstrates the need for formulation efforts to significantly improve solubility, especially if an intravenous drug delivery is to be pursued to reach the therapeutic concentrations. Erratic bioavailability also was found when orally dosing it unformulated.

Poorly-water soluble drugs represent a formulation challenge and it is pharmaceutical formulator's responsibility to find the optimum approach to overcome this limitation. Facing those challenges, we found nanoformulation technique is promising for this class of drug candidates that have low water solubility and require sustained exposure to achieve the maximum therapeutic effects. Therefore, we proposed that if we succeed in continuously delivering CZ48 at a low and sustained rate by a nanoformulation, we could

potentially provide sustained and prolonged concentration of CPT near or at the site of action, thus accomplishing an optimal therapeutic outcome.

The success of CZ48 nanosuspension preparation could increase the dissolution rate and the saturation equilibrium solubility by reducing the particle size of CZ48 to a nano-sized range. Then CZ48 nanosuspension could be administered by a variety of routes, such as oral, intravenous, ocular and pulmonary and so on. We aim to administer CZ48 nanosuspension by intravenous to avoid first-pass effect, providing the most rapid effect, and/or achieving a passive target effect. Moreover, the injection volume of nanosuspension will not exceed the limitation of the volume of i.v. administration owing to the its high drug load, and the therapeutic responses as well as associated toxicity can be more predictable (Wong J, 2008).

This project involved the development, optimization, and characterization of nanosuspension formulations of CZ48 for intravenous delivery. The formulation work was preceded by a thorough screening study of stabilizers and preparation time. CCD was also carried out to optimize the properties of CZ48 nanosuspensions.

From the obtained formulations, two formulations with different particle sizes were investigated for the pre-clinical pharmacokinetics and organ distribution patterns in two rodent species, rats and mice, upon i.v. administration, and were compared to those from CZ48 cosolvent administrations in an attempt to demonstrate the versatility of application of the developed formulation. Then based on the information obtained from

the pharmacokinetic and biodistribution studies, a lead formulation was selected and was subject to test the antitumor activity in a tumor bearing mouse model.

We were interested in lung cancer because it is the leading cause of cancer mortality in the United States, Europe, and many other industrialized countries. NSCLC differs from SCLC in that surgery can frequently be curative, albeit in a small subpopulation of patients (Devore RF and Johnson DH, 1996; Bonomi P, 1996). NSCLC displays the same characteristics as many solid tumors for which single-agent chemotherapy provides only a small response rate, and even combination chemotherapy produces only marginal survival improvements. This discouraging picture underscores the need for new therapeutic approaches for NSCLC. Besides the H460 cell line is very invasive. The average volume doubling time in the first passage in nude mice is around 7 days (Mattern J et al., 1985).

This project was unique in many perspectives:

First, it involved the development of a novel formulation, nanosuspension, for a novel CPT derivative, CZ48, for which superior lactone ring stability has been confirmed both *in vitro* and *in vivo*.

Second, a screening study was performed with 5 different stabilizers, used 3 concentrations, and their combinations. Moreover, the influences of the multiple preparation factors were evaluated and optimized with a surface response design using only a truncated set of empirical experiments and the statistical modeling of this empirical data, which were appropriate by meeting the assumptions.

Third, it proved the concept that achieving and sustaining therapeutic levels of the active moiety, CPT, in plasma and organ tissues were feasible upon i.v. administration of CZ48 nanosuspension formulation compared to CZ48 cosolvent.

Fourth, it demonstrated the significant antitumor activity with a higher tolerable dose by i.v. administration of CZ48 nanosuspension in xenograft tumor bearing mouse model.

5.1. CZ48 Nanosuspensions Preparation

Mainly there are two methods for the preparation of nanosuspensions: Bottom-up process and Top-down process (Verma S et al., 2009). In the bottom-up approach the drug is dissolved in an organic solvent and is then precipitated on addition of an anti-solvent in the presence of stabilizer. The limitation of this precipitation method is that the drug needs to be soluble in at least one solvent and this solvent needs to be miscible with nonsolvent. Moreover, this technique is not applicable to drugs that are simultaneously poorly soluble in aqueous and nonaqueous media (R.H Muller, handbook, 2000). The top-down method is the disintegration method and is preferred to the precipitation method. It includes media milling (nanocrystal), high pressure homogenization in water (dissocubes), high pressure homogenization (nanoedege) (Keck CM and Müller RH, 2006). Media milling method can be applied to the drugs that are poorly soluble in both aqueous and organic media. It is also easy to scale-up and has little batch-to-batch variation (Patravale VB et al., 2004). The final nano-sized product shows narrow size distribution. It's also flexibility in handling the drug quantity,

ranging from 1 to 400 mg/ml, enabling formulations of very dilute and highly concentrated.

Based on the above advantages, the media milling technique is used in nanosuspension preparation where the solid drug particles are sheared between the sliding surfaces of the moving glass beads. This shear movement imparts energy into the system leading to the reduction of the particle size. Due to the energy introduced into the system to reduce the particle size, the system becomes thermodynamically unstable due to the formation of fresh surfaces. It tends to reduce the high energy by re-agglomeration into larger particles to minimize the newly created surfaces. To overcome the agglomeration tendency, surface active compounds (surfactant) could be used to stabilize the suspension particles. There are only a limited numbers of nonionic and anionic surfactants that have been approved as excipients for parenteral use, including phospholipids, T-80, and poloxamers. There are many safety concerns about the use of anionic surfactants (Bummer P, 2000). With this consideration, 5 nonionic surfactants and there combinations with T-80 were investigated. T-80 and F-108 were selected from several stabilizer candidates as steric stabilizers to overcome the attractive interactions between the sheared particles. The surfactant F-108 has also been used in the formulation of i.v. injectable itraconazole and the clinical trial of its suspension has also been conducted (Mouton JW et al., 2006). The presence of the stabilizers keeps the particles apart and prevents the re-agglomeration.

To further reduce the particle size, the shear forces are increased by minimizing the distances that separate the sliding beads, using a mixture of glass beads with various

sizes to incorporate the smaller beads in-between the larger ones (Kesisoglou F et al., 2007). The single-sized glass beads produce particles with a larger polydispersity index (bi-modal size distributions), but a mixture of multi-sized glass beads produces a narrow polydispersity index (mono-modal particle size distribution). Similar results are reported by Yang (Yang JZ et al., 2008).

5.2. Central Composite Design (CCD)

Preparation of nanosuspensions is a complex procedure as it involves several processing variables and design components. These variables and system components also demonstrate significant interactions among themselves that affect the quality of final products. For a successful formulation development, it is extremely important to identify these critical factors ad their interactions that have potential impacts on the quality attributes and performance characteristics of the product.

The use of experimental techniques, such as CCD, is the most rational and systematic way for simultaneous identification, estimation, and analysis of influence of critical factors on the quality of final formulation (Zhang J et al., 2008; Kollipara S et al., 2010). Without the use of CCD, only a few variables can be studied at a limited number of levels because of the fact that many experiments are required to draw a significant conclusion. When cost and time of each experiment is very high, the use of CCD can offer possibility of analyzing a large number of variables with a limited experiment runs (Molpeceres J et al., 2009; Lewis GA et al., 1999; Aktas E et al., 2012; Hao J et al., 2012).

The tendency of smaller particles in a suspension to dissolve and re-grow on bigger particles presents a mode of instability, termed “Ostwald ripening”. It has been reported that too much dispersant used in the stabilization of a suspension could actually promote Ostwald ripening. The proposed weight ratio of drug to stabilizer was advocated to be in the range of 20:1 to 2:1 (Merisko-Liversidge E et al., 2003). This theory is consistent with our CCD results. Out of the three factors studied, CZ48 concentration and F-108/CZ48 ratio had considerable impacts on the mean particle size with a p value less than 0.05. Particle size changes steeply by varying CZ48 concentration, but changes in a relatively gradual fashion with the F-108/CZ48 ratios. Schubert and Muller-Goymann reported that an increase of stabilizer concentration led to a concentration dependent increase in particle size once the stabilizer concentration exceeded a critical concentration, which seems to be consistent with our study (Schubert MA and Müller-Goymann CC, 2003).

The zeta potential was not significantly affected by the experimental conditions employed in this study. A preferred zeta potential should provide a sufficient electric repulsion to prevent the nanoparticles from aggregation and agglomeration (Gao Y et al., 2010). In order to obtain a nanosuspension exhibiting a good stability, a minimum zeta potential of ± 20 mV is desirable (Müller RH and Jacobs C, 2002). Most of the nanosuspensions produced by FDA proved surfactants have a negative charge (Möschwitzer JP, 2012). For those positively charged surfactant, it is unsuitable for use in humans. Moreover, the negatively charged particles have a similar charge of the cellular membrane, and the particles will be strongly adsorbed onto the cellular membrane.

The particle size is the most basic property of a nanosuspension system. In addition, the other characterizations (saturation solubility, dissolution rate, physical stability, or even biological performances) of a nanosuspension system are also governed by the particle size (Gao L et al., 2008). According to Noyes-Whitney, the decreased particle size can increase the effective particle surface area and consequently, the dissolution rate (Patravale et al., 2004). It is well known that, a small particle size with a narrow size distribution can alleviate the agglomeration to ensure a stable and homogeneous system. As reported in the study of Wang et al. (Wang et al, 2010), nanosuspension A (642 ± 15 nm) and nanosuspension B (127 ± 2 nm) showed different bioavailability improvements with absolute bioavailability of 39.6% and 50.9%, respectively, compared to the unmilled suspension (17.4%) after oral administration. Previous research in our lab has proven that only the nanosuspension of size above 500 nm yields a significant difference in pharmacokinetic behavior *in vivo* from that of 200 nm (Qi YL, 2008). Therefore, the nanosuspensions with particle sizes of 200 nm and 600 nm were selected as the model formulations for further investigation. The zeta potential values of our final formulations are -26.5 ± 0.9 and -27.9 ± 0.8 mV for NS-S and NS-L, respectively, which would be sufficient to prevent the nanoparticles from aggregation and agglomeration.

5.3. Stability of CZ48 in Nanosuspension Formulations (NS-S and NS-L)

Physical stability evaluations of CZ48 in the two nanosuspensions revealed that the formulations were stable over 6 months. CZ48 chemical stability under different

conditions has already been established by Dr. Yousif Rojeab (Yousif R, 2007). Chemical stability of CZ48 solution at pH 7.4 as well as at pH 5.0 was evaluated under accelerated stability conditions to extrapolate the stability to room temperature. Particularly, from a drug development perspective, a shelf life of less than two years is usually required since batch approval, release and distribution; it can easily take up to six months. It also displayed consistency in CZ48 load 50 mg CZ48 per ml, from batch-to-batch, when prepared under the uniform conditions.

5.4. HPLC Assay

It is of crucial importance to be able to quantify the concentrations of CZ48 and the active moiety, CPT, simultaneously in the HPLC assay method used, since both species coexist in analytical samples generated from both *in vitro* and in vivo studies.

A previously developed isocratic HPLC method was used for the simultaneous quantifications of CZ48 and CPT concentrations in aqueous samples over the concentration range of 10 ~ 150 and 5 ~ 100 ng/ml for CZ48 and CPT, respectively (Li XH, 2004). With this assay, base-line peak resolution was achieved for all three species, CZ48, CPT and CZ44 (IS).

Another simple and sensitive gradient high-performance liquid chromatography (HPLC) assay for the analysis of CZ48, CPT in mouse plasma was developed and validated by Xin Liu (Liu X et al., 2008). The mean recoveries at three concentrations of 10, 100 and 900 ng/ml were 81.41 ± 0.035%, 86.00 ± 0.053% and 82.21 ± 0.020% respectively, for

CZ48 and 76.01 ± 0.028%, 77.04 ± 0.042% and 85.93 ± 0.023% respectively, for CPT. The calibration curves were linear (r^2=0.9999) over CZ48 and CPT concentrations ranging from 10 ~ 1000 ng/ml and 5 ~ 1000 ng/ml (n=6), respectively. The method had an accuracy of >95% and intra- and inter-day precisions of <1.2% and <2.2% respectively, for CZ48 and CPT, at three different concentrations (10, 100 and 900 ng/ml). The lower limits of quantification (LLOQ) using 0.1 ml mouse plasma were 10 ng/ml for CZ48 and 5 ng/ml for CPT.

Solid phase extraction (SPE) method was applied to prepare plasma samples in the originally developed method; however, organic solvent precipitation with diethyl ether was used to prepare mouse plasma in Liu's article. For our case, the HPLC assay method developed and validated by Liu was modified using organic solvent precipitation with acetonitrile to prepare plasma and organ samples from the pharmacokinetic studies and organ distribution studies in rats and mice. Organic precipitation yielded high recovery for CZ48 and CPT, about 96%. The lower limits of quantification (LLOQ) were 0.78 ng/ml for CZ48 and 0.55 ng/ml for CPT. A significant enhancement from the published method (Liu X et al., 2008).

In addition, it was cost-effective since SPE cartridges are for single-use. Organic precipitation with ice-cold acetonitrile added at a ratio of 5:1 to plasma or homogenized organ samples. The samples of clear supernatant after centrifugation were evaporated under air. The same volume of mobile phase was used to reconstitute the sample, which will not dilute the drug concentrations. It is critical especially for the last few time points when the concentrations of active metabolite, CPT, were very low. In conclusion, the

HPLC method was highly sensitive, reproducible and efficient in quantifying CZ48 and CPT concentrations simultaneously from *in vivo* studies.

5.5. In-vitro Release of CZ48 from Cosolvent and Two Nanosuspensions (NS-S and NS-L)

The *in vitro* release characteristics of CZ48 from the selected nanosuspension formulations of different particle sizes were evaluated in PBS and human plasma, as an essential characterization criterion and for selection optimal formulationfor the potential use for i.v. drug delivery. PBS can help to maintain a constant pH which is mimicking the human physiological environment. The osmolality and ion concentrations of the solution usually match those of the human body (isotonic).

The results showed that CZ48 nanosuspensions exhibited distinct release profiles from that of CZ48 cosolvent formulation. From the release study in aqueous PBS media, the release rate of CZ48 from cosolvent was very rapid, and a complete release was achieved within 2 hours. In contract, the release rates of CZ48 from nanosuspensions were significantly slower than that of CZ48 cosolvent, and reach a complete release by 6 hours. The CZ48 nanosuspension with a larger particle size (600 nm) exhibited significantly slower release rate compare to that of CZ48 nanosuspension with a smaller particle size (200 nm).

Similarly, *in vitro* release of CZ48 from nanosuspensions of various sizes in plasma was much slower than that of CZ48 cosolvent, as CZ48 was completed release from

cosolvent in 48 hours, while only 40% were released in 48 hours from nanosuspensions of the two sizes.

The immediate release profile of cosolvent and slower release profiles of CZ48 nanosuspensions, including NS-S and NS-L, could be explained by their different physical nature. In cosolvent formulation, CZ48 molecules are completely dissolved in the cosolvent mixture. The dissolved CZ48 molecules are readily to be transferred from the dialysis bag to the outside media. In contrast, nanosuspensions contain solid drug particles of nanomicron sizes, and the drug molecules need to be dissolved into the diffusion layer first and then into the bulk media before being released from the dialysis bag (Hsu WC and Lin SP, 1991). The slow dissolving process contributes to the slower/sustained release profiles of CZ48 from the nanosuspensions. The initial release rate of small-sized CZ48 nanosuspension (NS-S) was significantly higher than that of large-sized NS-L. The mean values of initial rates of nanosuspensions of various sizes increased as the particle size decreased, which is consistent with the previous work in our lab by Qi (Qi YL, 2008). According to Noyes-Whitney equation, the dissolution rate will increase due to the increase of surface area when particle size reduces (Aulton ME, 2002).

In vitro release study in plasma mimicked the release kinetics of CZ48 cosolvent and nanosuspensions in blood circulation after an i.v. injection. The distinct release profiles of CZ48 nanosuspensions from that of CZ48 cosolvent formulation in plasma suggests that these two types of formulations release CZ48 differently *in vivo*. However, there is no significantly different between the two nanosuspensions of different particle sizes that

might be due to the high protein binding of CZ48; 82.48 ± 2.52 %. The drug molecules also need to be dissolved into the diffusion layer first and then into the bulk media before being released from the dialysis bag. Then the drug molecules bind to the protein and hard to release from the dialysis bag. Therefore, the particle size of nanosuspensions did not apparently affect the *in vitro* release of CZ48 in plasma.

5.6. Pharmacokinetics and Organ Distribution of CZ48 NSs

Pharmacokinetic and organ distribution studies were conducted in SD rats and Swiss nude mice to comparatively evaluate the plasma pharmacokinetics and biodistribution of CZ48 cosolvent and nanosuspensions of two particle sizes (NS-S and NS-L). For nanosuspension system, studies have demonstrated that the particle size could also affect the *in vivo* performance, such as bioavailability and duration of drug effects (Chingunpitak J et al., 2008; Kassem MA et al., 2007; Wong J et al., 2008). Therefore, it is of great importance of this study to investigate the impact of physical nature of parenteral formulation on CZ48 disposition in rodent animals by comparatively establishing the plasma and organ profiles for different types of CZ48 parenteral formulations. The effects of the particle size of CZ48 nanosuspensions on the pharmacokinetics and biodistribution patterns were also established. Consequently, the different disposition of CZ48 yielded a significantly different pharmacokinetic and biodistribution behavior of its active metabolite CPT.

5.6.1. Plasma Pharmacokinetics of CZ48 Cosolvent and Nanosuspensions (NS-S, and NS-L) in Rats

From plasma pharmacokinetic results, CZ48 nanosuspensions exhibited distinct pharmacokinetic characteristics from that of CZ48 cosolvent.

Longer β half-life for CZ48 nanosuspensions than that from cosolvent was partially attributed to the sustained drug release from nanosuspensions. Another possible reason for prolonged β half-life could be due to the RES uptake of nanoparticles in nanosuspensions, and then the drug was released from phagocytic cells to blood circulation due to the drug concentration gradient, which resulted in a longer blood level compared to that from cosolvent (Liu Y et al., 2012). CZ48 nanosuspension also yielded much larger V_{ss} than cosolvent, which reflected significant dispositions of CZ48 in the peripheral compartments.

In the recent study of oridonin nanosuspensions in rabbits, the nanosuspensions of 897 nm was observed to exhibited distinct plasma pharmacokinetic properties from oridonin solution, such as a prolonged β half-life and large volume of distribution (Gao L et al., 2008). However, the oridonin nanosuspension of 103 nm exhibited a rapid *in vitro* dissolution as oridonin solution. As a result, the nanosuspension of 103 nm showed a similar plasma pharmacokinetics to that of the solution. In our studies, the *in vitro* dissolution profile of NS-S was similar to NS-L in plasma, while distinct from that of cosolvent. In this way, NS-S shared the similar plasma pharmacokinetic properties, such as low C_0, prolonged β half-life and large volume of distribution, as those of NS-L, while

those plasma pharmacokinetic properties were significantly different from that of cosolvent. The water solubility of oridonin is 0.7 g/L, significantly higher than that of CZ48 which is less than 63.2 ~ 57.2 ng/ml at pH 3 ~ 7. The solubility difference may explain the differences of *in vitro* dissolution and *in vivo* pharmacokinetics of nanosuspensions of 100 nm to 200 nm (Xu W et al., 2007). Other possible influencing factors could be the physiochemical differences in melting point and lipophilicity between oridonin and CZ48.

The particle size of nanosuspensions also has significant impacts on the plasma pharmacokinetics of CZ48 from nanosuspensions, which can be attributed to two reasons: size-dependent dissolution rate and RES uptake (Gao L et al., 2008; Manjunath K and Venkateswarlu V, 2005). The smaller-sized of CZ48 nanosuspenison (NS-S) yielded a significantly higher C_0 than the larger-sized nanosuspension (NS-L). The V_1 was smaller for NS-L than that of NS-S, indicating a greater drug uptake into the peripheral compartment from NS-L than NS-S. The nanoparticles with larger size are taken up more efficiently than those with smaller particle size in *in vitro* studies with macrophage cells (Allen TM and Everest JM, 1983; Chono S et al., 2006). Since the particle size of nanosuspension affect plasma pharmacokinetics, one can carefully select the particle size based on the therapeutic need.

The pharmacokinetic and distribution behaviors depend on the chemical properties, CZ48 disposition, as well as the transformation rate and capacity of CZ48 to CPT in each organ. Only free dissolved CZ48 can be converted to CPT. In this way, the CPT from NS-S also showed a significantly longer elimination half-life compared to those from

NS-L and cosolvent. There were a comparable V_{ss} among those three groups that could be interpreted as only the chemical properties could affect the CPT disposition at steady state.

5.6.2. Plasma Pharmacokinetics of CZ48 Cosolvent and Nanosuspensions (NS-S, and NS-L) in Mice

Athymic nude mice are animal models of choice for pharmacokinetics and pharmacodynamics studies of anticancer agents, because they can easily grow human tumor by injecting human tumor cells. Moreover, the Swiss nude mice will be the tumor model to test the efficacy of the lead nanosuspension. Therefore, the mouse model was also selected for the preclinical pharmacokinetic and biodistribution studies of CZ48 from cosolvent, and nanosuspensions in our project.

The blood volume of mice is 6-8% of the body weight and no more than 10-15% of total blood volume should be collected at one time (Hoff J, 2000). Due to this limitation, there were no more than three plasma samples could be obtained from each mouse for the plasma pharmacokinetic studies of CZ48 from cosolvent and nanosuspensions in mice. Therefore, combined with the organ distribution study, we withdraw only one additional plasma sample for each mouse before organ collection. A naïve averaged plasma approach was used to construct plasma-time profiles for CZ48 from cosolvent and nanosuspensions in mice. In naïve average plasma approach, the averaged plasma concentration at each time point was calculated. Based on the mean plasma concentration-time profile, the mean pharmacokinetic parameters which reflected

population pharmacokinetic properties were derived by WinNonlin (KuKanich B et al., 2007). Without pharmacokinetic parameters from each individual mouse, statistical comparison such as ANOVA test among those formulations could not be performed in our studies. Instead, the possible trend of changes of pharmacokinetic parameters between formulations was evaluated by comparing the magnitude of the values.

Similar as in rats, CZ48 nanosuspensions of two different particle sizes (NS-S and NS-L) also exhibited distinct plasma and biodistribution patterns from that of cosolvent. Significantly lower C_0 of CZ48 from both nanosuspensions than that from the cosolvent formulation could be due to the slower dissolution rates of CZ48 from the nanosuspensions than from cosolvent. The *in vitro* drug release studies demonstrated that CZ48 from cosolvent was rapidly and completely released, while CZ48 from nanosuspensions was released much slower in the plasma. Two-compartmental model was used to characterize the CZ48 plasma profiles from nanosuspensions, while one-compartmental model was used for the CZ48 profile from the cosolvent. It could be due to the drug accumulation in the peripheral compartment from CZ48 nanosuspensions. Longer elimination half-lives and larger V_{ss} were observed in nanosuspensions than those of CZ48 from cosolvent. The microconstants K_{21} of both nanosuspensions were slightly slower than K_{12}. No significant differences were observed between NS-S and NS-L.

The decreased C_0 and prolonged half-lives of nanosuspensions, as compared with cosolvent could be significant in clinical application of nanosuspensions. For example, the decreased C_0 could be beneficial in reducing side effects of the drug caused by the

excessively high C_0 (Kim WY et al., 2007). CZ48 nanosuspension with a prolonged half-life needs less frequent dosing to provide a sustained therapeutic plasma level of CPT, which is more convenient to patients and favors a better patient compliance.

More importantly, similar as the result in rats, the CPT from NS-S also showed a significantly longer elimination half-life compared to those from NS-L and cosolvent. There were a comparable V_{ss} of CPT among those three groups.

5.6.3. Organ Distribution of CZ48 Cosolvent and Nanosuspensions (NS-S, and NS-L) in Rats

Consistently distinct plasma pharmacokinetic properties of CZ48 nanosuspensions from those of cosolvent in rats and mice, such as prolonged β half-lives and large volume distribution for CZ48 nanosuspensions, drive our investigation to establish the biodistribution patterns of CZ48 from nanosuspension formulations, in contrast to that of cosolvent.

The organ distribution patterns of CZ48 from nanosuspensions were distinct from that of CZ48 cosolvent. CZ48 distributions among organs from cosolvent were relatively even among organs, due to the rapid dissolution and highly hydrophobic properties of CZ48, except a high accumulation in lung that may be due to the drug precipitation with subsequent retention in lung, which was consistent with the finding of bifendate nanosuspension study in rabbits (Liu Y et al., 2012). Further research was needed in the future. The liver and spleen were observed with the highest exposure of CZ48 from

nanosuspensions, which could be due to the RES uptake. Liver and spleen are known as two major sites containing the RES as the one of the body defense system to clear foreign particles (Brannon-Peppas L & Blanchette JO, 2004). The particles circulating in the blood stream, will be immediately uptaken by the RES (Burgess DJ, 2005; Gao L, 2008), as reported with high drug dispositions in liver and spleen from oridonin nanosuspensions of 897 nm (Gao L et al., 2008). The pattern of high drug distributions in liver and spleen from nanosuspensions is very similar to that of liposome and other nanoparticle formulations (Allen TM and Everest JM, 1984; Brannon-Peppas L & Blanchette JO, 2004; Freise J et al., 1981; Peters K et al., 2000). Following the uptake, the RES acts as a depot and drug can be released slowly back to the systemic circulation, which may contribute to the sustained plasma drug level achieved from nanosuspensions (Burgess DJ, 2005).

CZ48 exerts the antitumor activity by CEs mediated hydrolysis to the active metabolite CPT *in vivo* (Liehr JG et al., 2000). *In vitro* study of CZ48 metabolism has showed that among blood and CE-containing tissues such as liver, spleen, lung and kidney, the liver has the highest metabolic capacity to convert CZ48 to CPT (Satoh T and Hosokawa M, 1998) instead of in blood, consistent with the fact that the highest CEs activity is in the liver. For all three formulations, CPT showed the highest exposure in liver. Because the nanosuspension particles will be trapped by the RES cells and released slowly, and only the free CZ48 molecules can be biotransformed to CPT. As a result, the CPT from nanosuspension also yielded a significantly longer β half-life in different organs compared to those from cosolvent. CZ48 nanosuspensions showed a much higher

spleen exposure, which may be a concern of potential off-target accumulation and toxicity.

5.6.4. Organ Distribution of CZ48 Cosolvent and Nanosuspensions (NS-S, and NS-L) in Mice

Similar as in rats, CZ48 nanosuspensions of two different sizes (NS-S and NS-L) exhibited distinct biodistribution patterns from that of cosolvent in mice. CZ48 from cosolvent was distributed evenly in all organs. Rapid decline of the total drug concentration in all organs, which can be characterized by a one-compartment model, indicated a fast elimination of CZ48 from these organs.

CZ48 nanosuspension had the highest CZ48 exposure in liver, followed by spleen and lung, higher than in other organs. The high drug exposure in liver, spleen and lung from CZ48 nanosuspensions suggested the RES uptake of nanosuspensions, which was the same as in rats. Only the exposure of CZ48 in lung from NS-S showed a 3 times higher than that from NS-L which may be due to the extremely long half-life, 38.21 h and 3.07 h for NS-S and NS-L, respectively. And the prolonged half-life in lung could provide potential merits for lung cancer treatment. No significant difference was observed in other organs between NS-S and NS-L.

CPT from all these three formulations also showed the highest exposure in liver. However, the CPT from nanosuspensions had longer β half-lives in different organs compared to those from cosolvent.

All these properties may offer potential merits for CZ48 chemotherapy. Briefly, nanosuspensions after i.v. administration appeares to be a practical approach to introduce sustained levels of poorly soluble compounds over a period of hours, especially NS-S. It may the drug more effective or more tolerable by modifying and improving the drug performance, such as increasing the duration action and the reduced frequency of dosing (Wang Y et al., 2010).

5.6.5. Proof of Concept Efficacy of NS-S in Lung Cancer Tumor Bearing Mice Model

The present studies demonstrated that our nanosuspension formulation had substaintially lower toxicity than the cosolvent. Four times tail vein injection of cosolvent made severe tissue damage, but nanosuspension injection did not result in any damage. In addition, the blood was taken after the animal was sacrificed. Much darker and thicker blood was observed by cosolvent administration compared to no treatment goup and nanosuspension groups. Because of the low solubility of CZ48, the highest tolerate dose of CZ48 cosolvent was 5 mg/kg. Any increase of the cosolvent concentration will cause the animal death immediately due to the significant drug precipitation in the blood circulation. However, the dose of nanosuspension can be given up to 25 mg/kg due to the toxicity of the drug.

Cosolvent and NS-S-L at the same dose level (5 mg/kg) did not exhibit significant efficacy over the control/reference groups. For most of the chemotherapy agents, there is a therapeutic window. The phenomenon of lack of efficacy was not well understood,

but might be due to the dose level could not reach the minimum therapeutic concentration, or it failed to keep the therapeutic concentration for a long enough duration.

Wherevas, the treatment with NS-S-M yielded significant tumor growth suppression and prolonged animal median survival duration, compared to control groups. The significant onset tumor suppression was observed 3 days after the first dose given. This dose is the same as the pharmacokinetic study, which resulted in sustained circulation of CZ48 and CPT for more than 24 hours circulation in rodent animals. In this way, the significant efficacy may be attributable in part to the favorable pharmacokinetics of systemically delivery drugs, as well as to the inherent permeability by the tumor cells (Zou YJ et al., 2004).

For high dose group of CZ48 nanosuspension administration, it showed the highest tumor suppression, but after the first dose, two out of ten animals died. The death might be due to the toxicity of the high amount of CZ48. The dose was reduced from 50 mg/kg to 40 mg/kg twice weekly at the fourth dose, but still resulted in animal death (2 out of 7). Subsequently, the regimen was changed from 40 mg/kg twice weekly to once weekly. The significant tumor suppression could be investigated, but the toxicity caused 5 animals death. These results with the high dose group suggested that CZ48 nanosuspension could not be given more than 40 mg/kg at each time.

There was no significant body weight loss in any of these groups. Our promising results suggest that a therapeutic approach that uses nanosuspension delivery of this novel agent, CZ48, may warrant a further development.

Chapter 6 Summary

6.1. Formulation of CZ48 Nanosuspensions

The media milling technique was used in nanosuspension preparation where the solid drug particles were sheared between the sliding surfaces of the moving glass beads. T-80 and F-108 were added as steric stabilizers to overcome the attractive interactions between the nanoparticles. A narrow particle size distribution was achieved by using a mixture of glass beads with various sizes were used instead of single-sized glass beads.

6.2. Central Composite Design (CCD)

Three processing critical variables, CZ48 concentration, F-108/CZ48 ratio and T-80/CZ48 ratio, in the preparation method were identified and optimized by a scientifically and systematically efficient CCD design. The result of this mathematical analysis showed that CZ48 concentration and F-108/CZ48 ratio were the crucial parameters for the particle size of the nanosuspension prepared by media milling method; however, none of the factors investigated in this study had a significant quadratic relationship with the achieved zeta potential. Therefore, the statistical experimental methodology has clearly shown its usefulness in the optimization process and our study also serves as the groundwork for the understanding of nanosuspension formulation.

Based on the CCD results, NS-S (200 nm) and NS-L (600 nm) were developed for further *in vivo* pharmacokinetic and efficacy studies that were successfully proved the hypothesis of the project.

6.3. HPLC Assay

A previously developed HPLC method was modified and employed in quantifying CZ48 and CPT concentrations from *in vitro* and *in vivo* studies. The assay was highly sensitive, reproducible and efficient. Plasma and organic precipitation yielded CZ48 and CPT recovery of 96%. The lower limit of quantification (LLOQ) was 0.78 ng/ml for CZ48 and 0.55 ng/ml for CPT, improved from the previous LLOQ of the assay, 10 ng/ml for CZ48 and 5 ng/ml for CPT, respectively.

6.4. *In-vitro* Release of CZ48 from Cosolvent and Two Nanosuspensions (NS-S and NS-L)

The release profiles of the nanosuspensions in PBS and human plasma had similar pattern except for a lower release rate and smaller extent in plasma. Cosolvent formulation had the fastest release rate and the highest release extent than those of nanosuspension groups in PBS and plasma. The small particle NS-S (200 nm) had a faster release rate than that of NS-L (600 nm) group in PBS. However, they did not show significant difference in plasma. By comparing the release in PBS to plasma, there was a reduction in the rate and extent of release in plasma due to the high binding of CZ48 to plasma proteins. The release profiles differences might result in different pharmacokinetic characteristics of CZ48. The release profiles were best described by the 1^{st} -order kinetic equation in both release media.

6.5. Plasma Pharmacokinetics of CZ48 Cosolvent and Nanosuspensions (NS-S, and NS-L) in Rats

The rat plasma profile of CZ48 cosolvent was used as a reference for the profiles from the nanosuspensions. The plasma concentration-time profiles of CZ48 from cosolvent followed a one-compartment kinetics. However, the plasma concentration-time profiles of CZ48 from NS-S and NS-L followed a three-compartment model. The AUC of CZ48 from NS-S and cosolvent was comparable, but significantly higher than that from NS-L. The half-life of CZ48 from NS-S was the longest, which was about 4 times and 60 times of those from NS-L and cosolvent, respectively.

The plasma concentration-time profiles of CPT from cosolvent followed a one-compartment model. However, the plasma concentration-time profiles of CPT from NS-S followed a three-compartment model, and that from NS-L followed a one-compartment model. For NS-L, no distribution phase was observed, which might be due to the fact that the distribution kinetics of CPT was faster than that of the biotransformation. The AUC and half-life of CPT from NS-S was the highest followed by those from NS-L, and cosolvent. These properties might offer merits for the clinical application of CZ48.

6.6. Organ Distribution of CZ48 and Metabolite, CPT, from Cosolvent and Nanosuspensions (NS-S, and NS-L) in Rats (n=4)

Being a particulate system, the nanosuspensions have a higher RES uptake of CZ48 as compared to that of the reference cosolvent. There is no significant improvement on the CPT exposure. However, the elimination half-lives of CZ48 and CPT from the different organs after nanosuspension dosing ranged from 1.39 h to 16.50 h, substantially prolonged by 2 ~ 48 times from those of cosolvent.

6.7. Plasma Pharmacokinetics of CZ48 Cosolvent and Nanosuspensions (NS-S, and NS-L) in Mice (n=4)

The profiles of CZ48 and CPT from NS-S and NS-L are similar where the initial phase has a rapid decline followed by a slower phase of elimination. However, the profile of cosolvent showed rapid clearances of CZ48 and CPT. The relative systemic exposure of CZ48 from both nanosuspensions were comparable to that from cosolvent. However, the exposure of CPT from NS-S and NS-L were 2.39 times and 1.31 times higher than that from the cosolvent. The elimination half-lives of CZ48 and CPT from nanosuspensions were prolonged more than 8 times compared to that from cosolvent.

6.8. Organ Distribution of CZ48 and Metabolite, CPT, from Cosolvent and Nanosuspensions (NS-S, and NS-L) in Mice (n=4)

Being a particulate system, the nanosuspensions have a higher RES uptake of CZ48 as compared to that of the reference cosolvent. Similar to the result in rats, there is no significant improvement on the CPT exposure. However, the elimination half-lives of CZ48 and CPT from the different organs after nanosuspension dosing were prolonged 3 to 10 times of those from cosolvent.

6.9. NS-S Efficacy Study

The treatment with NS-S-M at 25 mg/kg yielded significant tumor growth suppression and prolonged animal survival with an early onsite after 3 days of the first dose, compared to control groups. The tolerable dose of CZ48 nanosuspension was substantially increased by 5 times from 5 mg/kg to 25 mg/kg, compare that of cosolvent. The same dose level with cosolvent at 5 mg/kg did not show any advantage. Our promising results suggest that an optimal therapeutic regimen that uses nanosuspension delivery of this novel agent, CZ48, may warrant a further development.

Reference

Aktas E, Eroglu H, Kockan U, Oner L. Systematic development of pH-independent controlled release tablets of carvedilol using central composite design and artificial neural networks. Drug Dev Ind Pharm. 2012 Jul 18. [Epub ahead of print]

Allen TM, Cullis PR. Drug delivery systems: entering the mainstream. Science. 2004; 303(5665): 1818-22.

Allen TM, Everest JM. Effect of liposome size and drug release properties on pharmacokinetics of encapsulated drug in rats. J Pharmacol Exp Ther. 1983; 226(2): 539-44.

Andes D. *In vivo* pharmacodynamics of antifungal drugs in treatment of candidiasis. Antimicrob Agents Chemother. 2003; 47(4): 1179-86.

Aulton ME, Pharmaceutics: the science of dosage form design. 2002

Bolton S. Factorial designs in pharmaceutical stability studies. J Pharm Sci. 1983; 72(4): 362-6.

Bonomi P. Non-small cell lung cancer chemotherapy. In: Pass HI, Mitchell JB, Johnson DH, Turrisi AT, editors. Lung Cancer. Principles and practice. Philadelphia: Lippincott-Raven; 1996. p.811-23.

Brannon-Peppas L, Blanchette JO. Nanoparticle and targeted systems for cancer therapy. Adv Drug Deliv Rev. 2004; 56(11): 1649-59.

Bummer P. Interficial phenomena, in: A Gennaro (Ed.), Remington: The Science and Practice of Pharmacy, 20th Ed., Lippincott Williams & Willkins, Baltimore. 2000; p. 285.

Burgess DJ. Injectable Dispersed Systems: Formulation, Processing, and Performance. Informa Health Care. 2005

Cao Z, Harris N, Kozielski A, Vardeman D, Stehlin JS, Giovanella B. Alkyl esters of camptothecin and 9-nitrocamptothecin: synthesis, *in vitro* pharmacokinetics, toxicity, and antitumor activity. J Med Chem. 1998; 41(1): 31-7.

Cao Z, Pantazis P, Mendoza J, Early J, Kozielski A, Harris N, Vardeman D, Liehr J, Stehlin JS, Giovanella B. Structure-activity relationship of alkyl camptothecin esters. Ann N Y Acad Sci. 2000; 922: 122-35.

Chen HJ, Hakka LE, Hinman RL, Kresge Aj and Whipple EB. The basic strength of carcazole. An estimate of the nitrogen basicity of pyrrole and indole. J of American Chem Society. 1971; 93: 20

Chingunpitak J, Puttipipatkhachorn S, Chavalitshewinkoon-Petmitr P, Tozuka Y, Moribe K, Yamamoto K. Formation, physical stability and *in vitro* antimalarial activity of dihydroartemisinin nanosuspensions obtained by co-grinding method. Drug Dev Ind Pharm. 2008; 34(3): 314-22.

Chono S, Tauchi Y, Morimoto K. Pharmacokinetic analysis of the uptake of liposomes by macrophages and foam cells *in vitro* and their distribution to atherosclerotic lesions in mice. Drug Metab Pharmacokinet. 2006; 21(1): 37-44.

Chow EC, Durk MR, Cummins CL, Pang KS. 1Alpha,25-dihydroxyvitamin D3 up-regulates P-glycoprotein via the vitamin D receptor and not farnesoid X receptor in both fxr(-/-) and fxr(+/+) mice and increased renal and brain efflux of digoxin in mice *in vivo*. J Pharmacol Exp Ther. 2011; 337(3): 846-59.

Cukierman E, Khan DR. The benefits and challenges associated with the use of drug delivery systems in cancer therapy. Biochem Pharmacol. 2010; 80(5): 762-70. Review.

Danhier F, Feron O, Préat V. To exploit the tumor microenvironment: Passive and active tumor targeting of nanocarriers for anti-cancer drug delivery. J Control Release. 2010; 148(2): 135-46. Review.

de Boer T, Bijma R, Ensing K. Modelling of conditions for the enantiomeric separation of beta2-adrenergic sympathicomimetics by capillary electrophoresis using cyclodextrins as chiral selectors in a polyethylene glycol gel. J Pharm Biomed Anal. 1999; 19(3-4): 529-37.

Dennis MJ, Beijnen JH, Grochow LB, van Warmerdam LJ. An overview of the clinical pharmacology of topotecan. Semin Oncol. 1997: S5-12-S5-18.

Devore RF, Johnson DH. Chemotherapy of small lung cell lung cancer. In: Pass HI, Mitchell JB, Johnson DH, Turrisi AT, editors. Lung Cancer. Principles and practice. Philadelphia: Lippincott-Raven; 1996. p.825-35.

Drulis-Kawa Z, Dorotkiewicz-Jach A. Liposomes as delivery systems for antibiotics. Int J Pharm. 2010; 387(1-2): 187-98. Review.

Fassberg J, Stella VJ. A kinetic and mechanistic study of the hydrolysis of camptothecin and some analogues. J Pharm Sci. 1992; 81(7): 676-84.

Freise J, Müller WH, Magerstedt P. Uptake of liposomes and sheep red blood cells by the liver and spleen of rats with normal or decreased function of the reticuloendothelial system. Res Exp Med (Berl). 1981; 178(3): 263-9.

Ganta S, Paxton JW, Baguley BC, GargS. Formulation and pharmacokinetic evaluation of an asulacrine nanocrystalline suspension for intravenous delivery. Int J Pharm. 2009; 367(1-2): 179-86.

Gao L, Zhang D, Chen M, Duan C, Dai W, Jia L, Zhao W. Studies on pharmacokinetics and tissue distribution of oridonin nanosuspensions. Int J Pharm. 2008; 355(1-2): 321-7.

Gao L, Zhang D, Chen M, Zheng T, Wang S. Preparation and characterization of an oridonin nanosuspension for solubility and dissolution velocity enhancement. Drug Dev Ind Pharm. 2007; 33(12): 1332-9.

Gao Y, Qian S, Zhang J. Physicochemical and pharmacokinetic characterization of a spray-dried cefpodoxime proxetil nanosuspension. Chem Pharm Bull (Tokyo). 2010; 58(7): 912-7.

Gerrits CJ, de Jonge MJ, Schellens JH, Stoter G, Verweij J. Topoisomerase I inhibitors: the relevance of prolonged exposure for present clinical development. Br J Cancer. 1997; 76(7): 952-62. Review.

Giovanella BC, Stehlin JS, Wall ME, Wani MC, Nicholas AW, Liu LF, Silber R, Potmesil M. DNA topoisomerase I--targeted chemotherapy of human colon cancer in xenografts. Science. 1989; 246(4933): 1046-8.

Giovanella BC, Stehlin JS, Wall ME, Wani MC, Nicholas AW, Liu LF, Silber R, Potmesil M. DNA topoisomerase I--targeted chemotherapy of human colon cancer in xenografts. Science. 1989; 246(4933): 1046-8.

Gottlieb JA, Guarino AM, Call JB, Oliverio VT, Block JB. Preliminary pharmacologic and clinical evaluation of camptothecin sodium (NSC-100880). Cancer Chemother Rep. 1970 Dec;54(6):461-70.

Gottlieb JA, Luce JK. Treatment of malignant melanoma with camptothecin (NSC-100880). Cancer Chemother Rep. 1972; 56(1): 103-5.

Grochow LB, Rowinsky EK, Johnson R, Ludeman S, Kaufmann SH, McCabe FL, Smith BR, Hurowitz L, DeLisa A, Donehower RC, et al. Pharmacokinetics and

pharmacodynamics of topotecan in patients with advanced cancer. Drug Metab Dispos. 1992; 20(5): 706-13.

Hao J, Wang F, Wang X, Zhang D, Bi Y, Gao Y, Zhao X, Zhang Q. Development and optimization of baicalin-loaded solid lipid nanoparticles prepared by coacervation method using central composite design. Eur J Pharm Sci. 2012; 47(2): 497-505.

Heldin CH, Rubin K, Pietras K, Ostman A. High interstitial fluid pressure - an obstacle in cancer therapy. Nat Rev Cancer. 2004; 4(10): 806-13.

Hertzberg RP, Caranfa MJ, Holden KG, Jakas DR, Gallagher G, Mattern MR, Mong SM, Bartus JO, Johnson RK, Kingsbury WD. Modification of the hydroxy lactone ring of camptothecin: inhibition of mammalian topoisomerase I and biological activity. J Med Chem. 1989; 32(3): 715-20.

Hoff J. Methods of blood collection in the mouse. Lab Animal. 2000; 29(10): 47-53.

Höfig I, Atkinson MJ, Mall S, Krackhardt AM, Thirion C, Anastasov N. Poloxamer synperonic F108 improves cellular transduction with lentiviral vectors. J Gene Med. 2012; 14(8): 549-60.

Hsiang YH, Hertzberg R, Hecht S, Liu LF. Camptothecin induces protein-linked DNA breaks via mammalian DNA topoisomerase I. J Biol Chem. 1985; 260(27): 14873-8.

Hsiang YH, Liu LF. Identification of mammalian DNA topoisomerase I as an intracellular target of the anticancer drug camptothecin. Cancer Res. 1988; 48(7): 1722-6.

Jani P, Halbert GW, Langridge J, Florence AT. Nanoparticle uptake by the rat gastrointestinal mucosa: quantitation and particle size dependency. J Pharm Pharmacol. 1990; 42(12): 821-6.

Kassem MA, Abdel Rahman AA, Ghorab MM, Ahmed MB, Khalil RM. Nanosuspension as an ophthalmic delivery system for certain glucocorticoid drugs. Int J Pharm. 2007; 340(1-2): 126-33.

Keck CM, Müller RH. Drug nanocrystals of poorly soluble drugs produced by high pressure homogenisation. Eur J Pharm Biopharm. 2006; 62(1): 3-16. Review.

Keck CM, Müller RH. Drug nanocrystals of poorly soluble drugs produced by high pressure homogenisation. Eur J Pharm Biopharm. 2006; 62(1): 3-16.

Kesisoglou F, Panmai S, Wu Y. Nanosizing--oral formulation development and biopharmaceutical evaluation. Adv Drug Deliv Rev. 2007; 59(7): 631-44.

Kesisoglou F, Panmai S, Wu Y. Nanosizing--oral formulation development and biopharmaceutical evaluation. Adv Drug Deliv Rev. 2007; 59(7): 631-44.

Kim WY, Nakata B, Hirakawa K. Alternative pharmacokinetics of S-1 components, 5-fluorouracil, dihydrofluorouracil and alpha-fluoro-beta-alanine after oral administration of S-1 following total gastrectomy. Cancer Sci. 2007; 98(10): 1604-8.

Kocbek P, Baumgartner S, Kristl J. Preparation and evaluation of nanosuspensions for enhancing the dissolution of poorly soluble drugs. Int J Pharm. 2006; 312(1-2): 179-86.

Kollipara S, Bende G, Movva S, Saha R. Application of rotatable central composite design in the preparation and optimization of poly(lactic-co-glycolic acid) nanoparticles for controlled delivery of paclitaxel. Drug Dev Ind Pharm. 2010; 36(11): 1377-87.

Korting HC, Schäfer-Korting M. Carriers in the topical treatment of skin disease. Handb Exp Pharmacol. 2010; (197): 435-68.

Kostanski JW, DeLuca PP. A novel *in vitro* release technique for peptide containing biodegradable microspheres. AAPS PharmSciTech. 2000; 1(1): E4.

KuKanich B, Huff D, Riviere JE, Papich MG. Naïve averaged, naïve pooled, and population pharmacokinetics of orally administered marbofloxacin in juvenile harbor seals. J Am Vet Med Assoc. 2007; 230(3): 390-5.

Lawrence MJ, Rees GD. Microemulsion-based media as novel drug delivery systems. Adv Drug Deliv Rev. 2000; 45(1): 89-121. Review.

Li Xiaohui. Preclinical Pharmacokinetics of CZ48, Lactone-stabilized Camptothecin, in Rats and Its Potential Routes of Administration for Therapy. Ph.D. Dissertation; University of Houston (2004)

Liehr JG, Harris NJ, Mendoza J, Ahmed AE, Giovanella BC. Pharmacology of camptothecin esters. Ann N Y Acad Sci. 2000; 922: 216-23. Review.

Liu X, Wang Y, Vardeman D, Cao Z, Giovanella B. Development and validation of a reverse-phase HPLC with fluorescence detector method for simultaneous determination

of CZ48 and its active metabolite camptothecin in mouse plasma. J Chromatogr B Analyt Technol Biomed Life Sci. 2008; 867(1): 84-9.

Liu Y, Zhang D, Duan C, Jia L, Xie P, Zheng D, Wang F, Liu G, Hao L, Zhang X, Zhang Q. Studies on pharmacokinetics and tissue distribution of bifendate nanosuspensions for intravenous delivery. J Microencapsul. 2012; 29(2): 194-203.

Lück M, Paulke BR, Schröder W, Blunk T, Müller RH. Analysis of plasma protein adsorption on polymeric nanoparticles with different surface characteristics. J Biomed Mater Res. 1998; 39(3): 478-85.

Manjunath K, Venkateswarlu V. Pharmacokinetics, tissue distribution and bioavailability of clozapine solid lipid nanoparticles after intravenous and intraduodenal administration. J Control Release. 2005; 107(2): 215-28.

Matsumura Y, Maeda H. A new concept for macromolecular therapeutics in cancer chemotherapy: mechanism of tumoritropic accumulation of proteins and the antitumor agent smancs. Cancer Res. 1986; 46(12 Pt 1): 6387-92.

Mattern J, Jäger S, Sonka J, Wayss K, Volm M. Growth of human bronchial carcinomas in nude mice. Br J Cancer. 1985; 51(2): 195-200.

McLeod AD, Lam FC, Gupta PK, Hung CT. Optimized synthesis of polyglutaraldehyde nanoparticles using central composite design. J Pharm Sci. 1988; 77(8): 704-10.

McLeod HL, Douglas F, Oates M, Symonds RP, Prakash D, van der Zee AG, Kaye SB, Brown R, Keith WN. Topoisomerase I and II activity in human breast, cervix, lung and colon cancer. Int J Cancer. 1994; 59(5): 607-11.

Merisko-Liversidge E, Liversidge GG, Cooper ER. Nanosizing: a formulation approach for poorly-water-soluble compounds. Eur J Pharm Sci. 2003; 18(2): 113-20. Review.

Moertel CG, Schutt AJ, Reitemeier RJ, Hahn RG. Phase II study of camptothecin (NSC-100880) in the treatment of advanced gastrointestinal cancer. Cancer Chemother Rep. 1972; 56(1): 95-101.

Molpeceres J, Guzman M, Aberturas MR, Chacon M, Berges L. Application of central composite designs to the preparation of polycaprolactone nanoparticles by solvent displacement. J Pharm Sci. 1996; 85(2): 206-13.

Möschwitzer JP. Drug nanocrystals in the commercial pharmaceutical development process. Int J Pharm. 2012. [Epub ahead of print]

Mouton JW, van Peer A, de Beule K, Van Vliet A, Donnelly JP, Soons PA. Pharmacokinetics of itraconazole and hydroxyitraconazole in healthy subjects after single and multiple doses of a novel formulation. Antimicrob Agents Chemother. 2006; 50(12): 4096-102.

Muggia FM, Creaven PJ, Hansen HH, Cohen MH, Selawry OS. Phase I clinical trial of weekly and daily treatment with camptothecin (NSC-100880): correlation with preclinical studies. Cancer Chemother Rep. 1972; 56(4): 515-21.

Müller RH, Jacobs C. Buparvaquone mucoadhesive nanosuspension: preparation, optimisation and long-term stability. Int J Pharm. 2002; 237(1-2): 151-61.

Müller RH, Jacobs C. Buparvaquone mucoadhesive nanosuspension: preparation, optimisation and long-term stability. Int J Pharm. 2002; 237(1-2): 151-61.

Patravale VB, Date AA, Kulkarni RM. Nanosuspensions: a promising drug delivery strategy. J Pharm Pharmacol. 2004; 56(7): 827-40. Review.

Peters K, Leitzke S, Diederichs JE, Borner K, Hahn H, Müller RH, Ehlers S. Preparation of a clofazimine nanosuspension for intravenous use and evaluation of its therapeutic efficacy in murine Mycobacterium avium infection. J Antimicrob Chemother. 2000; 45(1): 77-83.

Pfuma E. Pharmacokinetics and Pharmacodynamics of Combination CZ48 and Manumycin A in an Athymic Mouse Model. Ph.D. Dissertation; University of Houston (2009).

Pignatello R, Ricupero N, Bucolo C, Maugeri F, Maltese A, Puglisi G. Preparation and characterization of eudragit retard nanosuspensions for the ocular delivery of cloricromene. AAPS PharmSciTech. 2006; 7(1): E27.

Qi YL. Impacts of Size on Pharmacokinetics and Biodistributions of Mebendazole Nanoformulation in Mice and Rats. Dissertation; University of Houston (2008).

Rothenberg ML, Kuhn JG, Burris HA 3rd, Nelson J, Eckardt JR, Tristan-Morales M, Hilsenbeck SG, Weiss GR, Smith LS, Rodriguez GI, et al. Phase I and pharmacokinetic trial of weekly CPT-11. J Clin Oncol. 1993; 11(11): 2194-204.

Satoh T, Hosokawa M. The mammalian carboxylesterases: from molecules to functions. Annu Rev Pharmacol Toxicol. 1998; 38: 257-88. Review.

Schubert MA, Müller-Goymann CC Solvent injection as a new approach for manufacturing lipid nanoparticles--evaluation of the method and process parameters. Eur J Pharm Biopharm. 2003; 55(1): 125-31.

Schultz AG. Camptothecin. Chem Rev. 1973; 73(4): 385-405.

Sun W, Xie C, Wang H, Hu Y. Specific role of polysorbate 80 coating on the targeting of nanoparticles to the brain. Biomaterials. 2004; 25(15): 3065-71.

Takimoto CH, Wright J, Arbuck SG. Clinical applications of the camptothecins. Biochim Biophys Acta. 1998; 1400(1-3): 107-19.

Torchilin VP. Drug targeting. Eur J Pharm Sci. 2000; 11 Suppl 2: S81-91. Review

Vandamme TF. Microemulsions as ocular drug delivery systems: recent developments and future challenges. Prog Retin Eye Res. 2002; 21(1): 15-34. Review.

Verma S, Gokhale R, Burgess DJ. A comparative study of top-down and bottom-up approaches for the preparation of micro/nanosuspensions. Int J Pharm. 2009; 380(1-2): 216-22.

Wall ME, Wani MC, Cook CE, Palmer KH, McPhail HT, Sim G.A. Plant antitumor agents I: The isolation and structure of camptothecin, a novel alkaloidal leukemia and tumor inhibitor from Camptotheca acuminata. J Am Chem Soc. 1996; 88: 3888-3890.

Wall ME, Wani MC. Antineoplastic agents from plants. Annu Rev Pharmacol Toxicol. 1977; 17: 117-32. Review.

Wang Y, Liu Z, Zhang D, Gao X, Zhang X, Duan C, Jia L, Feng F, Huang Y, Shen Y, Zhang Q. Development and *in vitro* evaluation of deacety mycoepoxydiene nanosuspension. Colloids Surf B Biointerfaces. 2011; 83(2): 189-97.

Wang Y, Zhang D, Liu Z, Liu G, Duan C, Jia L, Feng F, Zhang X, Shi Y, Zhang Q. *In vitro* and *in vivo* evaluation of silybin nanosuspensions for oral and intravenous delivery. Nanotechnology. 2010; 21(15): 155104.

Wani MC, Ronman PE, Lindley JT, Wall ME. Plant antitumor agents. 18. Synthesis and biological activity of camptothecin analogues. J Med Chem. 1980; 23(5): 554-60.

Wong J, Brugger A, Khare A, Chaubal M, Papadopoulos P, Rabinow B, Kipp J, Ning J. Suspensions for intravenous (IV) injection: a review of development, preclinical and clinical aspects. Adv Drug Deliv Rev. 2008; 60(8): 939-54. Review.

Xiong R, Lu W, Yue P, Xu R, Li J, Chen T, Wang P. Distribution of an intravenous injectable nimodipine nanosuspension in mice. J Pharm Pharmacol. 2008; 60(9): 1155-9.

Yang JZ, Young AL, Chiang PC, Thurston A, Pretzer DK. Fluticasone and budesonide nanosuspensions for pulmonary delivery: preparation, characterization, and pharmacokinetic studies. J Pharm Sci. 2008; 97(11): 4869-78.

Yousif R. Microemulsion formulations of CZ48, lactone-stabilized camptothecin-C20-propionate, for transdermal delivery. Dissertation; University of Houston (2007).

Zhang J, Fan Y, Smith E. Experimental design for the optimization of lipid nanoparticles. J Pharm Sci. 2009; 98(5): 1813-9.

Zou Y, Fu H, Ghosh S, Farquhar D, Klostergaard J. Antitumor activity of hydrophilic Paclitaxel copolymer prodrug using locoregional delivery in human orthotopic non-small cell lung cancer xenograft models. Clin Cancer Res. 2004; 10(21): 7382-91.